UNIVERSIDADE FEDERAL DE VIÇOSA

Walking through space-time dynamics of the Southern Amazon's rainy season – deforestation impacts and hydroclimate variability at different scales

Luiz Felipe Sant' Anna Commar
Doctor Scientiae

VIÇOSA - MINAS GERAIS
2025

LUIZ FELIPE SANT' ANNA COMMAR

Walking through space-time dynamics of the Southern Amazon's rainy season – deforestation impacts and hydroclimate variability at different scales

Thesis submitted to the Applied Meteorology Graduate Program of the Universidade Federal de Viçosa in partial fulfillment of the requirements for the degree of *Doctor Scientiae*.

Adviser: Marcos Heil Costa

VIÇOSA - MINAS GERAIS
2025

Ficha catalográfica elaborada pela Biblioteca Central da Universidade Federal de Viçosa - Campus Viçosa

T
C734w
2025

Commar, Luiz Felipe Sant'Anna, 1995-
Walking through space-time dynamics of the Southern Amazon's rainy season : deforestation impacts and hydroclimate variability at different scales / Luiz Felipe Sant'Anna Commar. – Viçosa, MG, 2025.
1 tese eletrônica (100 f.): il. (algumas color.).

Texto em inglês.
Inclui apêndices.
Orientador: Marcos Heil Costa.
Tese (doutorado) - Universidade Federal de Viçosa, Departamento de Engenharia Agrícola, 2025.
Referências bibliográficas: f. 89-100.
DOI: https://doi.org/10.47328/ufvbbt.2025.301
Modo de acesso: World Wide Web.

1. Mudanças climáticas. 2. Desmatamento - Amazônia. 3. Modelos atmosféricos. I. Costa, Marcos Heil, 1965-. II. Universidade Federal de Viçosa. Departamento de Engenharia Agrícola. Programa de Pós-Graduação em Meteorologia Aplicada. III. Título.

CDD 22. ed. 551.5253

Bibliotecário(a) responsável: Alice Regina Pinto Pires CRB-6/2523

LUIZ FELIPE SANT' ANNA COMMAR

Walking through space-time dynamics of the Southern Amazon's rainy season – deforestation impacts and hydroclimate variability at different scales

Thesis submitted to the Applied Meteorology Graduate Program of the Universidade Federal de Viçosa in partial fulfillment of the requirements for the degree of *Doctor Scientiae*.

APPROVED: March 6, 2025.

Assent:

Luiz Felipe Sant' Anna Commar
Author

Marcos Heil Costa
Adviser

To my parents Diná and Sérgio.

ACKNOWLEDGMENTS

Aos meus pais pelo apoio em todas minhas decisões, conselhos de vida, incentivo em sempre buscar mais. Por ser exemplo de vida e por me levantarem em todas as minhas quedas. Por serem meu eterno porto seguro e por mostrar que muitas vezes o que buscamos tão longe pode ser encontrado o mais perto que imaginamos.

À Lívia, que me deu suporte, amor e incentivo nas horas de dificuldade, e compartilhou de minhas alegrias e conquistas tornando os momentos felizes em memórias inesquecíveis. Muito obrigado por fazer de Viçosa nosso lar e por transformar meus dias nessa jornada tão incrível. Pelas contribuições dadas a este trabalho.

Aos meus avôs, Pedro e Alcides (in memoriam) e avós, Ninita e Cida, que sempre demonstraram suporte e carinho. Também à minha bisavó Diná que um dia disse que eu seria doutor, acredito que ela se referiu à chance de ser médico, ao fim ela estava certa sobre o destino de uma maneira ou de outra.

Ao professor Marcos Heil Costa, pela oportunidade e confiança que me foi dada ao longo do desenvolvimento deste projeto. Por todos os anos de ensinamentos científicos, pelos desafios propostos. Por ser exemplo e inspiração sobre o que é produzir ciência de alta qualidade. Muito Obrigado!

A todos do Grupo de Pesquisa em Iteração Atmosfera-Biosfera e a meus colegas de departamento – Aninha, Pousa, Carlos, Flávia, Verônica, Júlia, Igor, Lucas, Gustavo, Daniel, Gabriel, Emily, Benezoli, Gabriel Peterle, Cláudio, Humberto, Laís – Agradeço muito pela amizade dentro e fora do trabalho. Em especial ao Lucas Louzada, que contribuiu brilhantemente com um dos capítulos deste trabalho, sem seu empenho este estudo não estaria tão completo.

Ao Gabriel, Pousa, Aninha, Flávia por tornar este tempo em Viçosa mais leve, por todas cervejas e conversas divididas. Em especial não poderia deixar de ressaltar meus agradecimentos ao Gabriel, sem qual o desenvolvimento desta tese seria mil vezes mais difícil. Muito obrigado por compartilhar suas simulações comigo, e por nossas conversas cientificas e casuais, sem sua ajuda e sua presença este estudo e estes anos teriam sido mais cinzas.

Aos meus amigos Mateus, Norberto, Tadeu, Yuri, Thiago, Fernando, Gonçalinho, Vitor, Yan que mesmo a distância sempre fizeram parecer que

nunca sai de casa.
Aos meus colegas da S&P Global, por me incentivarem nestes momentos finais e desafiadores desta jornada. A Sana, Chetan, Nuala, Patricia, Tristan e Duncan, por serem exemplos de liderança e companheirismo. E a Parvathi, Eli, Priscila, Débora, Antonio, Jaime, Ida, Oscar, Nolin, John e Austin, pelo apoio e parceria ao longo do caminho.
A todos os professores que fizeram parte desta trajetória pelos conhecimentos compartilhados.
A Graça Freitas por todo auxílio nessa trajetória acadêmica.
A Universidade Federal de Viçosa pela oportunidade de realizar o doutorado e por me acolher nos últimos, e intensos, 7 anos.
Ao Conselho Nacional de Desenvolvimento Científico e Tecnológico (CNPq), pela concessão da bolsa de estudos
This work has been sponsored by the following Brazilian research agencies: Coordination for the Improvement of Higher Education Personnel (CAPES; Financing code 001), Minas Gerais State Foundation for Research Aid (FAPEMIG) and National Council of Scientific and Technological Development (CNPq).

ABSTRACT

COMMAR, Luiz Felipe Sant' Anna, D.Sc., Universidade Federal de Viçosa, March, 2025. **Walking through space-time dynamics of the Southern Amazon's rainy season – deforestation impacts and hydroclimate variability at different scales**. Adviser: Marcos Heil Costa.

Deforestation profoundly impacts cloud dynamics and the hydroclimate system across tropical regions, with cascading effects on the onset and duration of the rainy season. This study integrates observational and simulated data to analyze these effects across different spatial scales: regional (highway BR-163), state (Mato Grosso, MT), and the broader southern Legal Amazon. At the regional scale, deforestation reduces cloud cover at fine spatial resolutions (11–25 km), resulting in shallower, warmer clouds that suppress deep convective cloud formation during the dry-to-wet season transition. At the state level, Mato Grosso's agricultural system, heavily reliant on its long rainy season for double cropping, is increasingly threatened by declining rainfall and delayed rainy season onset. Observational data from the past four decades show a worrying trend of reduced rainfall volumes, delayed onsets, and shorter rainy season durations, trends that may extend into the future as corroborated by Community Earth System Model (CESM) simulations under realistic deforestation scenarios. The rainy season onset is projected to shift to late October delaying in about two weeks, with durations falling below 200 days by mid-century. These changes could severely impact agricultural productivity, necessitating urgent sustainable practices and policy interventions to mitigate economic and ecological losses. Expanding to the southern Legal Amazon, CESM simulations reveal a yet unreported synoptic-scale circulation driven by extensive deforestation (ca. 40%). This anomalous circulation, linked to differences in surface heating, can persist for up to two months and delay the rainy season onset by 30–40 days compared to historical periods for the Legal Amazon. The implications of this persistent phenomenon extend beyond agriculture to include ecosystems and hydropower generation, highlighting the potential irreversibility of these changes under unabated deforestation trends. Together, this multi-scale analysis underscores the interplay of local land cover and large-scale processes in shaping the Amazon's hydroclimate. These findings emphasize the critical need for robust land-use policies, integrated climate modeling, and cross-sectoral strategies to address the widespread impacts of deforestation on atmospheric processes, agriculture, and regional livelihoods.

Keywords: deforestation; climate change; atmospheric modeling; Amazon; nexus food-energy-water

RESUMO

COMMAR, Luiz Felipe Sant' Anna, D.Sc., Universidade Federal de Viçosa, março de 2025. **Explorando as dinâmicas espaço-temporais da estação chuvosa no Sul da Amazônia – impactos do desmatamento e variabilidade hidroclimática em diferentes escalas**. Orientador: Marcos Heil Costa.

O desmatamento impacta profundamente a dinâmica das nuvens ea dinâmica hidroclimática em regiões tropicais, com efeitos em cascata sobre o início e a duração da estação chuvosa. Este estudo utiliza dados observacionais e simulados para analisar esses efeitos em diferentes escalas: regional (BR-163), estadual (Mato Grosso, MT) e mais amplamente no sul da Amazônia Legal. Na escala regional, o desmatamento reduz a cobertura de nuvens em resoluções espaciais finas (11–25 km), resultando em nuvens mais baixas e quentes que suprimem a formação de nuvens convectivas profundas durante a transição da estação seca para a estação chuvosa. Na escala estadual, o sistema agrícola de Mato Grosso, altamente dependente de sua longa estação chuvosa para a prática da segunda safra, está cada vez mais ameaçado pela redução do volume de chuvas e pelo atraso no início da estação chuvosa. Observações das últimas quatro décadas mostram uma tendência preocupante de redução nos volumes de chuva, atrasos nos inícios e diminuição na duração da estação chuvosa, tendências corroboradas por simulações do Community Earth System Model (CESM) sob cenários realistas de desmatamento. Nossas projeções apresentam atrasos no início da estação para o final de outubro, com durações abaixo de 200 dias em 2050. Essas mudanças podem impactar gravemente a produtividade agrícola, exigindo práticas sustentáveis urgentes e intervenções políticas para mitigar os potenciais perdas econômicas e ecológicas. Expandindo para o sul da Amazônia Legal, dados simulados revelam uma circulação em escala sinótica ainda não relatada, impulsionada por desmatamento extensivo (cerca de 40%). Essa circulação anômala, associada a diferenças no aquecimento da superfície, pode persistir por até dois meses e atrasar o início da estação chuvosa em 30–40 dias em comparação com os períodos históricos. As implicações desse fenômeno persistente vão além da agricultura, incluindo ecossistemas e geração de energia hidrelétrica, destacando a potencial irreversibilidade dessas mudanças sob tendências contínuas de desmatamento. Juntas, essas análises em diferentes escalas destacam a interação entre a cobertura do solo e os processos em larga escala na configuração hidroclimática da Amazônia. Os resultados enfatizam a necessidade de políticas robustas territoriais, modelagem climática integrada e estratégias intersetoriais para abordar

os impactos generalizados do desmatamento nos processos atmosféricos, na agricultura e nos meios de subsistência regionais.

Palavras-chave: desmatamento; mudanças climáticas; modelagem atmosférica; estação chuvosa; Amazônia; dinâmica de nuvens; nexus food-energy-water

LIST OF ILLUSTRATIONS

CHAPTER 1

CHAPTER 3

LIST OF TABLES

CHAPTER 3

SUMMARY

General Introduction

The Amazon's hydroclimate is associated and modulated with large-scale mechanisms, including the Intertropical Convergence Zone, the South American Monsoon system, and the South Atlantic Convergence Zone. These systems drive the seasonal rainfall patterns across Amazonia, with the most precipitation occurring during the austral summer (Wright *et al.*, 2017; Mu and Jones, 2022; Talamoni *et al.*, 2022). Another large-scale process is the influence of interannual variability by the El Niño-Southern Oscillation (ENSO), which has increasingly contributed to extreme droughts and delayed rainy season onsets in the Amazon (Cai *et al.*, 2020; Marengo *et al.*, 2021b; Espinoza *et al.*, 2022).

While the northern Amazon remains humid throughout the year, the Southern Amazon (SA) exhibits a pronounced seasonal climate, where the timing and duration of the rainy season are critical for both natural ecosystems and agricultural activities. The onset of the rainy season in SA generally follows a northwest-southeast pattern influenced by regional convection driven by heterogeneous solar heating, which is the main driver of the convective energy, and those large-scale circulation mechanisms (Yin *et al.*, 2014; Wright *et al.*, 2017; Rodrigues *et al.*, 2021; Talamoni *et al.*, 2022). However, in recent decades the rainy season onset has been delayed, a trend attributed to regional deforestation and the variability of those large-scale atmospheric circulation changes (Fu *et al.*, 2013; Leite-Filho *et al.*, 2020; Staal *et al.*, 2020; Bochow and Boers, 2023).

Deforestation in the Amazon disrupts the surface energy balance, evapotranspiration, and atmospheric moisture recycling, resulting in reduced rainfall and delayed rainy seasons (Stickler *et al.*, 2013; Lawrence and Vandecar, 2015; Staal *et al.*, 2020; Mu and Jones, 2022). Deforestation patterns are now more fragmented, creating localized thermal circulations, leading to small and mesoscale feedback, including anomalous subsidence and diminished rainfall upwind of cleared areas (Saad *et al.*, 2010; Lawrence and Vandecar, 2015; Fassoni-Andrade *et al.*, 2021).

These small to mesoscale hydroclimatic changes become evident along critical deforestation frontiers such as the highway BR-163 corridor. As roads supply infrastructure to previously remote regions, they facilitate land use change, i.e., conversion of forests to pasture and agricultural lands (Wang *et al.*, 2009; Li *et al.*, 2019; Ferrante *et al.*, 2021). This process increases surface albedo, reduces surface roughness, and decreases evapotranspiration, thereby

altering the regional energy balance (Wang *et al.*, 2009; Khanna *et al.*, 2017; Wright *et al.*, 2017). The disturbance in regional energy directly impacts the convective energy, a critical factor for cloud formation (Wang *et al.*, 2009; Luo *et al.*, 2024). In deforested areas, shallow clouds prevail over deep convective clouds (Duveiller *et al.*, 2021; Funatsu *et al.*, 2021; Xu *et al.*, 2022a).

Similarly, early modeling studies suggested that large-scale deforestation clearing the Amazon would reduce precipitation by increasing surface albedo, disrupting monsoon circulation, and altering the rainy season (Shukla *et al.*, 1990; Eltahir and Bras, 1996; Costa and Foley, 2000; Sampaio *et al.*, 2007). Analyses of intermediate-scale deforestation also have associated deforestation with rainfall decrease (Costa *et al.*, 2007; Sampaio *et al.*, 2007; Pires and Costa, 2013). However, the coarse-resolution models used in these analyses might not have correctly represented the mesoscale and the large-scale circulation processes. (Vc nao vai comentar nada nos estudos que fazem uma combinacao de desmatamento e aumento de CO2)?

Properly resolving these hydroclimatic scales is crucial for the region since the rainy season significantly affects agriculture in the SA. In this region, some states, such as Mato Grosso (MT), are particularly vulnerable due to their high economic dependence on rainfed agriculture. Over the past three decades, MT has emerged as one of Brazil's largest agricultural producers, driven by double-cropping systems like soy-maize and soy-cotton rotations (Arvor *et al.*, 2014; Abrahão and Costa, 2018). However, the delayed onset and shortened duration of the rainy season, largely attributed to deforestation and climate variability, present significant risks to these rainfed systems, threatening crop yields and economic stability. In addition to agriculture, the SA economy is deeply intertwined with ecosystem services and planned infrastructure projects, such as the expansion of hydropower plants on the Tapajós and Xingu river basins (Strand *et al.*, 2018; Couto *et al.*, 2021). The compounded effects of deforestation, climate variability, and infrastructure development could thus undermine both economic and environmental sustainability in the region.

The challenges of deforestation and climate change in agriculture, ecosystem services, and hydropower in the Southern Amazon highlight the need for realistic land-use scenarios. CMIP5's RCP8.5 projects 20% of Amazon deforestation by 2050 (Pires *et al.*, 2016), a level already reached by 2020 (Souza *et al.*, 2020), indicating more rapid forest losses. To address this, I used two realistic deforestation pathways from environmental policy scenarios (Rochedo *et al.*, 2018): one emphasizing strong conservation and another projecting weak environmental governance, reaching ~40% by 2050. These pathways, modeled at fine spatial resolution, better

capture the hydroclimatic impacts of deforestation, bridging global projections and local vulnerabilities. This approach supports policies that balance economic growth with ecological sustainability, safeguarding critical ecosystem services and reducing risks to agriculture and hydropower.

In this context, this thesis investigates the impacts of deforestation on the hydroclimatic variability in the southern Amazon, focusing on the intricate linkages between land-use change, atmospheric processes, and seasonal rainfall dynamics. Chapter 1 explores the effects of deforestation on cloud dynamics and the onset of the rainy season along the BR–163 corridor. In Chapters 2 and 3, I used a fully coupled climate model forced by realistic deforestation scenarios. More specifically, Chapter 2 addresses the implications of delayed rainy season onset and reduced rainfall in agriculture in Mato Grosso through trends in rainfall patterns and rainy season characteristics using climate modeling forced by realistic deforestation scenarios. Chapter 3 evaluates the broader impacts of deforestation on the Amazon's hydroclimate using fine-resolution climate models by simulating weak and strong environmental governance scenarios under Different climate change scenarios.

Chapter 1: Head in the clouds and feet on the ground: the effects of deforestation on clouds and rainy season onset

Abstract

The dynamics of the Amazon's rainy season are governed by complex atmospheric interactions. Over recent decades, variability in the region’s climatic drivers and increasing deforestation have disrupted rainfall patterns, altering the onset of the rainy season and cloud dynamics processes. However, the interplay between cloud dynamics and the characteristic of the rainy season remains overlooked. Here, I explore the relationship between deforestation, cloud dynamics, and rainy season onset in the Amazon across varying spatial scales and land cover types. My findings show that deforestation reduces cloud cover at fine scales (11–25 km) and promotes shallower, warmer clouds, inhibiting deep convective cloud formation. This persistent effect lasts nearly two months during the dry-to-wet season transition. Deforestation in tropical regions alters cloud dynamics and delays the onset of the rainy season by disrupting regional energy and moisture availability. This study emphasizes the need to consider both land-use changes and large-scale climatic mechanisms' impacts on cloud dynamics in future climate modeling and policy decisions.

1.1. Introduction

The Amazon hydroclimate is driven by complex interactions between atmospheric circulation and surface energy fluxes (Yin *et al.*, 2014; Wright *et al.*, 2017; Mu and Jones, 2022). While a wet climate prevails near the equator, regions beyond 5°S exhibit significant seasonality in precipitation patterns. Convective processes play a critical role in rainfall occurrence (Wang *et al.*, 2009; Wright *et al.*, 2017; Duveiller *et al.*, 2021; Xu *et al.*, 2022a; Abera *et al.*, 2024). The seasonal variability of the Sun heating energy is the main driver of convective energy seasonal availability. The rainy season onset typically follows a northwest-southeast pattern (Figure 1. 1c) related to the availability of convective energy and large-scale circulation mechanisms (Rodrigues *et al.*, 2021; Talamoni *et al.*, 2022). Still, especially during the dry-to-wet season transition, this large-scale driver may be delayed or disrupted by disturbances in the local energy balance, such as those induced by deforestation (Leite-Filho *et al.*, 2020).

Deforestation in the Amazon is often associated with expanding infrastructure, such as the BR-163 highway (Figure 1. 1a–b). As roads provide access to previously remote areas, they facilitate land use change, particularly converting forests to pasture and agricultural lands (Wang *et al.*, 2009; Li *et al.*, 2019; Ferrante *et al.*, 2021). These changes in land cover increase surface albedo, reduce surface roughness, and decrease evapotranspiration, thereby altering the regional energy balance (Wang *et al.*, 2009; Khanna *et al.*, 2017; Wright *et al.*, 2017; Leite-Filho *et al.*, 2020).

The disturbance in regional energy directly impacts the convective energy, a critical factor for cloud formation (Wang *et al.*, 2009; Luo *et al.*, 2024). As deforestation expands, surface properties change, increasing surface temperature and reducing cloud top heights (CH) and cloud fraction (CF) in deforested regions at sub-daily, monthly, and yearly scales (Wang *et al.*, 2009; Teuling *et al.*, 2017; Xu *et al.*, 2022a; Abera *et al.*, 2024; Leung *et al.*, 2024). In these regions, shallow clouds prevail over deep convective clouds, essential for rainfall (Duveiller *et al.*, 2021; Funatsu *et al.*, 2021; Xu *et al.*, 2022a).

In this study, I investigate the impact of deforestation, particularly along the BR-163 corridor, on cloud dynamics and the onset of the rainy season in the Amazon. Specifically, I analyze anomalies in cloud top height, fraction, and top temperature across regions with varying land cover types, deforestation levels, and spatial scales. Additionally, I assess how the cloud variable correlates with the onset of the rainy season. By comparing these regions, I aim to

elucidate the effects of deforestation on atmospheric processes and their role in altering local hydroclimatic patterns.

1.2. Methods

1.2.1. Study region

The study focuses on two primary regions along the BR-163 highway within the Brazilian Legal Amazon. Over the last decades, road expansion in the Amazon has driven deforestation (Commar *et al.*, 2023a), although early impacts were moderated by the challenging conditions of unpaved, often impassable roads. However, the recent paving of BR-163 has significantly increased accessibility to these areas, prompting extensive land occupation for agricultural expansion and accelerating deforestation rates (Soares-Filho *et al.*, 2004).

The two regions exhibit distinct land use and cover dynamics. Case 1 presents a relatively homogeneous forest cover, which transitions mostly to pasture, reflecting a concentrated pattern of land use change (Figure 1. 1). In contrast, Case 2 presents a more heterogeneous landscape, combining forest and savanna ecosystems with pasture and agricultural land transitions, showing a more complex land use pattern (Figure 1.1).

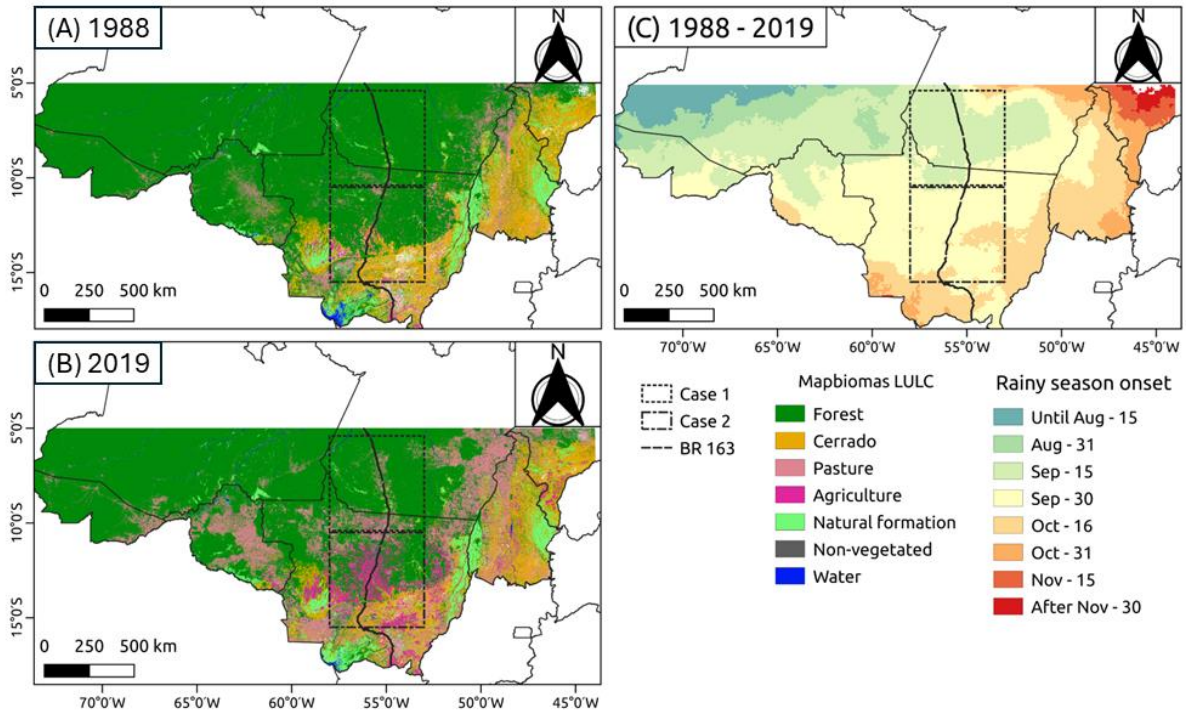

Figure 1.1 – Land use and land cover (LULC) dynamics and rainy season onset within the study area in the southern part of Brazil's Legal Amazon. (A) LULC for 1988. (B) LULC for 2019. (C) Average rainy season onset for 1988-2019. Case 1 (upper square box) and Case 2

(lower square box) highlight two focus areas with distinct LULC characteristics. The dashed line represents the BR-163 highway.

1.2.2. Land use and land cover data

For land use and land cover (LULC) data, I utilized MapBiomas Collection 7, which provides annual classifications for Brazil derived from semi-automatic classification approaches applied to Landsat satellite data (Souza *et al.*, 2020). I utilized the period from 1988 to 2019, including detailed classifications for multiple land use categories, such as forest, agriculture, pasture, and savanna, with a horizontal resolution of 30 m. I aggregated this dataset into a lower resolution to match the other datasets through area fractions.

1.2.3. Rainy season onset

1.2.3.1. Rainfall data

I used daily precipitation from two databases, from 1988 to 2019, to define the rainy seasons for the study region. First, the Brazilian daily weather gridded data (referred to as 'Xavier' (Xavier *et al.*, 2022) with a spatial resolution of 0.1° × 0.1° (~11 km). This dataset is derived from the spatialization of observational data from rainfall gauges and meteorological stations allocated across the country. The second, the Climate Hazards Group Infrared Precipitation with Stations (CHIRPS) dataset, with a spatial resolution of 0.05° × 0.05° (~5.5 km), combines satellite cold cloud durations and rain gauge data (Funk *et al.*, 2015). These observed datasets have been used in several Amazon studies and demonstrated high accuracy in seasonal and daily rainfall representation.

1.2.3.2. Onset definition

In climatological studies, the onset of the rainy season is defined using long-term statistical average rainfall as the threshold for the region, offering a generalized understanding of seasonal patterns across broad spatial and temporal scales (Arvor *et al.*, 2014, Liebmann, *et al.*, 2007). In contrast, for applied studies—particularly those focused on agricultural systems—an applied approach better captures the dynamics relevant to crop planning and land management. In this context, I adopted a modified version of the anomalous accumulation (AA) method, as proposed by Arvor *et al.* (2014), which identifies the onset of the rainy season as the day following the start of the longest period during which anomalous accumulation remains positive, relative to a crop, i. e., the period when rainfall consistently exceeds the crop water need, signaling effective water availability for agricultural use.

Unlike climatological definitions, that emphasize historical averages and interannual variability, this agriculturally oriented method prioritizes functional rainfall thresholds relevant

to planting and productivity. While the two definitions serve different purposes, their divergence highlights the importance of methodological alignment with the study's specific goals.

I used the modified anomalous accumulation (AA) method to define the onset of the rainy season (Arvor *et al.*, 2014). This method associates a daily rainfall (R_n) and a reference value (R_{ref}) (Equation 1) and has proven helpful in studies across Brazil, utilizing both observed and modeled data (Abrahão and Costa, 2018; Commar *et al.*, 2023a, 2024). The accumulation starts on 1 July, aligning with the dry season midpoint of the region.

$$AA_t = \sum_n^t R_n - R_{ref} \quad (1)$$

where AA_t is anomalous accumulation at day *t*, R_n is daily rainfall (mm d^{-1}) on day *n*, and R_{ref} is the reference value. Intending an agricultural perspective, I used a reference value of 2.5 mm d^{-1}, which is the precipitation requirement for soybean seedlings (Abrahão and Costa, 2018).

1.2.4. Satellite cloud data

The dataset employed in this study is the PATMOS-x AVHRR + HIRS cloud Climate Data Record (CDR) version 6.0 (PATMOS-x), provided as a level-2b product on a 0.1° × 0.1° (~10 km) horizontal resolution (Foster *et al.*, 2023). This product is generated by using inter-calibrated radiance data from the Advanced Very High-Resolution Radiometer (AVHRR) global area coverage sensor, which is collocated with High-Resolution Infrared Radiation Sounder (HIRS) measurements on compatible NOAA POES and EUMETSAT/MetOp satellite platforms (Heidinger *et al.*, 2014; Foster *et al.*, 2023). Additionally, the AVHRR + HIRS radiances have been cross-calibrated with radiance data from NASA's Moderate Resolution Imaging Spectroradiometer (MODIS) sensor to ensure continuity and accuracy across different sensor types (Cao *et al.*, 2008: 200; Zhao *et al.*, 2024).

The analysis incorporates four cloud-related variables derived from the ascending orbits of the PATMOS-x dataset. These orbits cross the equator during the afternoon, which corresponds to the period of highest incoming solar energy in the study region—making them particularly relevant for capturing cloud dynamics under peak atmospheric activity. (i) cloud optical depth (CD), (ii) cloud cover fraction (CF), (iii) cloud top height (CH), and (iv) cloud top temperature (CT). My study focuses on identifying both potential deep convective clouds (DCCs) and non-deep convective clouds (N-DCCs) within the region of interest, limiting data usage to the period from 1988 onward to align with the land-use and land-cover (LULC) dataset.

The 1988–2019 PATMOS-x daily records were further processed into 5–day and 15–day composites spanning August through November yearly to capture the seasonal dynamics within the Amazon's rainy season.

Following criteria from previous studies for continental and oceanic regions(Yuan and Li, 2010; Yuan *et al.*, 2010; Zhao *et al.*, 2024), I identified DCCs using three specific conditions: CT < 245 K, CH > 6 km, and CD > 23. These thresholds exclude unknown cloud types, dust, smoke, and fire.

1.2.5. Spatial scale assessment

To explore the impact of forest loss across scales, I analyzed the impacts of deforestation on concurrent rainy season and cloud dynamics at a series of horizontal resolutions ranging from ~11 km to 111 km (0.1°, 0.25°, 0.5°, and 1.0°) by creating correlations with the LULC data derived from the MapBiomas and the hydroclimate variables.

1.2.6. Assessment of annual cloud anomalies composites

I calculated annual standard anomalies for cloud variables (DCC and N-DCC) across deforestation intervals, extracting Pearson correlation coefficients and p-values from linear regressions. These anomalies reveal how seasonal variability in cloud variables correlates with increasing deforestation percentages in each study region. Additionally, I correlated cloud variables and onset anomalies by applying the same analysis to rainy season onset anomalies. This approach provides insights into how changes in cloud properties relate to variations in the timing of the rainy season.

1.3. Results

Delayed onsets correlate well with deforestation percentages for different horizontal resolutions smaller than 0.5° (Figure 1.2). Both study regions demonstrated a good fit with at least one rainfall product, but the Xavier stood out for Case 2, where the land cover is more heterogeneous (Figure 1.2e–g).

In Case 2, I noticed negative anomalies up to 25% of deforestation in higher resolutions (Figure 1.2a–b) for Xavier´s dataset. These negative values cease to exist above 25% of deforestation. Also, the persistency of negative anomalies in the CHIRPS extends to the 50% deforestation level (Figure 1.2a–c). For Case 2, negative anomalies were restricted to 15% of deforestation, considering the Xavier´s dataset (Figure 1.2e–g). At higher deforestation levels, the onsets demonstrated a higher anomalie values. The CHIRPS product demonstrated no tendency with constant values and no significative results (Figure 1.2e–h).

I observed higher positive anomalies above 50% of deforestation in the areas. However, the increase in deforestation percentages always leads to increased anomalies, indicating a linear delay of the onset of the rainy season as deforestation expands. Furthermore, aggregating the variables to larger scales increases the variability of the anomalies to the point where the correlation disappears at a 1.0° scale (~111 km).

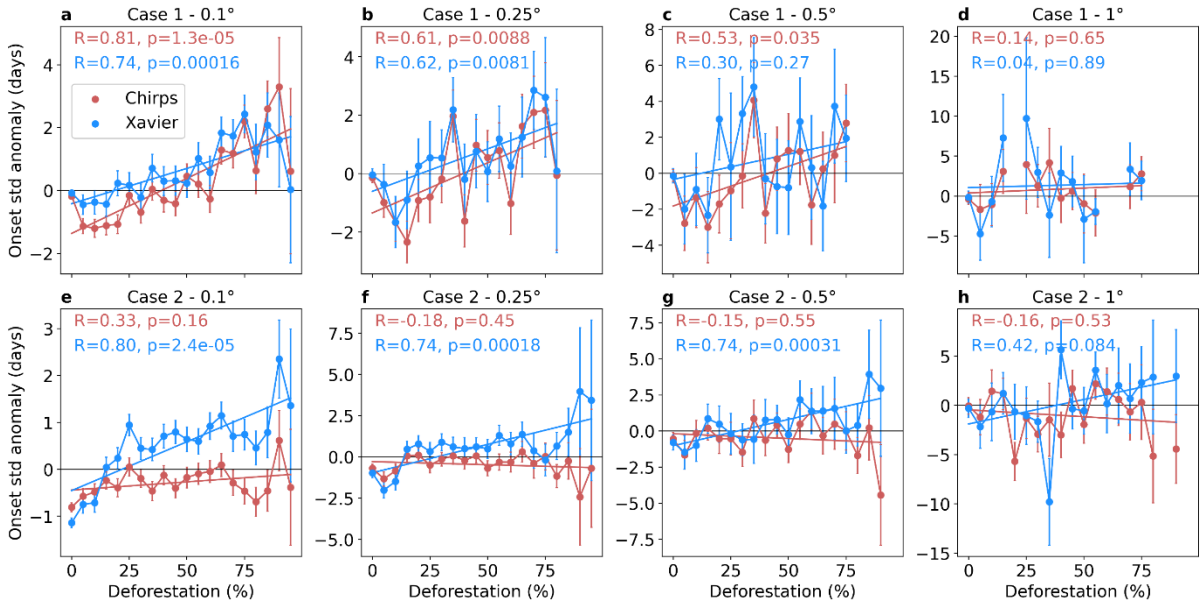

Figure 1.2 – Relationship between mean annual rainy season onset anomalies and deforestation percentages at various horizontal resolutions for two rainfall products, CHIRPS (in red) and Xavier (in blue) for Case 1 (a–d) and Case 2 (e–h). Each plot displays Pearson correlation coefficients from linear regression analyses and p-values indicating statistical significance. Error bars represent the standard error of the mean onset anomaly within each deforestation interval.

The correlation between cloud variable anomalies and deforestation levels demonstrates mixed patterns across horizontal resolutions, cases, and cloud types. Until the end of October, the correlations show how the cloud variables interplay with the onset, but after this date, most of the grid cells reached the onset (Figure 1.1c).

At finer scales, particularly for 0.1° and 0.25°, there are significant correlations (hatched shading) between 15-day composites of cloud fraction (CF), cloud top temperature (CT), and cloud height (CH) anomalies with deforestation (Figure 1.3). Larger spatial scales (0.5°–1.0°) often fail to capture significant patterns, particularly for non-deep convective clouds (N-DCC). This behavior is similar to the 5–day composite (Supplementary Figure 1.1).

Cloud fraction (CF) typically exhibits significant positive correlations with deforestation levels for N-DCC and negative significant correlations with the deep convective clouds (DCCs) at the microscale (0.1° resolution) (Figure 1.3 and Supplementary Figure 1.1).

This physically consistent result indicates that the advance of deforestation leads to fewer deep convective clouds and more shallow clouds, especially before October. In Case 1, correlations are not significant after October. CF typically does not correlate significantly with deforestation at larger scales, indicating a phenomenon predominantly microscale driven.

Cloud top temperature (CT) generally shows consistent positive correlations with increasing deforestation levels in both cases and cloud types, indicating higher CT occurs within more deforested areas (Figure 1.3). These remain significant across multiple resolutions and time composites (Figure 1.3 and Supplementary Figure 1.1). However, I noted that Case 2 showed higher correlations with more significative values for CT (Figure 1.3i–p and Supplementary Figure 1.1i–p), indicating higher dependence of CT on land cover for Case 2, with higher latitudes and less incoming solar radiation for the same period of the year when compared to Case 1. This suggests a higher dependence on lower albedos to provide energy for convection in Case 2. Cloud top height (CH) anomalies are the opposite of the CT, with significant negative correlations for the regions and cloud types (Figure 1.3), demonstrating that both cloud types (DCCs and N-DCCs) become shallower as deforestation advances.

I observed that Case 1 and Case 2 exhibit similar responses to deforestation. However, Case 2 displays stronger correlations independent of the cloud types (Figure 1.3 and S1). Additionally, DCC displays stronger correlations across all variables when compared to N-DCC clouds, especially in Case 1 (Figure 1.3). N-DCC correlations are slightly weaker but it is also statistical significant.

Overall, deforestation reveals strong interactions with cloud dynamics, with higher correlations at finer resolutions. The distinct behavior of cloud cover between cloud types indicates that deforestation favors shallow clouds, and forested regions favor deep convective clouds, colder cloud top temperatures.

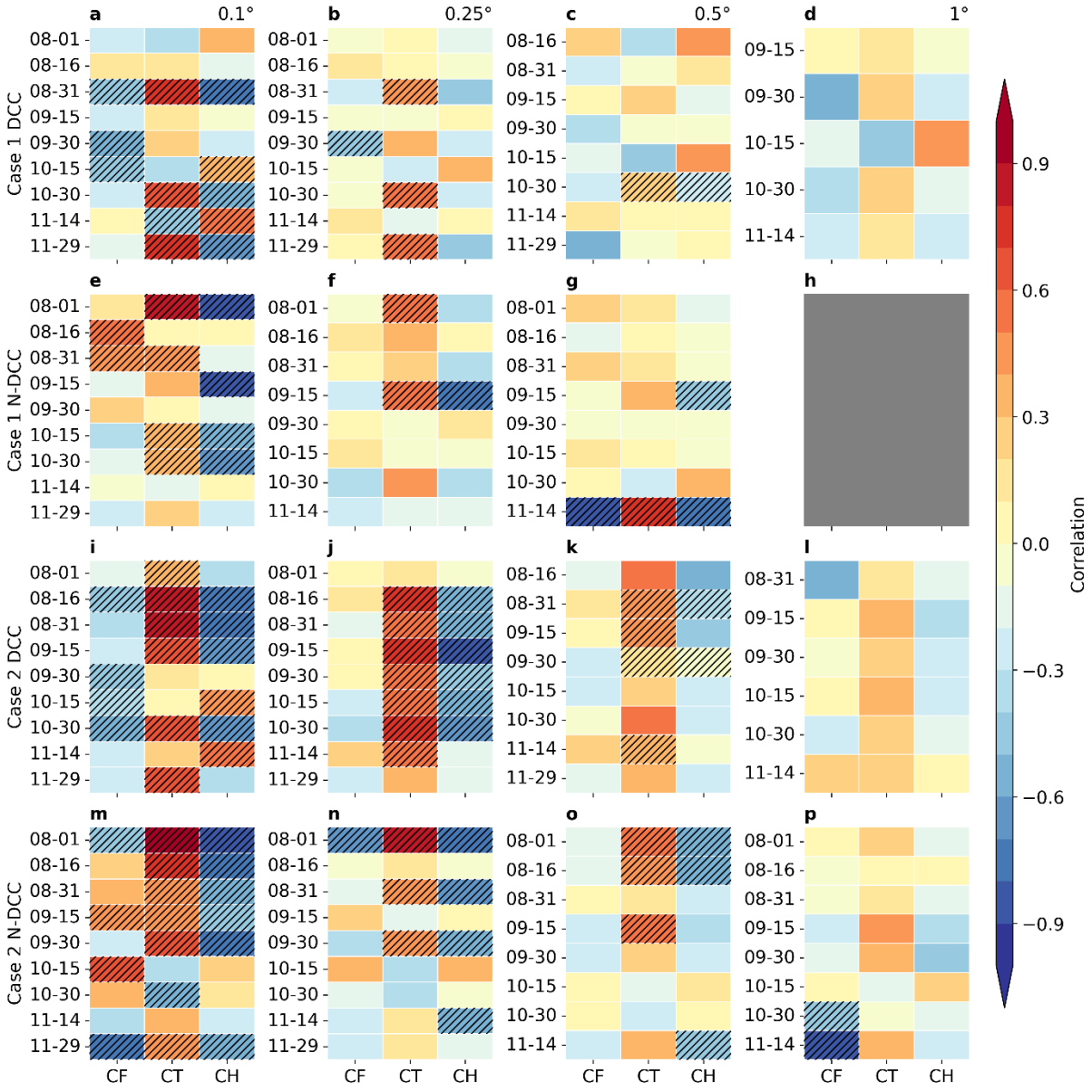

Figure 1.3 – Assessment of the correlation between cloud fraction (CF), cloud top temperature (CT), and cloud height (CH) standardized anomalies with deforestation levels for 15-day composites. The results are grouped by Case 1 DCC clouds (a–d), N-DCC clouds (e–h), Case 2 DCC clouds (i–l), and N-DCC clouds (m–p). Each column represents different horizontal resolutions –0.1°, 0.25°, 0.5°, and 1°. Positive values indicate that the standardized anomalies positively correlate with increasing deforestation. Shaded areas indicate results significant at $\alpha = 0.1$. Grey boxes indicate there is not enough data to calculate the correlation.

Strong positive correlations exist between CT and the rainy season onset (Figure 1.4). This figure results connect the results of Figure 1.2 and Figure 1.3, indicating that higher CT contributes to a delayed onset of the rainy season. Moreover, the correlation exhibits a temporal persistence, with positive correlations extending from early August to late October (Figure 1.4 and Supplementary Figure 1.2), particularly at smaller spatial scales. This suggests a potential

lagged response or cumulative effect of the LULC on the region's cloud dynamics and rain production mechanisms. The proposed mechanism here is that, as time progresses from August to November, surface energy for convection increases, forming deeper and colder clouds that are more likely to produce higher amounts of rainfall and define the onset of the rainy season.

Similar to Figure 1. 3, Case 2 showed higher correlations than Case 1. This indicates that the surface energy balance mechanism (more energy available in lower albedo rainforest areas) connects to the early onset of the rainy season through deep convective cold clouds. However, despite this relationship, the process also depends on the availability of regional moisture, which is essential for the rainfall formation and occurence.Conversely, cloud top height (CH) anomalies negatively correlate with rainy season onset anomalies (Figure S1.3–S1.4). This implies that clouds tend to become shallower in areas with increasing deforestation, contributing to delays in the rainy season onset. Notably, the persistent effects of CH anomalies mirror those observed for CT correlations, extending their influence over time (Figure S1.3–S1.4). Additionally, N-DCCs showed more significant correlations than DCCs, suggesting that the prevalence of shallower clouds poses a substantial challenge to the onset of the rainy season. This effect is particularly evident before October (Figure S1.3–S1.4), coinciding with the period leading up to the average rainy season onset dates in these regions (Figure 1.1c).

The relationship between cloud fraction (CF) and rainy season onset reveals distinct spatial and temporal patterns depending on cloud type (Figure S1.5–S1.6). For DCCs, significant negative correlations are predominant during the early months of August and September, indicating that lower CF values are associated with rainy season onset delays in highly deforested areas (Figure S1.5–S1.6). Conversely, for N-DCCs, positive correlations are observed, particularly under 5–day composites and at coarser resolutions during the same period. This suggests that deforested regions experience an increase in N-DCCs, contributing to delayed rainy season onset. These findings highlight the roles of contrasting cloud types in mediating the atmospheric response to land-use changes. The time-related change in correlation implies that N-DCCs become DCCs as the onset date approaches. This dipole behavior between cloud types is more pronounced in Case 1.

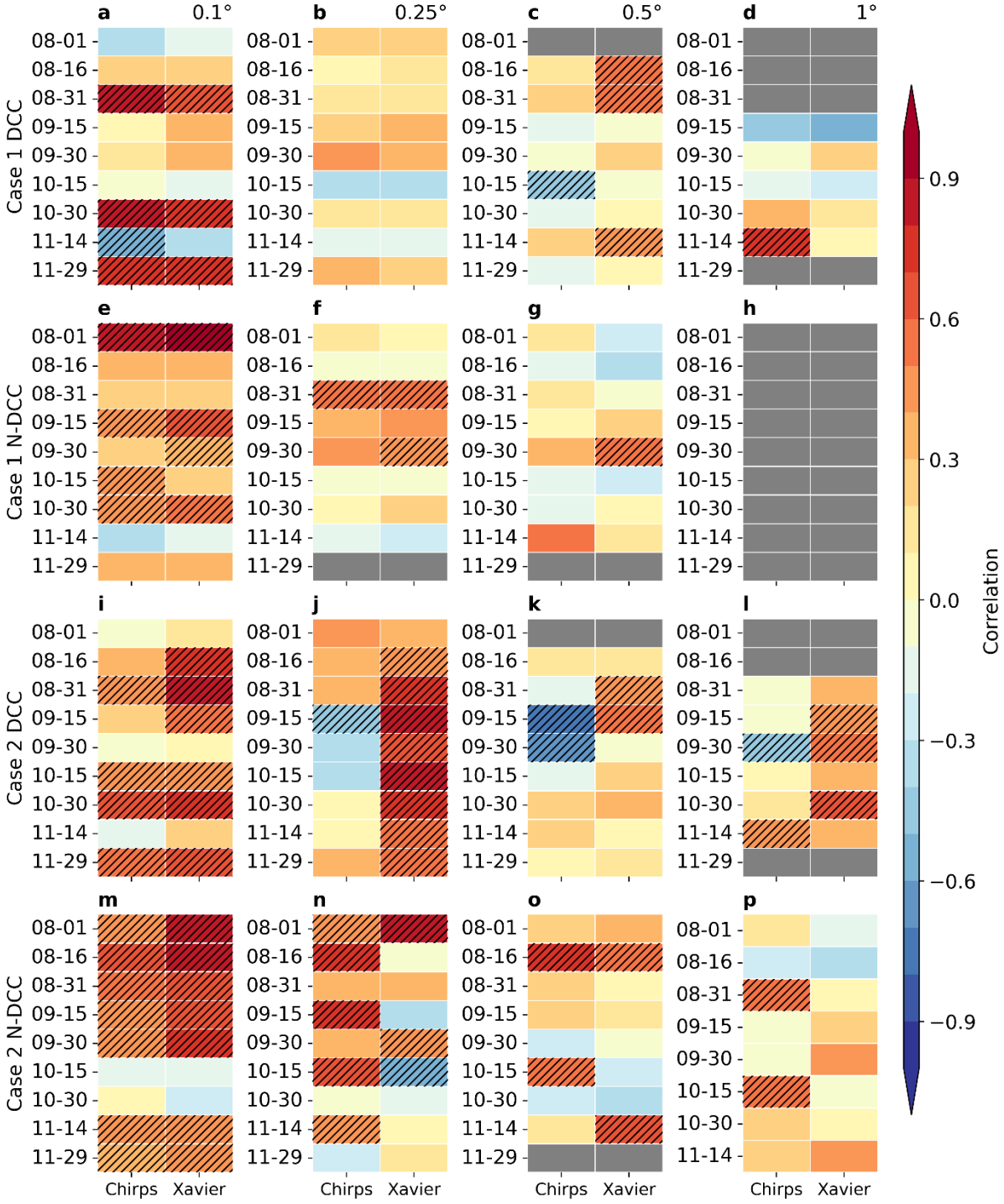

Figure 1.4 – Assessment of the correlation between cloud top temperature (CT) with rainy season onset anomalies for 15–day composites. The results are grouped by Case 1 DCC clouds (a–d), N-DCC clouds (e–h), Case 2 DCC clouds (i–l), and N-DCC clouds (m–p). Each column represents different horizontal resolutions – 0.1°, 0.25°, 0.5°, and 1°. Positive values indicate that the higher cloud temperatures (lower cloud top heights) are positively correlated with the

delay in the onset of the rainy season. Shaded areas indicate significant results at α = 0.1. Grey boxes indicate there is not enough data to calculate the correlation.

1.4. Discussion

The paving of the BR-163 highway has been an essential driver of increased deforestation in the Amazon (Figure 1.1), where much of the LULC changes from pristine tropical vegetation (forests) to pasture, and agricultural land occurs alongside the road. This pattern resembles the impacts along other major highways, such as the BR-230 (Trans Amazon), BR-364 (Cuiabá-Porto Velho), and the recently expanded BR-319 (Porto Velho-Manaus), all of which have facilitated access to previously remote forested regions, accelerating deforestation rates (Wang *et al.*, 2009; Khanna *et al.*, 2017; Li *et al.*, 2019; Ferrante *et al.*, 2021). The resulting land-cover changes disrupt the regional energy balance, as deforested areas exhibit reduced surface roughness, altered albedo, and diminished evapotranspiration (Lawrence and Vandecar, 2015; Khanna *et al.*, 2017). At smaller scales (0.1°–0.25°, 11–28km), these effects directly impact the precipitation, thus influencing the onset of the rainy season.

Previous studies investigating the relationship between deforestation and precipitation at different spatial resolutions from 0.25° to 2° have often reported that rainfall declines with increased deforestation, although small deforestation is sometimes associated with increased precipitation (Leite-Filho *et al.*, 2021; Smith *et al.*, 2023). Furthermore, research has shown that increasing deforestation leads to delayed rainy season onset (Butt *et al.*, 2011; Leite-Filho *et al.*, 2020), a finding consistent with my results (Figure 1.2). A main new result of this study is that, while previous research highlights stronger deforestation-precipitation responses at coarser resolutions (Leite-Filho *et al.*, 2021; Smith *et al.*, 2023), my results reveal a stronger signal at finer scales (0.1°–0.25°) for both onset and cloud variable anomalies. This discrepancy highlights the importance of using higher-resolution datasets to capture the localized interactions between deforestation and rain-producing atmospheric processes.

Differences between CHIRPS and Xavier´s datasets highlight challenges in precipitation estimation for deforested regions. CHIRPS, reliant on cloud-top temperature (CT), may underestimate precipitation where deforestation reduces deep convective clouds. Changes in LULC lead to altered surface heat fluxes, reducing moisture uplift, which is critical for cloud development (Luo *et al.*, 2024). While CHIRPS performs well in capturing extreme events with intense DCCs (Funatsu *et al.*, 2021), the accuracy might diminish over deforested areas with reduced cloud cover and higher CT, which could reduce the correlation magnitude and significance in my analyses. Similarly, the reliance on observational datasets—such as those

used in Xavier's study, which are predominantly located in urban or deforested areas, introduces a potential source of uncertainty, especially in regions with sparse gauge coverage.

The strong positive correlations observed between CT anomalies and rainy season onset align with previous research linking deforestation to higher temperatures, altered atmospheric energy, and circulation (Wang *et al.*, 2009; Khanna *et al.*, 2017; Abera *et al.*, 2024; Luo *et al.*, 2024). My findings suggest that increased CT in deforested areas derives from atmospheric thermal stabilization, and delays the onset of the rainy season.

Similarly, the negative correlations between CH anomalies and onset anomalies indicate that deforestation promotes the development of shallower clouds. This reduction in vertical cloud development reflects weakened convective activity derived from deforestation (Wang *et al.*, 2009; Duveiller *et al.*, 2021; Leung *et al.*, 2024), further contributing to the delayed rainy season onset. The more significant correlations observed for N-DCCs compared to DCCs highlight the sensitivity of shallower clouds to LULC changes and their role as indicators of atmospheric disturbance driven by deforestation.

For DCCs, lower CF values were associated with delayed rainy season onset, corroborating previous findings of reduced convective activity and cloud cover in deforested areas (Teuling *et al.*, 2017; Leung *et al.*, 2024; Luo *et al.*, 2024). In contrast, N-DCCs showed positive correlations, particularly at coarser resolutions and during the late dry season–August, indicating a shift toward shallower, less convective cloud types in response to deforestation. This effect of increased shallower clouds might be associated with mesoscale circulations, reduced convective energy, and increased albedo driven by deforestation (Wang *et al.*, 2009; Teuling *et al.*, 2017; Luo *et al.*, 2024).

However, significant correlations for N-DCCs were negative, especially in September and October (Supplementary Figure 1.5e-f, m-n), indicating a cloud cover reduction. Similar assessments observed this behavior over African and Asian tropical forests and temperate forests on monthly and yearly scales (Teuling *et al.*, 2017; Duveiller *et al.*, 2021; Xu *et al.*, 2022a; Abera *et al.*, 2024), although the 5–day to 15–day composites allow for a better understanding of the dynamics of this process during the dry-to-wet transition period.

Recent studies have connected CF reduction with the reduction of moisture and latent heat, alongside increases in sensible heat (Xu *et al.*, 2022a; Luo *et al.*, 2024). These changes in heat fluxes can be coupled with shifts in the regional energy balance mentioned earlier, where deforestation has a critical role, e.g., increasing surface albedo and altering the distribution of

surface energy and wind patterns (Khanna *et al.*, 2017; Maeda *et al.*, 2021; Mu and Jones, 2022). Simultaneously, deforestation reduces local evapotranspiration, a crucial moisture source for the rainy season (Wright *et al.*, 2017; Versieux and Costa, 2024). Therefore, my results underscore the intricate relationship between energy balance and moisture availability, emphasizing how these factors influence atmospheric dynamics, reduce cloud fractions and height, and increase temperature in DCCs and N-DCCs. Moreover, how the continuous temporal dynamics of this process are critical, underscoring the complexity involved in biosphere-atmosphere interactions (Teuling *et al.*, 2017).

The differences between Case 1 and Case 2 highlight the complexity of deforestation's impact on the rainy season onset, shaped by hydroclimatic and land-use factors. The southern Amazon relates to large-scale climate mechanisms and the energy balance in the regions that promote convection (Leite-Filho *et al.*, 2020; Espinoza *et al.*, 2022; Commar *et al.*, 2023a). These features generate convective energy and an onset with a northwest-southeast progression (Figure 1.1c) (Rodrigues *et al.*, 2021; Talamoni *et al.*, 2022). Thus, Case 2, located at a higher latitude, has a later onset and increased correlation values later in my timeline compared to Case 1.

Unlike Case 1, where deforestation primarily involves converting dense pristine forests to agricultural land, with major changes in albedo and energy balance components, the transition from Cerrado to agriculture in Case 2 sets a less dramatic shift in energy balance and evapotranspiration (Caballero *et al.*, 2022a). Despite these distinctions, the contrasting energy balances and land-cover changes between forests and Cerrado are likely to modulate the intensity of micro and mesoscale feedback. Case 2 shows a gradual, persistent disruption to cloud formation and rainy season dynamics.

The persistent effects of deforestation on energy balances and circulation have been widely observed in modeling studies (Commar *et al.*, 2023a; Sierra *et al.*, 2023). Reductions in cloud cover due to deforestation have been documented on monthly and seasonal scales (Teuling *et al.*, 2017; Duveiller *et al.*, 2021), in global modeling studies (Hua *et al.*, 2023), and even at hourly resolutions (Leung *et al.*, 2024). My findings of persistent cloud reduction over 5–day to 15–day composites align with these monthly-scale observations while enabling a deeper seasonal assessment of the Southern Amazon’s rainy season dynamics. Furthermore, the observed effects of reduced clouds and disrupted energy balances (Commar *et al.*, 2023a; Hua *et al.*, 2023; Sierra *et al.*, 2023) highlight the significant impact of deforestation on the

Amazon's hydroclimatic dynamics. These results emphasize the critical need for skillful representation of cloud processes in modeling studies.

Nevertheless, the persistence of the correlation highlights a time-related dynamic in the rainy season process. As the rainy season approaches, energy increases, allowing the N-DCCs to transition into DCCs gradually (Chakraborty *et al.*, 2020; Henkes *et al.*, 2021), suggesting a cumulative process where cloud development intensifies over time.

While I did not specifically investigate deforestation thresholds, it is essential to analyze the Brazilian Forest Code, which sets a maximum deforestation limit of 20% within the Amazon biome (Soares-Filho *et al.*, 2014). Notably, a significant shift in cloud dynamics, such as reduced cloud height and increased cloud top temperature, at 20% deforestation— aligns with the legal deforestation limit in the region for heterogeneous forests (Figure 1.5a–b). However, the heterogeneous area showed a less pronounced impact on cloud variables above the legal deforestation threshold (Figure 1.5c–d). Nonetheless, its rainy season onset was still delayed by five days compared to preserved regions (Figure 1.5c–d).

These findings indicate that even legally permissible deforestation levels can significantly disrupt atmospheric processes, particularly cloud dynamics in heterogeneous forests. While the impacts on cloud variables in heterogeneous regions may be less pronounced, the onset is still delayed, highlighting a cumulative disruption to the regional energy and moisture balance (Wang *et al.*, 2009; Xu *et al.*, 2022a; Luo *et al.*, 2024). This threshold demonstrates that even within legal limits, deforestation can destabilize critical feedback mechanisms, emphasizing the urgent need for robust conservation efforts, law enforcement, and enhanced monitoring of Amazonian land use.

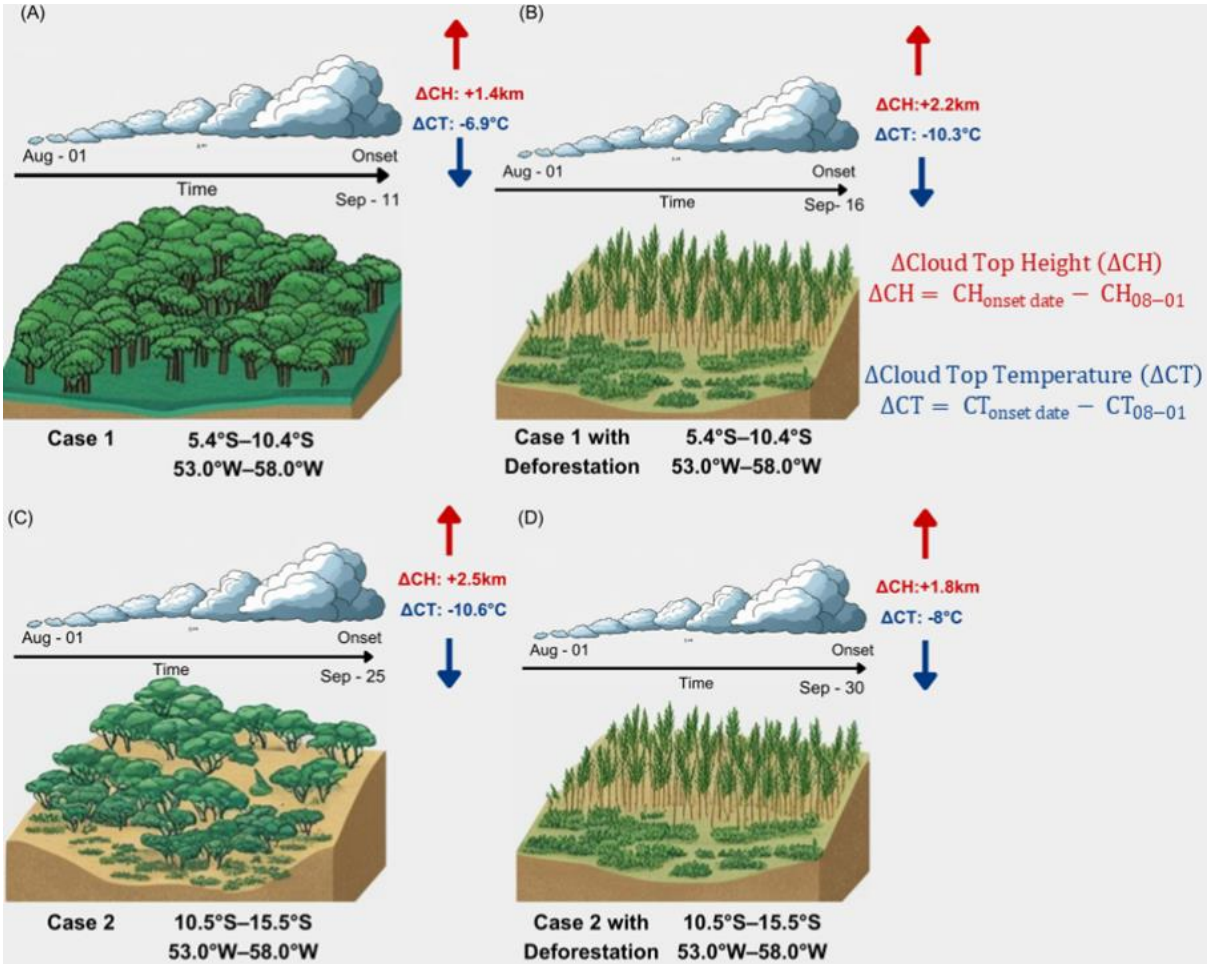

Figure 1.5 – Variation in cloud top height (ΔH) and cloud top temperature (ΔT) from August 1st to the rainy season onset across two regions with and without deforestation. (A) Case 1 without deforestation. (B) Case 1 with a 20% deforestation. (C) Case 2 without deforestation. (D) Case 2 with 20% deforestation.

In this study, I highlighted the intricate relationship between deforestation, cloud dynamics, and the onset of the rainy season. My findings highlight that deforestation alters local and regional cloud dynamics. Additionally, I observed a persistent temporal effect, with correlations extending from early August to late October, underscoring the lasting influence of deforestation on seasonal climate patterns, favoring environmental conditions that delay the transition to the rainy season.

1.5. Supplementary material

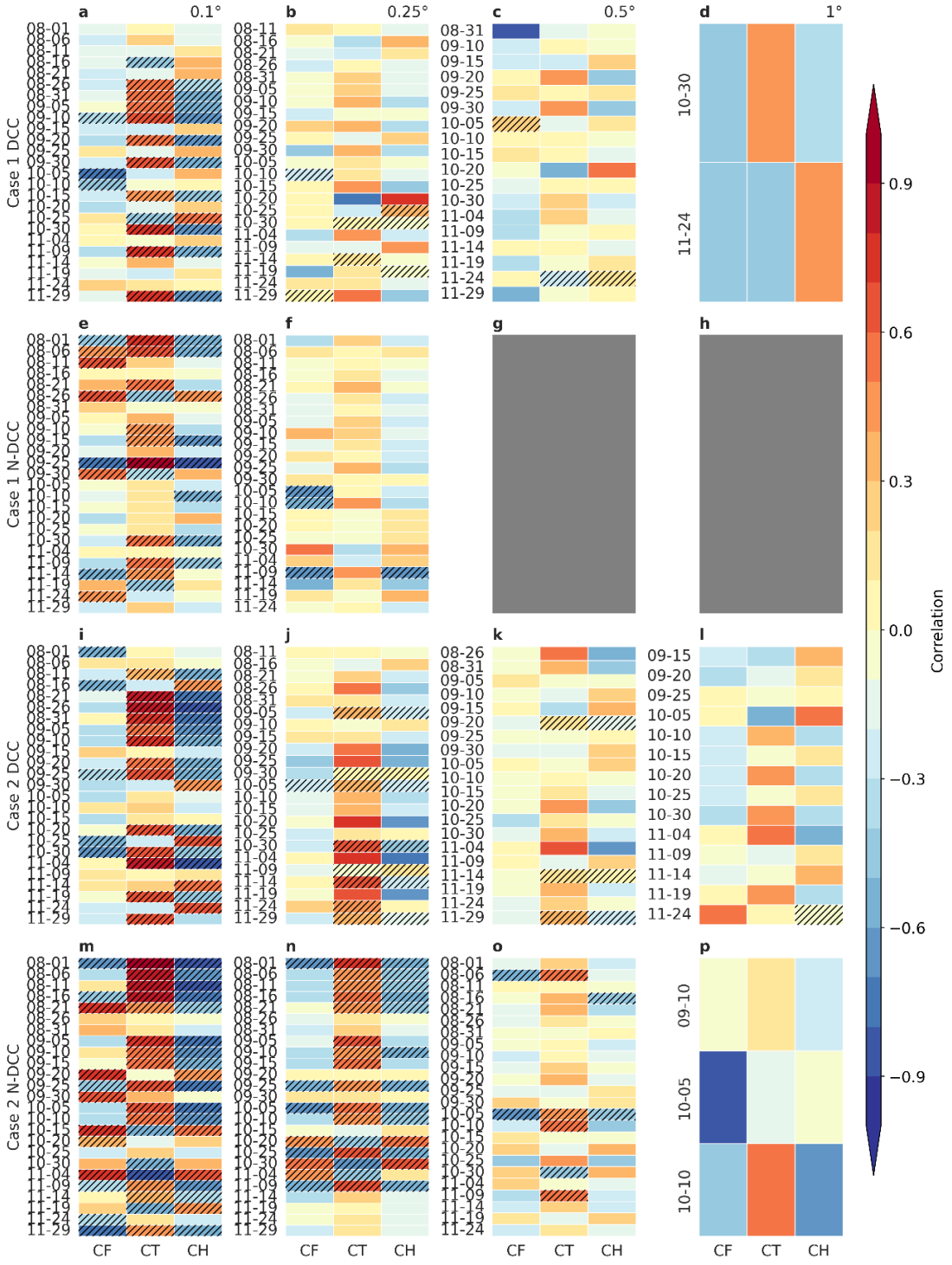

Figure S1.1 – Assessment of mean annual cloud fraction (CF), cloud top temperature (CT), and cloud height (CH) anomalies across deforestation levels for 5–day composites. The results are grouped by Case 1 DCC clouds (a–d), N-DCC clouds (e–h), Case 2 DCC clouds (i–l), and N-DCC clouds (m–p). Each column represents different horizontal resolutions–0.1°, 0.25°, 0.5°, and 1°. Positive values indicate that the standard anomalies are positively correlated with increasing deforestation, while negative values suggest that the standard anomalies decrease as

deforestation intensifies. Shaded areas indicate results significant at α = 0.1. Grey boxes indicate there is not enough data to perform the correlation.

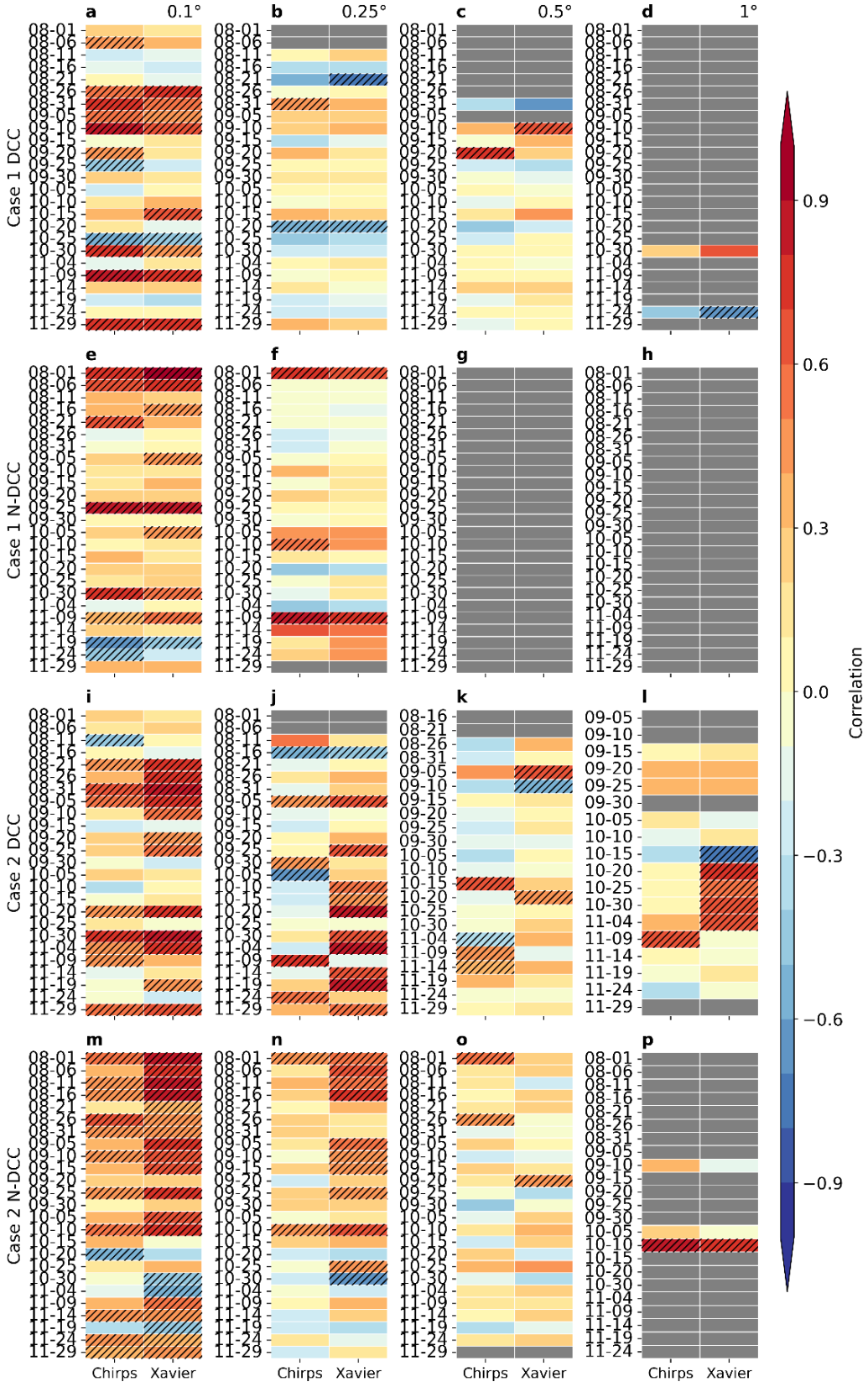

Figure S1.2 – Assessment of mean annual cloud top temperature (CT) correlated with mean annual rainy season onset anomalies across deforestation percentages for 5–day composites.

The results are grouped by Case 1 DCC clouds (a–d), N-DCC clouds (e–h), Case 2 DCC clouds (i–l), and N-DCC clouds (m–p). Each column represents different horizontal resolutions—0.1°, 0.25°, 0.5°, and 1°. Positive values indicate that the standard anomalies are positively correlated with the rainy season's onset delay, while negative values suggest a negative correlation with the delay of the rainy season. Shaded areas indicate significant results at α = 0.1. Grey boxes indicate there is not enough data to perform the correlation.

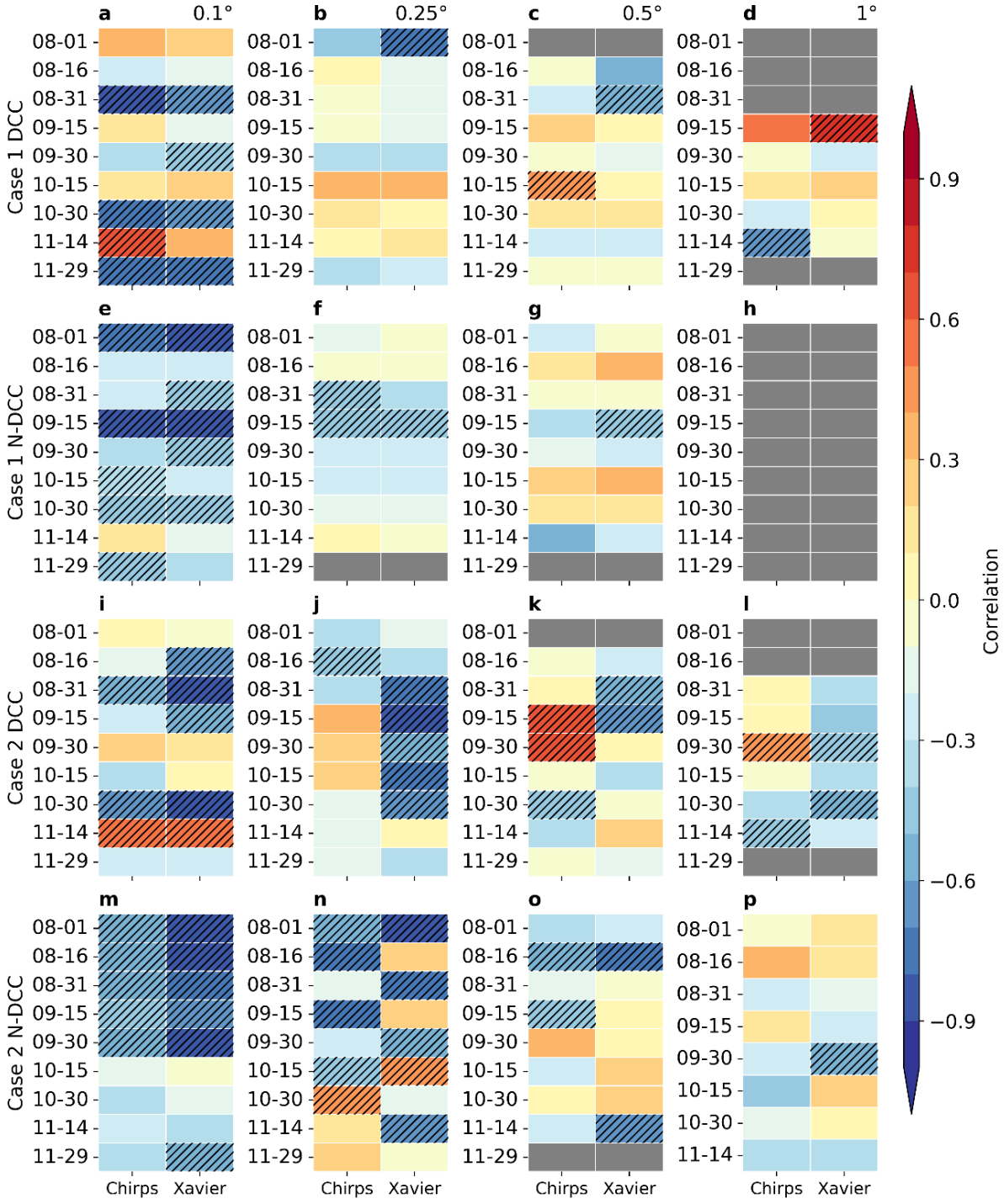

Figure S1.3 – Assessment of mean annual cloud top height (CH) correlated with mean annual rainy season onset anomalies across deforestation percentages for 15–day composites. The results are grouped by Case 1 DCC clouds (a–d), N-DCC clouds (e–h), Case 2 DCC clouds (i–l), and N-DCC clouds (m–p). Each column represents different horizontal resolutions—0.1°,

0.25°, 0.5°, and 1°. Positive values indicate that the standard anomalies are positively correlated with the rainy season's onset delay, while negative values suggest a negative correlation with the delay of the rainy season. Shaded areas indicate significant results at α = 0.1. Grey boxes indicate there is not enough data to perform the correlation.

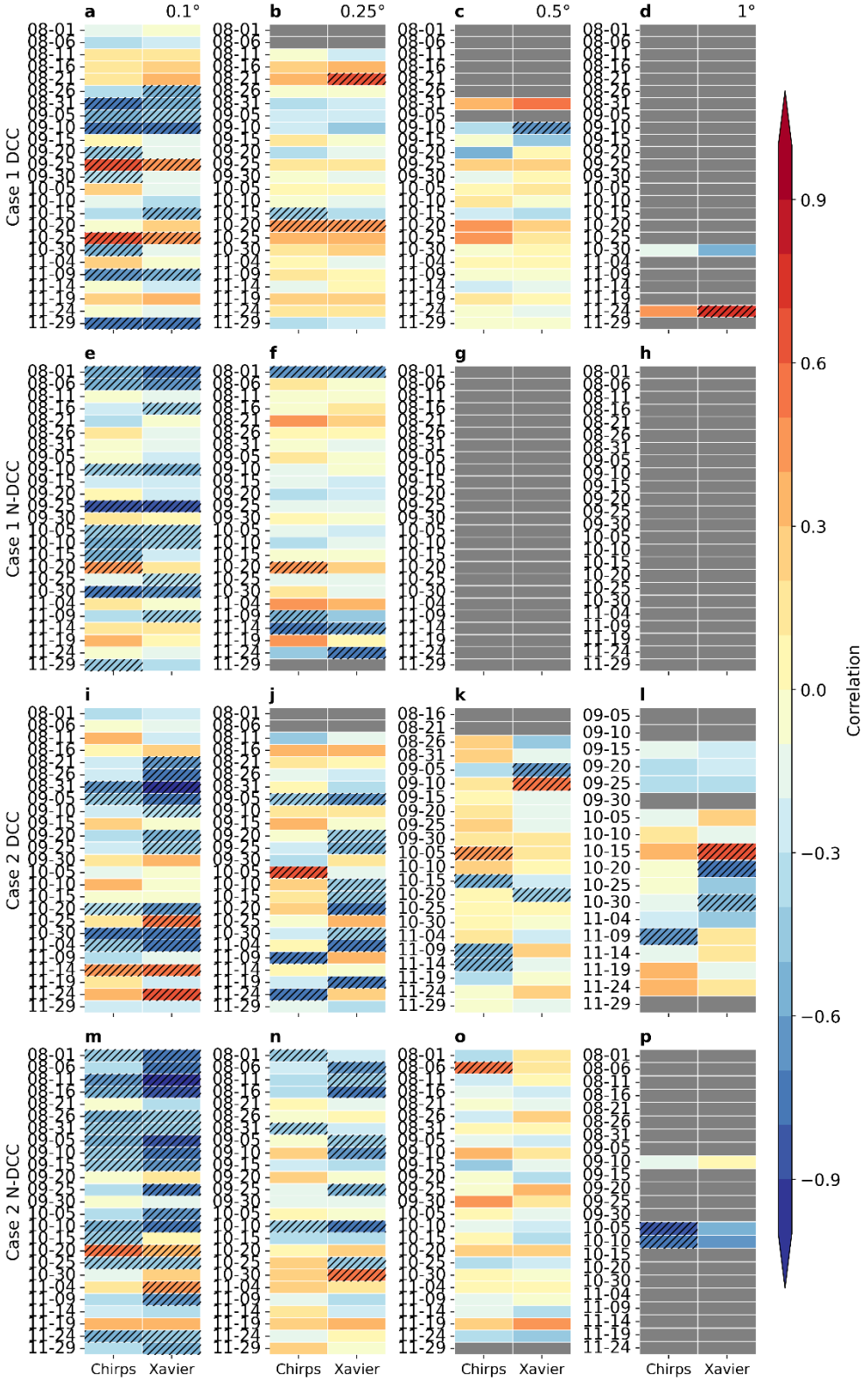

Figure S1.4 – Assessment of mean annual cloud top height (CH) correlated with mean annual rainy season onset anomalies across deforestation percentages for 5–day composites. The

results are grouped by Case 1 DCC clouds (a–d), N-DCC clouds (e–h), Case 2 DCC clouds (i–l), and N-DCC clouds (m–p). Each column represents different horizontal resolutions—0.1°, 0.25°, 0.5°, and 1°. Positive values indicate that the standard anomalies are positively correlated with the rainy season's onset delay, while negative values suggest a negative correlation with the delay of the rainy season. Shaded areas indicate significant results at α = 0.1. Grey boxes indicate there is not enough data to perform the correlation.

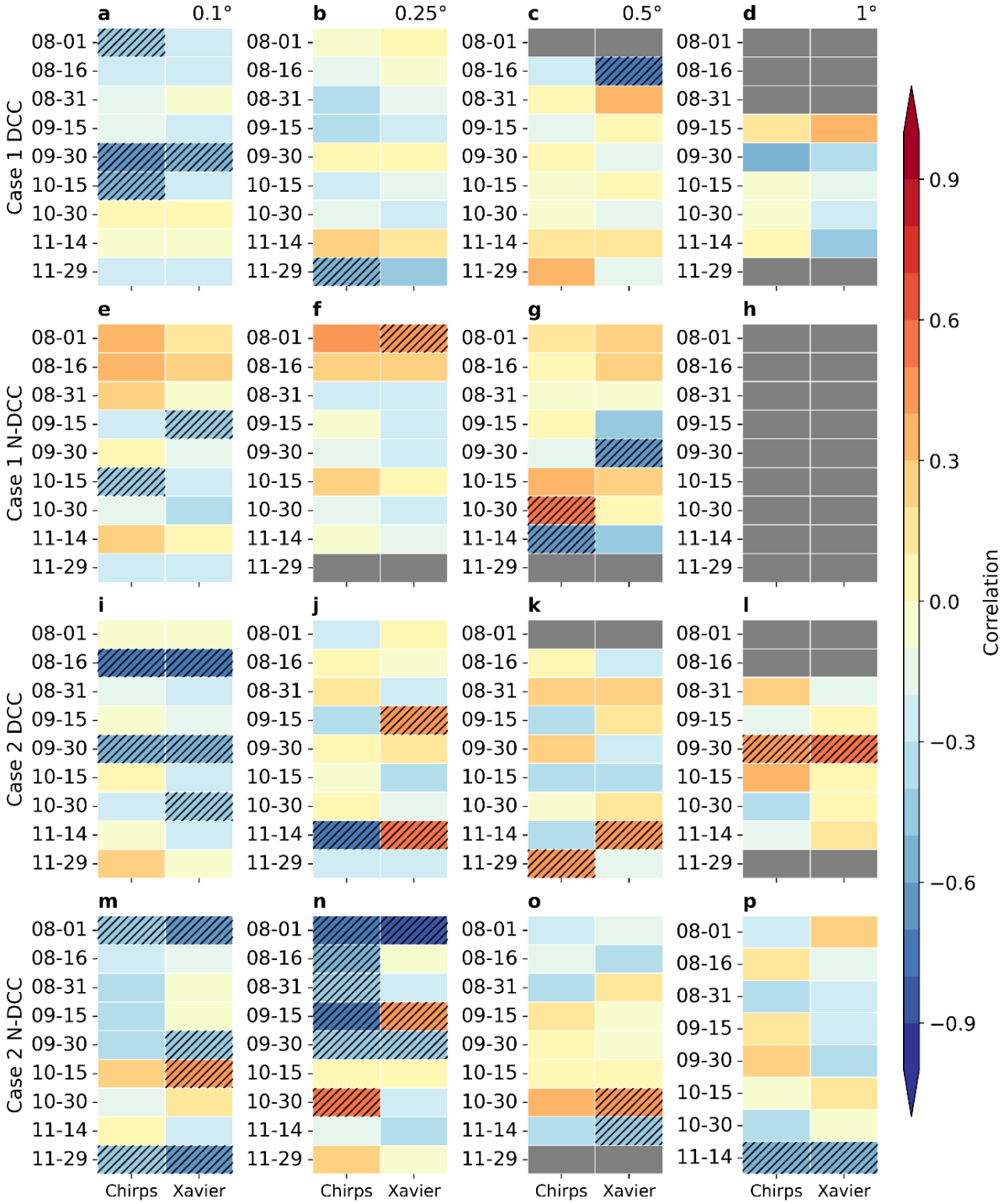

Figure S1.5 – Assessment of mean annual cloud fraction (CF) correlated with mean annual rainy season onset anomalies across deforestation percentages for 15–day composites. The results are grouped by Case 1 DCC clouds (a–d), N-DCC clouds (e–h), Case 2 DCC clouds (i–l), and N-DCC clouds (m–p). Each column represents different horizontal resolutions—0.1°,

0.25°, 0.5°, and 1°. Positive values indicate that the standard anomalies are positively correlated with the rainy season's onset delay, while negative values suggest a negative correlation with the delay of the rainy season. Shaded areas indicate significant results at α = 0.1. Grey boxes indicate there is not enough data to perform the correlation.

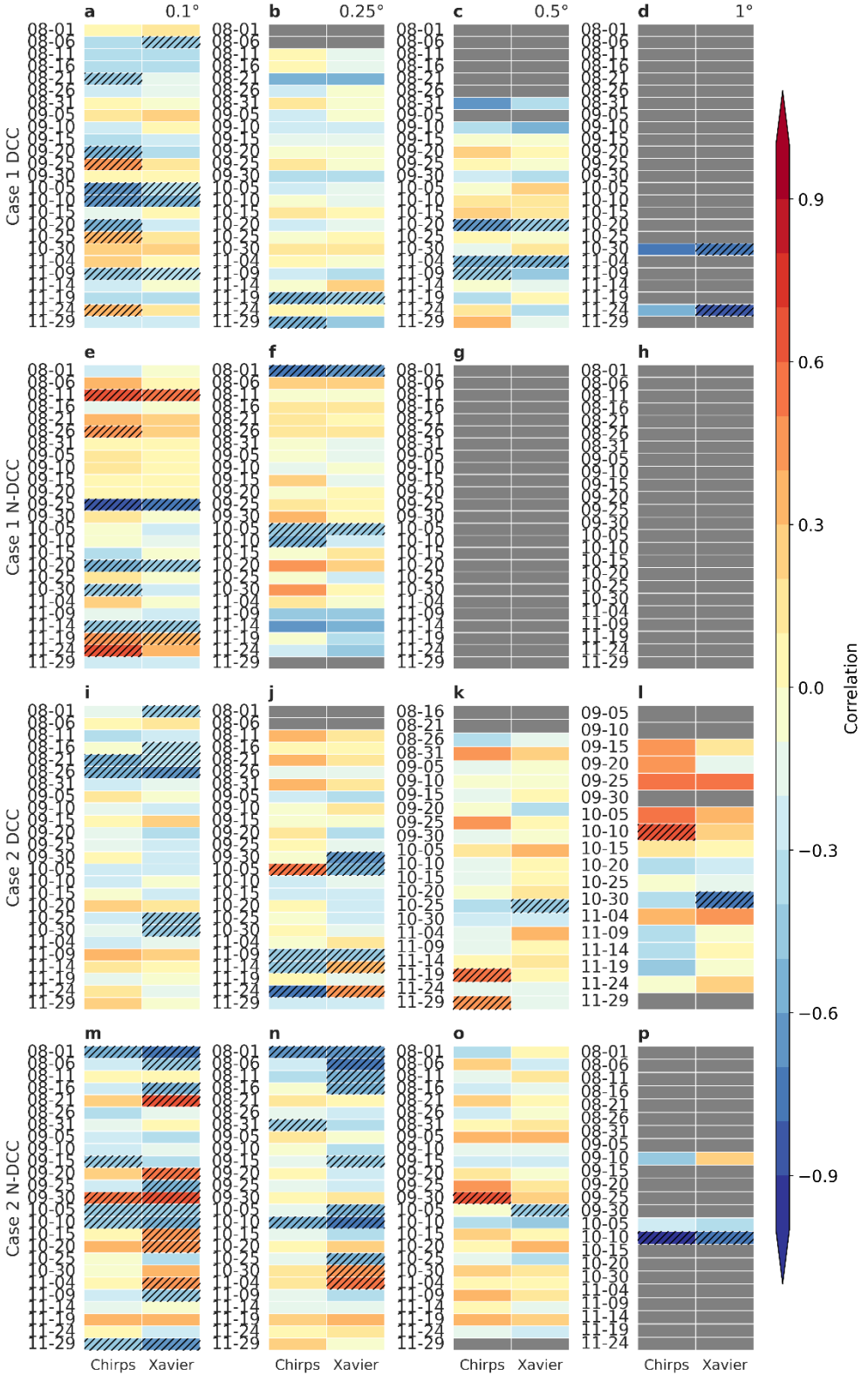

Figure S1.6 – Assessment of mean annual cloud fraction (CF) correlated with mean annual rainy season onset anomalies across deforestation percentages for 5–day composites. The

results are grouped by Case 1 DCC clouds (a–d), N-DCC clouds (e–h), Case 2 DCC clouds (i–l), and N-DCC clouds (m–p). Each column represents different horizontal resolutions—0.1°, 0.25°, 0.5°, and 1°. Positive values indicate that the standard anomalies are positively correlated with the rainy season's onset delay, while negative values suggest a negative correlation with the delay of the rainy season. Shaded areas indicate significant results at $\alpha = 0.1$. Grey boxes indicate there is not enough data to perform the correlation.

Chapter 2: Mato Grosso’s rainy season: Past, present, and future trends justify immediate action

Commar LFS, Louzada L, Costa MH, Brumatti LM, Abrahão GM. 2024. **Mato Grosso’s rainy season: past, present, and future trends justify immediate action**. *Environmental Research Letters*, 19(11): 114065. https://doi.org/10.1088/1748-9326/ad8588.

Abstract

Mato Grosso state, the agricultural giant of Brazil, owes its success partially to the long rainy season that has allowed for the extensive adoption of double cropping, elevating the region to one of the world's leading grain producers. However, recent studies warn of the adverse impacts of deforestation and climate variability, which are causing a decrease in rainfall and a delay in the rainy season onset. These changes pose significant threats to both ecosystems and intensive agriculture. To assess these threats, I compared past and present rainfall and rainy season duration in Mato Grosso and conducted robust climate projections using climate simulations forced by realistic deforestation scenarios. My analysis of observed rainfall data from the past four decades and Community Earth System Model simulations affirmed a worrying trend of decreasing rainfall volumes, delayed rainy season onset, and shorter rainy season length. Climate projections indicate that this pattern will intensify, with onsets expected in late October and rainy season durations shorter than 200 days by mid-century. These findings underscore the potential impact on Mato Grosso's double-cropping system, a cornerstone of the region's agricultural success, and emphasize the urgent need for sustainable large-scale agricultural practices and strategic interventions by regional decision-makers to mitigate agricultural losses and ecosystem degradation.

2.1. Introduction

Mato Grosso (MT) is a state in Brazil that has undergone significant growth in recent decades. In 1980, the state's population was 1.1 million, and by 2000, it had doubled to 2.1 million. As of 2022, the population has further increased to 3.6 million. Agriculture in Mato Grosso has also experienced rapid growth, especially in the production of soy and maize. In 1980, the total production of these crops was only 260,000 tons, while in 2023, it reached 90 million tons over 12 million ha.

Most of the maize production increase relates to its adoption as a second crop, given that regions with longer rainy seasons, like MT, can support a double-cropping system as an intensification method (Arvor *et al.*, 2014; Abrahão and Costa, 2018).

Mato Grosso has been under a double-cropping system for the last three decades, especially using soy-maize and soy-cotton combinations, with the second crop becoming as economically important as the first (Abrahão and Costa, 2018; Brumatti *et al.*, 2020). Currently, about 70% (8.5 Mha) (Zhang *et al.*, 2021) of cropland area in Mato Grosso is cultivated with two crops per year, significantly increasing the state's grain production (Hampf *et al.*, 2020).

Although agriculture is well established in the state, it is heavily influenced by climate variability, since most double-cropping areas are rainfed (Brumatti *et al.*, 2020; Hampf *et al.*, 2020). A reduced rainy season might pose a severe challenge for farmers. Deforestation in concert with climate variability is delaying the rainy season onset, lengthening the dry season over the different parts of the state, and thereby impacting agribusiness and natural ecosystems within the biomes (Araujo *et al.*, 2018; Leite-Filho *et al.*, 2019; Marengo *et al.*, 2021a; Hofmann *et al.*, 2023). The enhanced dry period has harmed rainfed agriculture, where soybean and maize experienced yield losses of 26 and 892 kg ha^{-1} per season, respectively (Rattis *et al.*, 2021). This elevates concern for the feasibility of double cropping in light of reduced rainy season duration over MT in the future (Cohn *et al.*, 2016; Costa *et al.*, 2019).

Reduced rainfall, delayed onset of the rainy season, and lengthening of the dry season have been attributed to both large-scale (warming of the oceans) and local-scale (deforestation) factors and their interactions (Costa *et al.*, 2019; Commar *et al.*, 2023a; Smith *et al.*, 2023). Modeling studies have effectively represented the link between hydroclimate and deforestation. These studies reveal that deforestation disrupts the energy balance, evapotranspiration, and surface roughness, leading to feedback mechanisms with a drier atmosphere and shifting the circulation, reducing the rainfall, and delaying the rainy season onset (Fu *et al.*, 2013; Khanna *et al.*, 2017; Staal *et al.*, 2020; Commar *et al.*, 2023a).

Nevertheless, recent research highlighted a compelling association between declining Amazon rainfall and the intensification of the Hadley and Walker cells (Fu, 2015; Espinoza *et al.*, 2019; Arias *et al.*, 2020). The strengthening of the Hadley cell reduces precipitation through increased subsidence, influenced by elevated sea surface temperatures in the Pacific and Atlantic, alongside a decline in deep convective circulation (Fu, 2015; Espinoza *et al.*, 2021; Bochow and Boers, 2023). Additionally, the Walker circulation, particularly during the warm phase of El Niño-Southern Oscillation, exacerbates this effect by inducing subsidence over the continent, leading to severe droughts and delayed rainy seasons (Cai *et al.*, 2020; Leite-Filho *et al.*, 2020).

This interaction between Amazon climatic dynamics and the Hadley and Walker circulations reflects the interconnected nature of these atmospheric phenomena. These interactions profoundly influence the region's hydroclimatic patterns, particularly in response to anthropogenic changes (Ruiz-Vásquez *et al.*, 2020; Sierra *et al.*, 2022).

The expansion of agricultural areas has been characterized as a no-win situation for agribusiness. The conversion of natural vegetation to agriculture is usually associated with a delay in the rainy season onset (Leite-Filho *et al.*, 2021). Adding climate change scenarios to this equation intensifies the consequences, resulting in an even later onset and a shorter rainy season (Pires *et al.*, 2016; Costa *et al.*, 2019; Commar *et al.*, 2023a). These extensive effects could cause economic losses of millions and heavy ecosystemic damage (Brumatti *et al.*, 2020; Carauta *et al.*, 2021; Leite-Filho *et al.*, 2021). The potential losses should arouse the concern of regional leaders. Even changing sowing dates and adopting shorter-cycle cultivars might decrease gross revenues when deforestation and climate change are considered (Brumatti *et al.*, 2020; Carauta *et al.*, 2021).

Although the correlation between the rainy season onset and duration to climate change and deforestation is recognized, a thorough assessment focused on agricultural and ecosystem impact is still overlooked. Therefore, this study aims to comprehensively evaluate changes and trends in Mato Grosso state's rainfall and rainy season onset and duration. Using coupled climate models forced by realistic deforestation scenarios, I also seek to provide a robust climate projection for MT. Having such foresight will allow decision-makers to prepare effectively, mitigating agricultural losses and averting ecosystem degradation.

2.2. Methods

2.2.1. Study area

Mato Grosso, situated in Central-West Brazil within the southern legal Amazon, encompasses three distinct biomes: the Amazon in the northwest, the Pantanal in the southwest, and the Cerrado across the remainder of the state. Primarily an agricultural region (Figure 2.1a), Mato Grosso predominantly cultivates crops such as soybeans, maize, and cotton (Arvor *et al.*, 2014; Abrahão and Costa, 2018; Zhang *et al.*, 2021).

The agricultural expansion in the region prompted the development of significant agricultural hubs such as Sorriso and Primavera do Leste (Figure 2.1a–b). This expansion of crops across the state contrasts with the presence of vast conservation units and indigenous lands, which predominantly maintain their native vegetation (Figure 2.1).

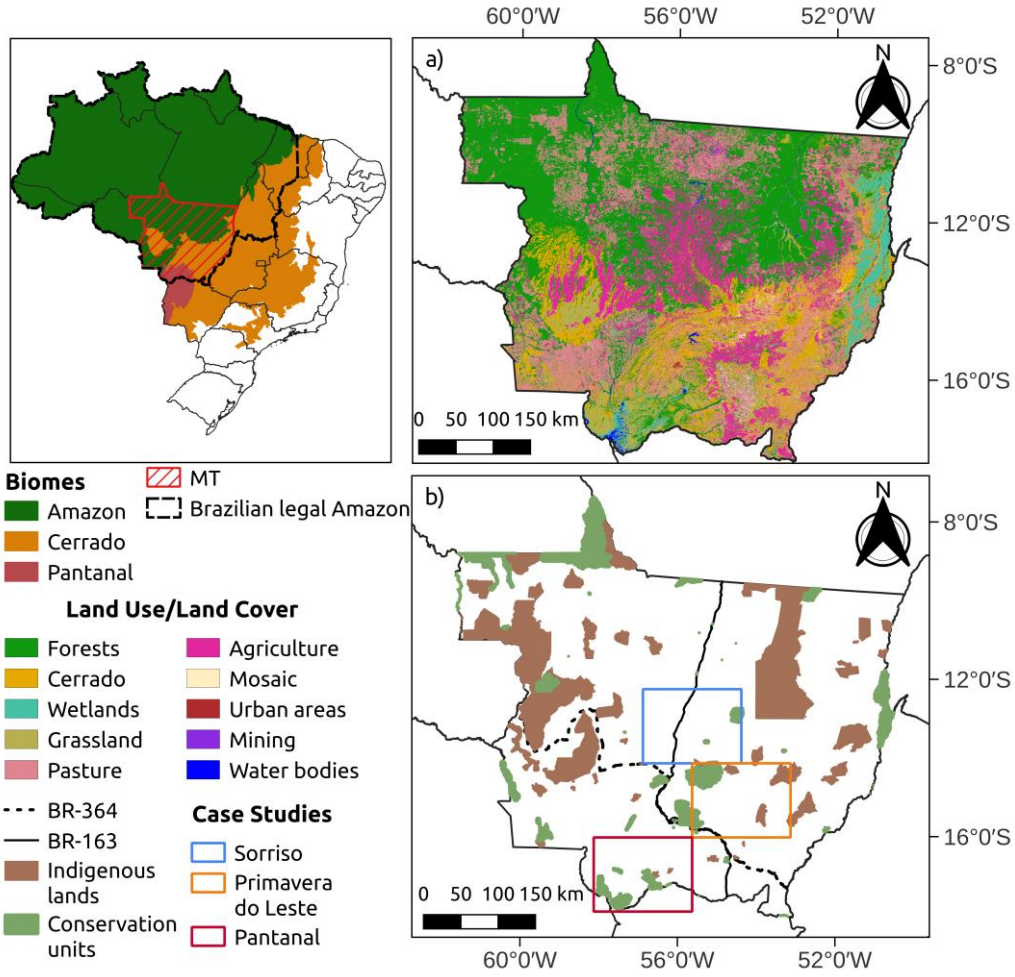

Figure 2.1 – Study area showing (a) land use and land cover for Mato Grosso in 2020 and (b) locations of indigenous lands, conservation units, and case study regions. Main roads are also shown.

2.2.2. Study period and data

I used daily precipitation from two databases, extending from 1981 to 2020, to diagnose past and current behavior of rainfall and rainy seasons for Mato Grosso: (i) The first is Brazilian daily weather gridded data with a spatial resolution of 0.1° × 0.1° (~11 km) for the whole of Brazil; this dataset is derived from the spatialization of observational data from 11,473 rain gauges and 1,252 meteorological stations distributed across the country (Xavier *et al.*, 2022) and is from now on referred to simply as "Xavier." (ii) The second, the Climate Hazards Group Infrared Precipitation with Stations (CHIRPS) dataset, with a spatial resolution of 0.05° × 0.05° (~5 km), combines satellite and rain gauge data; CHIRPS is widely used in Brazil (Funk *et al.*, 2015). I divided these datasets into two periods, representing past and more recent decades, 1981–2000 (P1) and 2001–2020 (P2).

I used the Community Earth System Model version 1.0.6 (CESM) (Hurrell *et al.*, 2013) to produce the future projection. CESM is a fully coupled model, combining atmospheric, surface, ocean, river, and cryosphere models, producing adequate simulations of earth system interactions (Hurrell *et al.*, 2013; De Hertog *et al.*, 2023). I reproduced the original RCP2.6 and RCP8.5 CMIP5 simulations coupled with all the components cited above, excluding the land use/land cover inside Brazil, where the RCP land model was replaced by environmental governance (EG) scenarios derived from recent Brazilian environmental policy, land use, and cover.

The EG scenarios represent strong (SEG) and weak (WEG) environmental governance. The weak scenario mirrors historical trends pre-2005, characterized by policies supporting agriculture with limited sustainability, thereby increasing deforestation in the Amazon and Cerrado regions. The strong scenario considers a shift towards sustainability with robust governmental support and preservationist practices (Rochedo *et al.*, 2018).

With this setup, I conducted four initializations for each scenario with global domain, with initial historical conditions from four ensemble members of the historical experiment from the original CESM, thus replicating the original initial conditions in the RCP scenarios. Here, I used precipitation data with a spatial resolution of 0.9° × 1.25° (~100 km) from the historical CESM simulations ranging from 1990 to 2000 and a projection for the four combined scenarios—RCP2.6-WEG, RCP2.6-SEG, RCP8.5-WEG, and RCP8.5-SEG—from 2020 to 2050. For more comprehensive insights into the CESM simulations, readers are referred to (Commar *et al.*, 2023a).

2.2.3. Rainy season onset and duration

I employed a modified anomalous accumulation (AA) method to define the onset and duration of the rainy season (Arvor *et al.*, 2014). This method establishes a relationship between daily rainfall (R_n) and a reference value (R_{ref}) (Eq. 1) and has proven effective in studies across agricultural regions in Brazil, utilizing both observed and modeled data (Abrahão and Costa, 2018; Commar *et al.*, 2023a, 2023b).

In my investigation, I initiated accumulation on July 1, aligning with the midpoint of the dry season in Mato Grosso. The onset of the rainy season coincides with the day of minimum AA, while its demise corresponds to the day of maximum AA. Consequently, the duration of the rainy season spans the interval between these dates (Arvor *et al.*, 2014).

$$AA_t = \sum_n^t R_n - R_{ref} \quad (1)$$

where AA_t = anomalous accumulation at day t; R_n = daily rainfall (mm day^{-1}) on day n; and R_{ref} = reference value. I used a reference value of 2.5 mm day^{-1}, which is the precipitation requirement for soybean seedlings (Abrahão and Costa, 2018).

2.3. Results

2.3.1. Rainy season changes and trends

Rainfall exhibited heterogeneous patterns over time. During period P1, higher precipitation levels were observed in southern MT, contrasting with period P2, where a considerable decrease occurred, with the rainfall decreasing across the state (Figure 2.2a–b, Figure S2.2 1a–b). Significant reductions were observed in the Pantanal region, with anomalies exceeding 150 mm and prominent decreasing trends (Figure 2.2c–d, Figure S2.2 1c–d). Similarly, Primavera do Leste experienced substantial decreases in rainfall, accompanied by significant downward trends (Figure 2.2c–d, Figure S2.2 1c–d). By contrast, the patterns observed for rainy season onset and length were more homogeneous. Across most of the state, a trend toward later onset and shorter duration of the rainy season was noticeable (Figure 2.2e–l, Figure S2.2 1e–l). Excluding northwestern MT, the trend of the later onset and shorter rainy season is apparent, and most of the eastern and southern regions exhibited significant changes in P2 (Figure 2.2g–h, k–l).

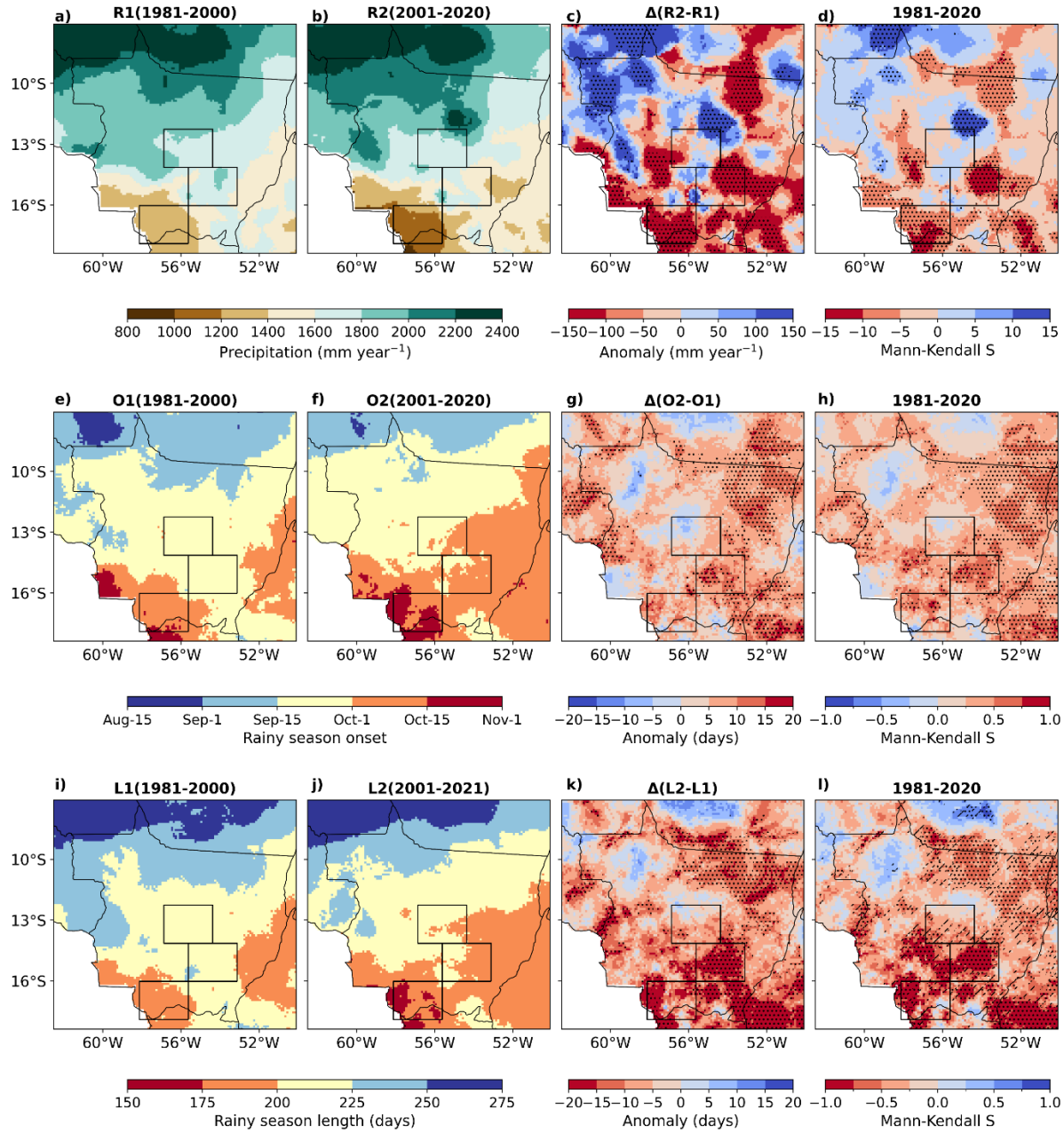

Figure 2.2 – Changes in rainfall patterns and rainy season over four decades using Xavier data, with comparative analysis and significance testing. Maps represent mean rainfall (R), rainy seasons onsets (O), and length (L) for two periods, R1, O1 and L1 (a, e, i) and R2, O2 and L2 (b, f, j), shown alongside the differences between P1 and P2 (c, g, k), and the Mann-Kendall S statistic for the entire period (d, h, l). Dotted areas denote significant differences at $\alpha = 0.05$ via Student's t-test (c, g, k) or the Mann-Kendall test (d, h, l). Oblique diagonal lines indicate significance at $\alpha = 0.10$ according to the Mann-Kendall test (d, h, l). The black rectangles represent the three case studies—Sorriso, Primavera do Leste, and Pantanal—as defined in Figure S2.2

Sorriso, Primavera do Leste, and Pantanal showed at least five days of delay in onset and a rainy season shorter by ten days (Figure 2.2g, k). Furthermore, trends in rainy season

delay and reduction over these regions were significant (Figure 2.2h, l, Figure S2.2 1h, l), suggesting a drier P2.

The Sorriso and Primavera do Leste regions showed a decreasing rainy season duration trend, accentuating the concern regarding intensive agriculture, the main economic activity in these regions. This same trend in the Pantanal region may influence local biodiversity. Thus, these regions highlight potential economic and ecosystem impacts of a reduced rainy season.

Moreover, the historical analyses reveal reductions in precipitation (Figure 2.2c-d), delayed onset (Figure 2.2g-h) and reduced length of the rainy season (Figure 2.2k-l) in the Primavera do Leste region, coinciding with areas dominated by agriculture (Figure 2.1a).

2.3.2. Climate projections

The cumulative distribution function (CDF) of the rainy season onset shows the likelihood of the rainy season onset occurring before a given day of the year (Figure 2.3). The CDF of the onset dates for both observed and CESM data ranging between August 15 and November 15, for the period 1990-2000 is shown in Figure 2.3a–c.

To evaluate the model's skill in defining rainy season onset probabilities, I computed the mean errors in the onset within probability intervals of 10% (Figure 2.3d). Primavera do Leste is the region with the least accurate model representation, which is particularly evident for earlier onsets (cumulative probability < 50%), with errors in the range of 20 days (Figure 2.3d). Conversely, Sorriso and the Pantanal exhibit anomalies below 10 days for the cumulative probability of onset > 30% (Figure 2.3d). Furthermore, the model demonstrates a skillful representation of rainy season onset across all three regions, notably capturing late onsets better than early ones.

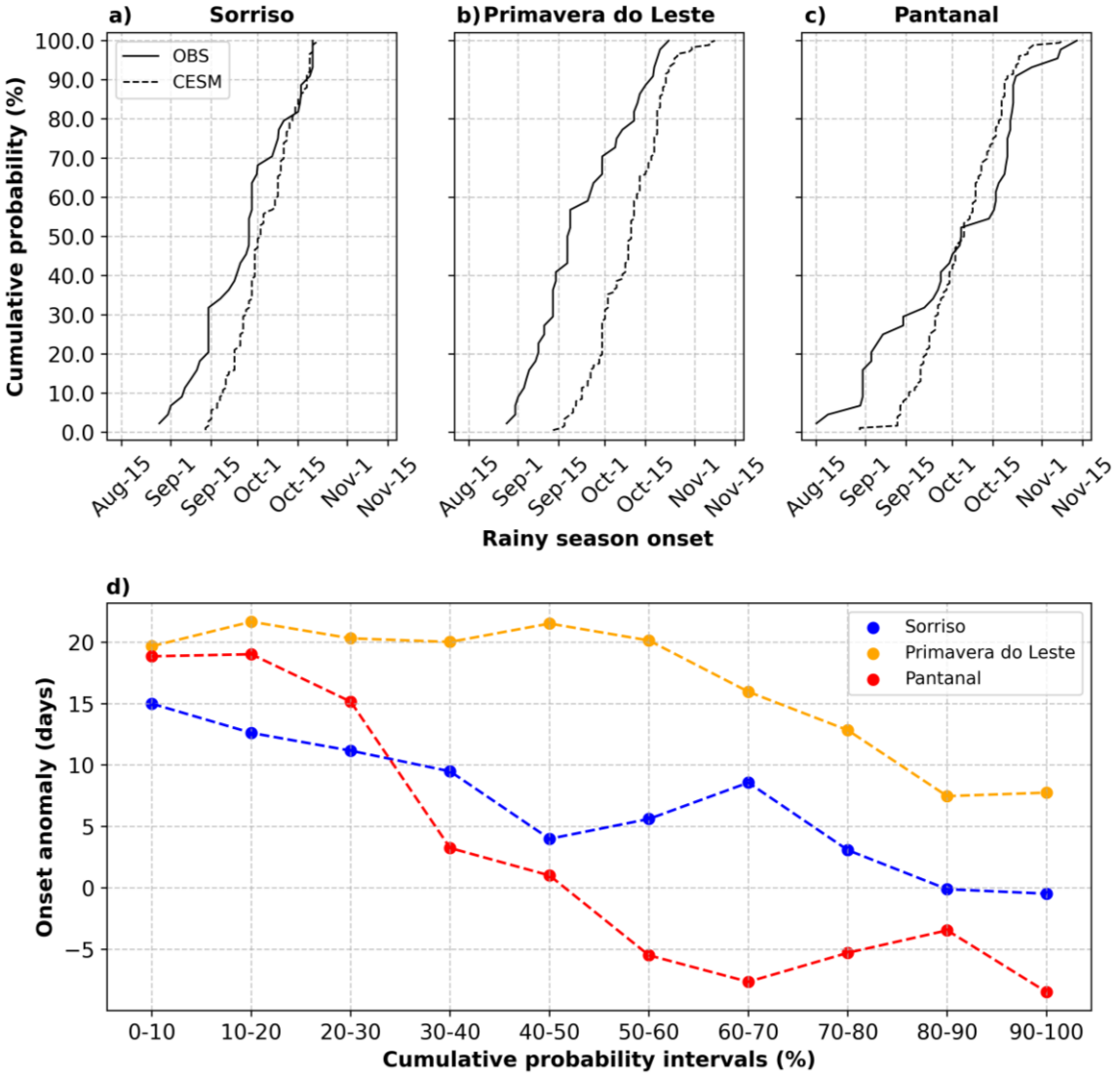

Figure 2.3 – Cumulative probability of rainy season onset for the Xavier observed data (OBS) and CESM historical simulations from 1990 to 2000 for each case study region: (a) Sorriso, (b) Primavera do Leste, and (c) Pantanal. (d) illustrates the difference in the cumulative probability of rainy season onset between CESM simulations and observed data, calculated at various probability intervals. Positive values indicate that the simulated rainy season happens with later onset than was observed, while negative values indicate earlier onset. The error varies between +20 and −10 days.

Figure 2.4 summarizes the three regions observed and simulated CDFs for the rainy season onset. Consistent with the anomalies and trends observed in rainy season onset (Figure 2.2g–h), P2 (2001–2020) shows later onset dates than P1 (1980–2000) for all probability levels across all three regions (Figure 2.4a–c). Analysis of observed data indicates a decrease in the probability of early-onset dates (before Sep 30) in Sorriso (Figure 2.4a) and in the Pantanal (Figure 2.4c) and, in particular, a remarkable reduction in Primavera do Leste (Figure 2.4b). This analysis of past and present underscores a reduction of early-onset years between P1 and P2, with an increased frequency of late-onset years.

The CESM cumulative distribution indicates that future decades will likely experience later rainy season onsets compared to P2, suggesting a delay in the onset dates at all probability levels for Sorriso and Primavera do Leste (Figure 2.4a, b). As time progresses, projected onsets tend to occur later, with even later onsets projected for the 2041–2050 period. The impact of these shifts is notably pronounced in Sorriso and Primavera do Leste, with their onset distributions shifting by up to 15 days when compared to observed data, and 10 compared to historical simulations (Figure 2.4a–b). Although the Pantanal region exhibits later onset dates in the observations than the projections (Figure 2.4c), early-onset dates still lag those observed in P1.

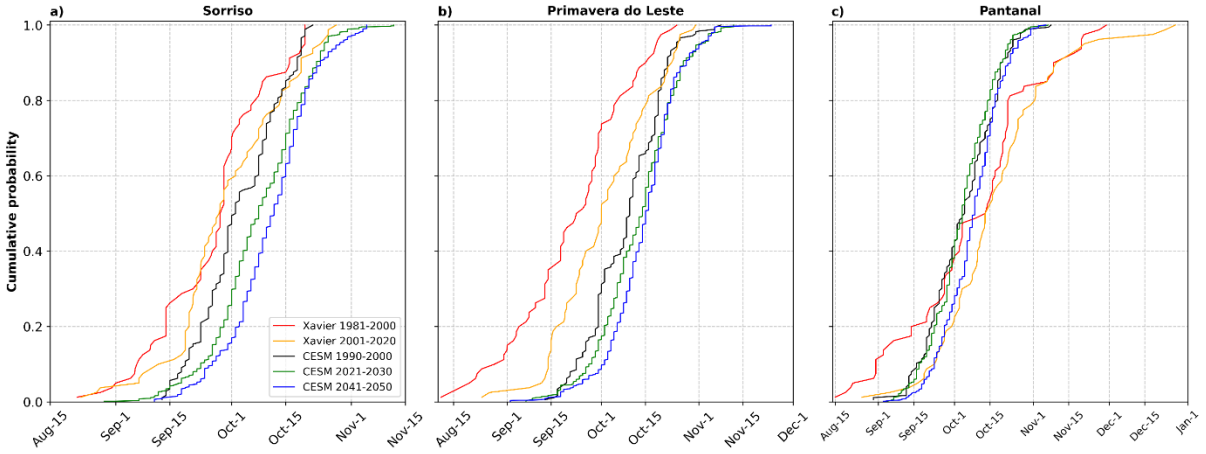

Figure 2.4 – Cumulative probability of rainy season onset. Comparison between Xavier for periods P1 (1981–2000) and P2 (2001–2020) and climate simulations (CESM) for the historical period (1990–2000), and future decades across each case study (a–c).

I define an early rainy season onset as occurring on or before September 30. A rainy season starting on or before this date typically indicates a larger rainy period and the potential for successful double cropping in Mato Grosso. However, with onsets occurring after October 1, the likelihood of failure for double cropping increases, resulting in lower yields for the second crop. Onsets after November 1 prompt farmers to refrain from planting a second crop due to climate risks associated with later sowing dates.

The probabilities of projected rainy season onset dates exhibit a distinct gradient across Mato Grosso, with early onsets concentrated in the northwestern region (Figure 2.5a, e, i). A northwest–southeast gradient of onset dates is apparent (Figure 2.5b–d). In the northwest part of the state, over the decades the probability of early onset decreases from 60%–80% in the 2000s to 40%–60% in the 2040s (Figure 2.5a, e, i). Onsets between October 1 and 15 show an

increasing probability in the northwest and southwest regions. A similar trend is observed in the eastern part of the state for later October dates.

Notably, Sorriso and Primavera do Leste demonstrate an increase in the probability of onset occurring between October 16 and 31, rising from 20%–40% in 2021–2030 to a 40%–60% chance by mid-century (Figure 2.5g, k). Concurrently, the likelihood of an early onset decreases to 20% for these regions (Figure 2.5e, i). There is a noticeable shift in the probability distribution across these date thresholds as the decades progress, with the probability of an early onset shifting from September to early and later October dates, indicating a progressive delay for the climate change and deforestation projection scenarios. This same shift in onset dates can be noticed in the Pantanal region, with most of the region maintaining a high probability of onset in early October.

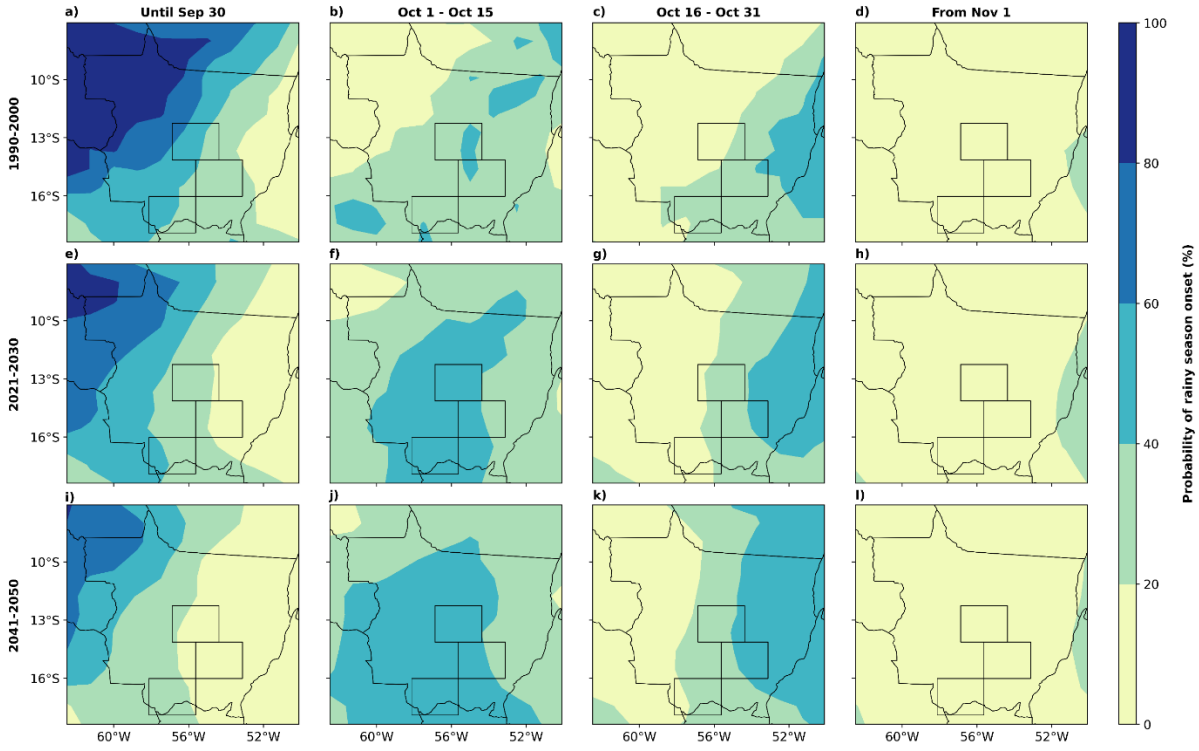

Figure 2.5 – Probability of rainy season onset occurrence within specific time ranges. Each column represents the probability of onset for certain dates: on or before Sep 30 (a, e, i), Oct 1–Oct 15 (b, f, j), Oct 16–Oct 31 (c, g, k), and on or after Nov 1 (d, h, l). The rows represent three different decades: 1990–2000 (a–d), 2021–2030 (e–h), and 2041–2050 (i–l). The black rectangles indicate the three case study regions—Sorriso, Primavera do Leste, and Pantanal—as defined in Figure S2.2

Complementary to my analysis of onset thresholds, I defined intervals for the rainy season length. Rainy seasons lasting more than 220 days indicate a prolonged rainy period that leads to successful double cropping. As the rainy season shortens towards 180 days, the

probability of failure for double cropping increases, leading to an increased possibility of low yields for the second crop. If the rainy season lasts less than 180 days, sowing a second crop becomes unfeasible for farmers.

Probabilities for rainy season length show a similar gradient to that of onset, with longer rainy seasons concentrated in the northwestern region (Figure 2.6d, h, l). Over the decades, the probability of extensive rainy seasons decreases, while areas with durations shorter than 180 days come to cover half of MT with probabilities exceeding 30% (Figure 2.6e, i). Lengths of 181–200 days show increasing probabilities in central MT, and by mid-century, most of the state exhibits more than a 50% chance of being in this range (Figure 2.6f, j). Similarly to rainy season onset, there is a transition towards shorter rainy season lengths, and the probability for these shorter rainy periods increases across the state (Figure 2.6m).

Additionally, Sorriso, Primavera do Leste, and Pantanal demonstrate a decrease in the probability of longer rainy season lengths, with durations of 181–200 days notably increasing from 2021–2030 to 2041–2050 (Figure 2.6n–p). Concurrently, the likelihood of a rainy season shorter than 200 days for these regions surpasses 80% (Figure 2.6n–p).

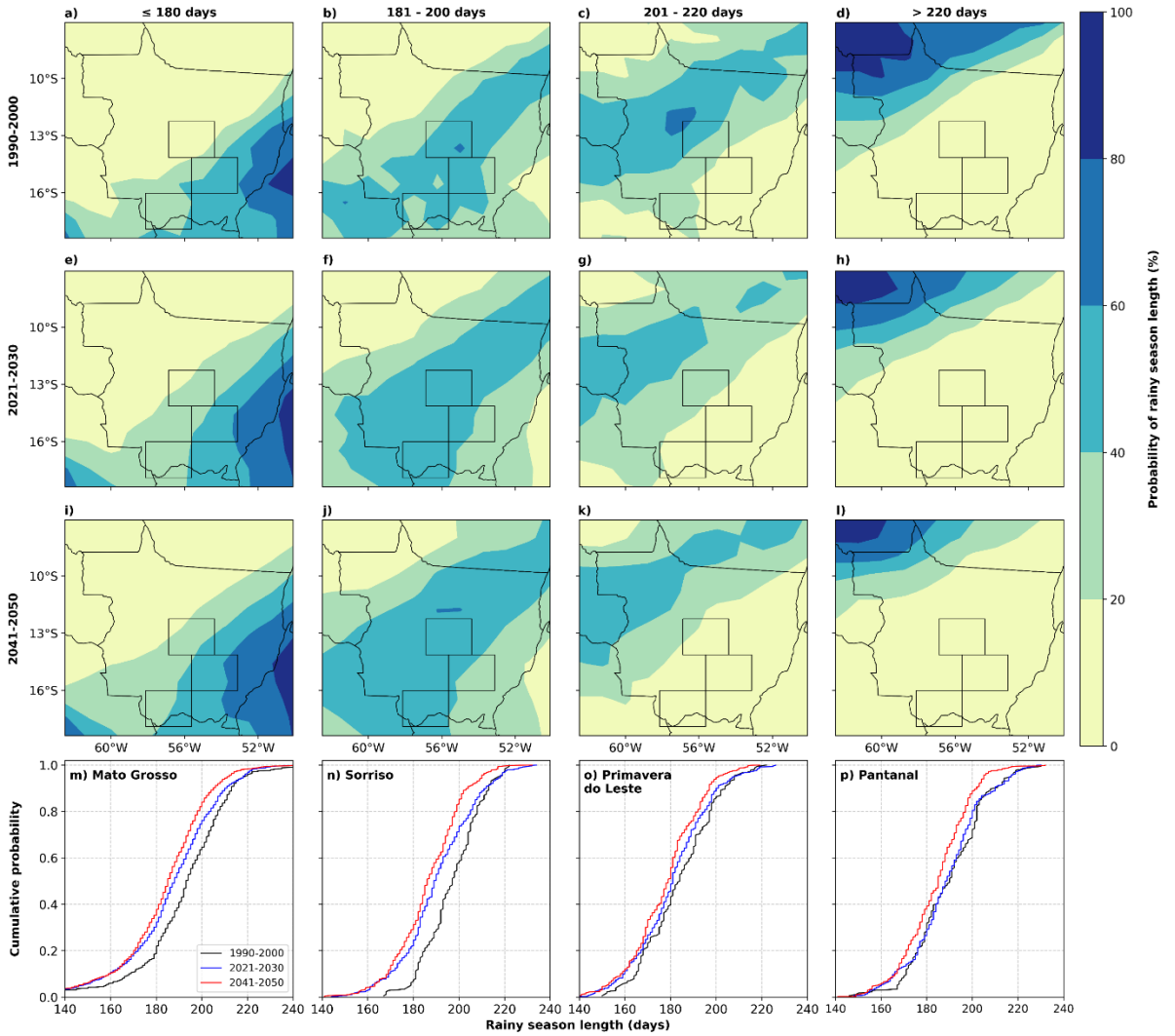

Figure 2.6 – Probability of rainy season length occurrence within specific time ranges and cumulative probability of rainy season duration. Each column represents a specific duration in days: less than 180 (a, e, i), 181–220 (b, f, j,), 201–220 (c, g, k), and more than 220 (d, h, l). The top three rows represent three different decades: 1990–2000 (a–d), 2021–2030 (e–h), and 2041–2050 (i–l). The black rectangles indicate the three case study regions— Sorriso, Primavera do Leste, and Pantanal—as defined in Figure S2.2. The bottom row shows cumulative probability for the whole of Mato Grosso state (m) and each case study: Sorriso (n), Primavera do Leste (o), and Pantanal (p).

2.4. Discussion

2.4.1. Rainy season diagnosis

Previous studies investigating precipitation across areas broader than MT have consistently registered decreasing rainfall over MT. Specifically, eastern, southwestern, and southern MT have shown increased drought and diminishing rainfall trends (Araujo *et al.*, 2018; Marengo *et al.*, 2021b; Hofmann *et al.*, 2023), which corroborates my diagnosis (Figure 2.2). These trends are particularly pronounced during the transition from dry to wet periods (Araujo *et al.*, 2018; Hofmann *et al.*, 2023), marked by the rainy season onset. Furthermore, the expansion of drier trends has been observed in the Cerrado and Pantanal regions of the state

(Araujo *et al.*, 2018; Hofmann *et al.*, 2023). In addition to analyzing the region's rainfall, I explored trends and anomalies in rainy season onset and duration, enhancing my understanding of the changing climatic patterns in the region.

Among the possible causes of these changes are the shifts in regional atmospheric circulation induced by land use and land cover within the region (Araujo *et al.*, 2018; Michot *et al.*, 2024). Extensive deforestation in tropical areas promotes a negative effect on precipitation (Smith *et al.*, 2023) and, for Amazon areas comprising northern MT, each 10% increment of deforestation might delay the rainy season onset by 1.7 days (Leite-Filho *et al.*, 2019). Also, modulations in the South Atlantic Convergence Zone (SACZ) characterized by increased intensity might promote a subsidence movement, affecting the rainy season and precipitation amounts (Arvor *et al.*, 2017; Michot *et al.*, 2024). I consider these sources of variation likely to be among the causes since these studies have shown similar results to mine, with a delayed onset and consequent shorter rainy season length.

With agriculture as the main economic activity in MT, the current behavior of the rainy season onset and duration, along with the observed trends, have raised concern for farmers. Similar studies have verified that a decrease of 100 mm in precipitation might reduce the possibility of double cropping by 3.6% (Rattis *et al.*, 2021). Similarly, delayed onset and shorter length of the rainy season severely affect or even eliminate the possibility of a second crop (Abrahão and Costa, 2018; Rattis *et al.*, 2021; Leite-Filho *et al.*, 2024). My analysis found rainfall anomalies surpassing 150 mm, with significant decreasing trends in onset and length, with anomalies of up to 20 days between two 20-year periods (Figure 2.2k). However, trend analyses indicate a trend of up to 1-day reduction of rainy season duration per year, equivalent to a trend of nearly 40 days in 40 years from 1981 to 2020 (Figure 2.2l). These results, together with the previous findings, are especially concerning Sorriso and Primavera do Leste, which rely on agricultural development. Despite the potential for irrigation to mitigate yield losses, similar studies for Mato Grosso have reported reductions in yields even in irrigated areas (Rattis *et al.*, 2021).

The economic consequences of agriculture are not the only concern for Mato Grosso. In 2020, the Pantanal region experienced an unusually long and severe drought associated with a heat wave, leading to massive, widespread fires (Marengo *et al.*, 2021a; Libonati *et al.*, 2022). This reduction in rainfall and delayed rainy season onset could present challenges for the region's biodiversity and society (Mataveli *et al.*, 2021; Libonati *et al.*, 2022). My analysis of

observed trends in the Pantanal over the last four decades reveals a significant reduction in rainfall and a delayed onset of the rainy season, aligning with previous studies.

2.4.2. Model skill and projection configuration

As I am aiming to provide valuable information to Mato Grosso decision-makers regarding sowing dates and double cropping feasibility, the distribution of rainy season onset probability was my main concern. Thus, errors of less than 10 days by the end of my probability spectrum (Figure 2.3) emerge as a reliable representation of the onset for the regions, given the region's seasonal precipitation variability (Hofmann *et al.*, 2023; Michot *et al.*, 2024). Moreover, CESM has presented consistent rainfall volumes for dry-to-wet transition months (Commar *et al.*, 2023a), with comparable behavior to studies using multimodel ensembles, including underestimated rainfall in the Brazilian Amazon region (Monteverde *et al.*, 2022; Olmo *et al.*, 2022).

Concerning CESM configuration, the Community Land Model (CLM) represents surface processes as having higher evapotranspiration than observed for tropical regions with C4 plants (Spracklen *et al.*, 2018; Boysen *et al.*, 2020). Since my simulations replace the natural vegetation with C4 grasses, this parametrization might impact local rainfall values. However, this setup preserved the original CMIP5 configuration.

I grouped CESM simulations into decades comprising all four scenarios (RCP2.6-WEG, RCP2.6-SEG, RCP8.5-WEG, and RCP8.5-SEG), enabling the occurrence of extreme-onset events (early and delayed) in my probability distributions. This promoted the understanding of how the extremes place in each projected decade since, for decision-makers, extreme events are the major cause of disasters in planning and yield failures.

2.4.3. Climate projections

Studies using models have shown a strong correlation between deforestation, precipitation, and the duration of the rainy season. These studies demonstrate that widespread deforestation can seriously disrupt the energy balance, evapotranspiration, and surface roughness, ultimately triggering feedback mechanisms that reduce rainfall and delay the onset of the rainy season by up to 40 days (Khanna *et al.*, 2017; Staal *et al.*, 2020; Commar *et al.*, 2023a). This delay in rainfall increases the dry season duration in several studies using CMIP5 due to the increase in temperature, the raised concentration of greenhouse gases, the intensification of El Niño, changes in the behavior of the subtropical jet, or changes in the moisture transport (Fu *et al.*, 2013; Costa *et al.*, 2019; Brumatti *et al.*, 2020; Douville *et al.*,

2023). Likewise, my MT results show a considerable shift towards a later onset and shorter length of the rainy season in climate change scenarios.

Increased deforestation scenarios combined with climate change could lead to a US$2.8 billion gross revenue decrease by 2050, and even using more adapted cultivars aiming for mitigated impact for double cropping does not maintain healthy revenue values (Brumatti *et al.*, 2020). Indeed, climate change is expected to reduce second-crop productivity by 17% in 2040 (Hampf *et al.*, 2020). Considering the Amazon biome, which is part of the MT ecosystem, agriculture might lose US$15 billion yearly due to the advance of deforestation (Commar *et al.*, 2023a). My finding that there is a higher probability of shorter rainy seasons with later onset reaffirms these disastrous scenarios from previous studies but adds graduated information about the progress of these changes decade by decade to help with developing mitigation strategies.

Deforestation scenarios analogous to ours have demonstrated a 20% loss in double-cropping yield for Mato Grosso, with projections indicating that regions such as Sorriso and Primavera do Leste may face yield losses of up to 15% under similar conditions (Spera *et al.*, 2020). This is particularly concerning, as climate projections suggest that these regions are among the most vulnerable to potential losses in second crops (Hampf *et al.*, 2020; Carauta *et al.*, 2021). Thus, combining these effects can severely harm the double-cropping potential for those regions.

Other agricultural regions in Brazil increased their production through agricultural intensification practices, especially irrigation. However, this intensification, together with precipitation variability, has triggered regional water stress (Pousa *et al.*, 2019; Santos *et al.*, 2020; Commar *et al.*, 2023b). While sustainable intensification of agriculture may offer a partial solution for MT (Rattis *et al.*, 2021; Marin *et al.*, 2022), it is crucial to acknowledge and address this potential conflict.

Compared to agricultural areas, the Pantanal region faces ecological issues instead. Details about the 2020 drought (Marengo *et al.*, 2021a; Libonati *et al.*, 2022) support my observations concerning reduced rainfall (Figure 2.2c) and shortened rainy seasons (Figure 2.2k). This severe dryness has significant consequences for the local economy, population, and ecosystems, all of which rely on the biome (Tomas *et al.*, 2019; Mataveli *et al.*, 2021; de Moraes *et al.*, 2022). The 2024 widespread fire event and the potential amplification of other severe events due to the rainfall and rainy season characteristics presented here cannot be ignored. Regional policies must consider these projections to secure the welfare of Pantanal biodiversity, economy, and local population.

2.5. Conclusions: a call for action

The past and present diagnostic analysis and the projected analysis for future climate indicate consistent patterns. The trends towards late onset of the rainy season and reduced duration of the rainy season, trends that started in the last few decades, are expected to continue. Those who moved to Mato Grosso in the late 20th century and got used to its rainy climate and long rainy season should not expect a similar climate in the first half of the 21st century. Agricultural and ecological conservation practices used before are no longer sustainable in the 21st century.

This highlights the urgent need for action to adapt to climate change. These climate projections, which are consistent with recent climate changes, represent a critical opportunity. Regional decision-makers might use these projections and develop regional adaptation strategies to make agriculture and ecosystem conservation more sustainable in future decades.

For agriculture, despite the state's historical reliance on agricultural intensification through rainfed double cropping over the past several decades, climate projections indicate that this practice is under increasingly severe climate risk, which may lead to reduced yields in the first or second crop. A possible solution lies in irrigation. Supplementary irrigation during the beginning of the first crop season and the end of the second crop season might resolve the problem without using much water. Yet, while this solution is promising, it will be a challenge. Because of Mato Grosso's climate, irrigation was virtually non-existent in the state until 2000 and has been increasing since then. Still, Mato Grosso had less than 200,000 ha irrigated in 2020, while the need for irrigation now amounts to ~10 Mha (Rocha Junior *et al.*, 2020), a 50-fold difference. This brings significant challenges in terms of energy production and distribution, and availability of credit to farmers. In addition, careful monitoring of water resources is essential to mitigate the risk of water stress and water use conflicts.

The challenges are even stronger for ecosystem conservation. Future climate projections indicate that the Pantanal is a region highly susceptible to desertification (de Moraes *et al.*, 2022). Desertification in this region increases the probability of fires and results in low river levels that limit the population's mobility and the transport of commodities to the Atlantic Ocean via the Paraná–Paraguay waterway (Marengo *et al.*, 2021a). Solutions for the Pantanal drought that preserve the functioning of this delicate ecosystem are still to be proposed.

In summary, Mato Grosso faces significant challenges due to ongoing and upcoming climate change. Previous agricultural and conservation practices are no longer viable, and immediate action is needed. Specific agricultural policies that facilitate the implementation of

irrigation systems without compromising water security are as urgent as specific ecosystem conservation policies that realize that the Pantanal is at imminent risk of desertification through fire.

2.6. Supplementary material

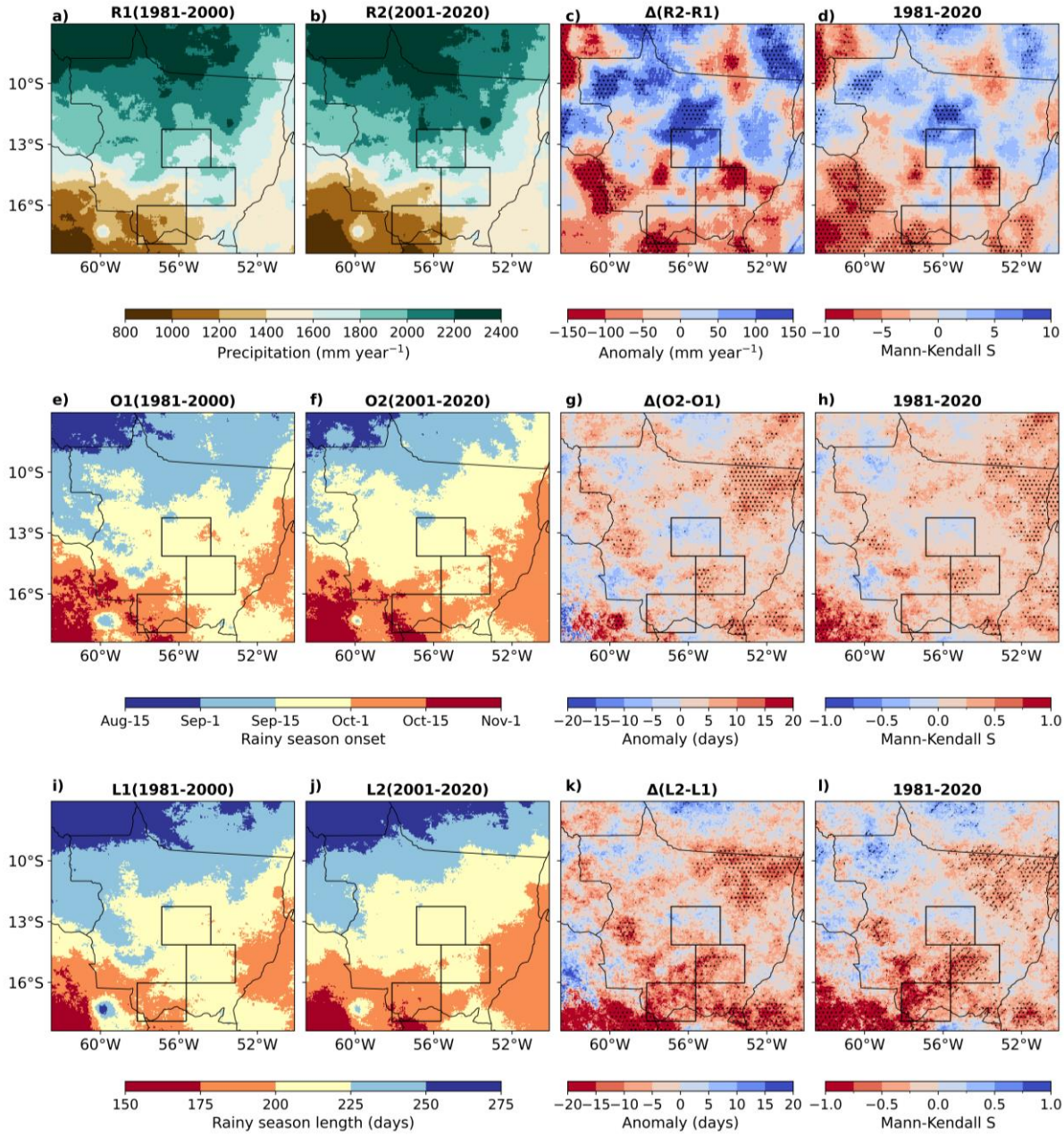

Figure S2.1 – Changes in rainfall patterns and rainy season over four decades using CHIRPS data, with comparative analysis and significance testing. Maps represent mean rainfall (R), rainy seasons onsets (O), and length (L) for two periods, R1, O1 and L1 (a, e, i) and R2, O2 and L2 (b, f, j), shown alongside the differences between P1 and P2 (c, g, k), and the Mann-Kendall S statistic for the entire period (d, h, l). Dotted areas denote significant differences at $\alpha = 0.05$ via Student's t-test (c, g, k) or the Mann-Kendall test (d, h, l). Oblique diagonal lines indicate significance at $\alpha = 0.10$ according to the Mann-Kendall test (d, h, l). The black rectangles represent the three case studies—Sorriso, Primavera do Leste, and Pantanal—as defined in Figure 2.1.

Chapter 3: A possible deforestation-induced synoptic-scale circulation that delays the rainy season onset in Amazonia

Commar LFS, Abrahão GM, Costa MH. 2023. **A possible deforestation-induced synoptic-scale circulation that delays the rainy season onset in Amazonia**. *Environmental Research Letters*, 18(4): 044041. https://doi.org/10.1088/1748-9326/acc95f.

Abstract

The physical hydroclimate system of the Amazon functions on several spatial and temporal scales. Large-scale processes control the main seasonal patterns of atmospheric circulation and rainfall. Seasonal variability in solar forcing, associated with the low rainforest albedo, provides energy for continental heating, convection, and the onset of the South American monsoon. Mesoscale processes cause localized circulation such as river breeze and deforestation breeze. I assessed the impact of different deforestation scenarios for the mid-century last decade rainy season. Here I describe a yet unreported synoptic-scale circulation that delays the rainy season onset in southern Amazonia. This model-predicted circulation is driven by extensive (ca. 40%) deforestation patterns and may last as long as two months. This persistent anomalous circulation may result in a rainy season onset delay of 30 – 40 days compared to the historical period. Like other synoptic-scale phenomena, differences in surface heating drive this circulation. Given the unabated deforestation trends, the consequences for local ecosystems, agriculture, and power generation of delayed rainy season onset associated with this circulation may be difficult to revert.

3.1. Introduction

The seasonal behavior of the Amazon's hydroclimate is related to large-scale mechanisms such as the Intertropical Convergence Zone and the South American Monsoon System, which cause most of the region's rain to fall during summer (Wright *et al.*, 2017; Mu and Jones, 2022; Sierra *et al.*, 2022; Talamoni *et al.*, 2022). In addition, the South Atlantic Convergence Zone is a monsoon trough convergence band oriented in the northwest–southeast direction and ranging from the Amazon basin to the tropical South Atlantic Ocean (Sierra *et al.*, 2022; Talamoni *et al.*, 2022). Moreover, the El Niño–Southern Oscillation controls the main interannual hydroclimate variability in Amazon (Marengo *et al.*, 2021b; Espinoza *et al.*, 2022) and has contributed to severe droughts in the basin recently (Marengo *et al.*, 2021b; Mu and Jones, 2022).

Northwestward of an SW–NE diagonal ranging from 16° S, 60° W to 4° S, 45° W, the Amazon climate is humid, with either no dry season or just a less rainy season (Koppen's Af and Am) (Alvares *et al.*, 2013). As this diagonal is crossed, in southern Amazonia (SA), the climate transitions from humid to seasonal (Koppen's Aw). The onset of the rainy season in SA is related to large-scale mechanisms and heterogeneous solar heating promoting convection in the region (Leite-Filho *et al.*, 2020; Espinoza *et al.*, 2022). The heating promotes evapotranspiration, increasing atmospheric moisture and preconditioning the regional convection for the rainy season onset (Wright *et al.*, 2017; Talamoni *et al.*, 2022).

In the last few decades, the rainy season onset in SA has been delayed(Fu *et al.*, 2013; Leite-Filho *et al.*, 2020). This behavior relates to changes in atmospheric circulation, regional convective energy (Wright *et al.*, 2017; Talamoni *et al.*, 2022), and land-use change by deforestation (Leite-Filho *et al.*, 2020; Staal *et al.*, 2020). Specifically, deforestation can change the surface energy balance and surface roughness, creating feedbacks that reduces rainfall and delays the rainy season onset (Stickler *et al.*, 2013; Lawrence and Vandecar, 2015; Khanna *et al.*, 2017; Staal *et al.*, 2020; Caballero *et al.*, 2022b; Mu and Jones, 2022).

Early studies that analyzed the effects of complete Amazon deforestation on climate simulated a reduction in the evapotranspiration and precipitation proportional to the increase in the land surface albedo, which would impact the surface energy fluxes (latent and sensible heat) (Shukla *et al.*, 1990; Dirmeyer and Shukla, 1994; Eltahir and Bras, 1996; Costa and Foley, 2000; Sampaio *et al.*, 2007). In the simulations, these energy fluxes promoted a change in the atmospheric circulation, impacting the rainfall volume and rainy season timing due to anomalous subsidence over the region.

However, current deforestation patterns are fragmented and on the scale of a few tens of kilometers. Mesoscale forest clearing creates a thermally driven mesoscale (10–100 km) circulation called the deforestation breeze (Saad *et al.*, 2010; Lawrence and Vandecar, 2015; Fassoni-Andrade *et al.*, 2021). This circulation may promote subsidence, diminishing rainfall upwind of the deforested areas (Saad *et al.*, 2010; Khanna *et al.*, 2017).

Analyses of intermediate-scale deforestation scenarios in the last two decades have associated deforestation with rainfall decrease (Costa *et al.*, 2007; Sampaio *et al.*, 2007; Pires and Costa, 2013; Spracklen and Garcia-Carreras, 2015), but the coarse-resolution models (~300 km) used in these analyses might not have correctly represented the circulation dynamics between the mesoscale and the large-scale processes. Those models' resolutions might also have affected land-atmosphere interactions since there is an apparent relationship between the deforestation scale and rainfall impact (Spracklen and Garcia-Carreras, 2015; Leite-Filho *et al.*, 2021; Caballero *et al.*, 2022b; Mu and Jones, 2022; Smith *et al.*, 2023).

Here I use a fine-resolution (0.9° × 1.25°) coupled climate system model to investigate the effects of realistic deforestation scenarios on the Amazon's climate and increasing atmospheric CO_2 concentrations. While I follow the representative concentration pathways (RCPs) of the Coupled Model Intercomparison Project Phase 5 (CMIP5), I consider their land-use scenarios too optimistic for Amazonia. RCP8.5 assumed Amazon deforestation of 20% by 2050 (Pires *et al.*, 2016), which is close to estimates of the current (2020) levels of Amazon deforestation (~838,000 km²) (Souza *et al.*, 2020). Instead of using the default CMIP5 scenarios, I used two realistic deforestation pathways that emerged from different environmental policy scenarios (Rochedo *et al.*, 2018). The strong environmental governance (SEG) scenario enhances forest legislation and conservation, while the weak environmental governance (WEG) scenario renounces deforestation control and reinforces predatory practices (Rochedo *et al.*, 2018; Leite-Filho *et al.*, 2021). In the SEG pathway, the deforested area will be ~23% in 2050, while with WEG, deforestation could reach ~1,700,000 km² (~40%) by the same time (Rochedo *et al.*, 2018).

3.2. Methods

3.2.1. Climate simulations

I used the Community Earth System Model version 1.0.6 (CESM) (Hurrell *et al.*, 2013). CESM is a fully coupled model capable of simulating interactions between the different components of the climate system, such as the atmosphere, oceans, cryosphere, and land surface (Hurrell *et al.*, 2013; Sampaio *et al.*, 2021). I arranged the simulations to reproduce the original

RCP2.6 and RCP8.5 CMIP5 simulations with coupled atmosphere, ocean, sea, and ice, except for the land-use patterns inside Brazil, where the original RCP land-use patterns were replaced by those of two locally informed environmental governance (EG) scenarios (see below).

The Community Land Model version 4 (CLM) is the component that represents surface processes in CESM (Hurrell *et al.*, 2013). It represents the transient land-cover change between the fractions of 15 plant functional types (PFTs), each with its own set of physiological parameters and RCP's emissions effects on it.

Four initializations were performed for each scenario, with initial historical conditions taken from four ensemble members of the historical experiment with the original CCSM4 (Community Climate System Model version 4, former name of CESM) for the year 2005, thus replicating the original initial conditions of the scenarios present in the RCP simulations from CMIP5.

3.2.2. Environmental governance scenarios

Inside Brazil, land-use patterns for CLM were taken from two scenarios representing land-use futures under two levels of environmental governance: weak environmental governance (WEG) and strong environmental governance (SEG). Both EG scenarios considered the trajectory of Brazilian environmental policy, land use, and occupation in recent years (Rochedo *et al.*, 2018).

The WEG scenario represents the worst possible case for the environment, indicating policies to support the development of agriculture with zero sustainability. WEG was designed to replicate the deforestation trends of the pre-2005 period when the environmental governance of the Amazon and Cerrado was at its lowest. The SEG scenario assumes that environmental policies will be enforced and have government support, with conservationist practices and economic incentives for preservation, replicating deforestation rates from the 2005–2012 period when environmental governance was substantially reinforced (Rochedo *et al.*, 2018).

The EG scenarios consist of yearly land-cover information on a 25 ha grid discriminated into 31 classes. These were reclassified into crops, pasture, natural vegetation, and planted forest, and then further reclassified into CLM’s 15 PFTs (Table S3.1). Natural vegetation was mapped to a combination of PFTs with the same fraction as those in the primary vegetation maps from Ramankutty and Foley (Ramankutty and Foley, 1999). For a more detailed description of the mappings, refer to Oleson et al. (Oleson *et al.*, 2010).

3.2.3. Anomalies for the decade 2040–2050

I ran the simulations for 2012–2050 for four scenarios that combined climate forcings and EGs: RCP2.6-WEG, RCP2.6-SEG, RCP8.5-WEG, and RCP8.5-SEG. I calculated anomalies between the EG scenarios (WEG − SEG) to assess their effects on the rainy season onset. The onset is defined as the start of the lengthiest period when rainfall exceeds the established threshold for a specific region (Supplementary methods – Eq. 1). I calculated monthly averages for zonal, meridional, and vertical wind, rainfall, net radiative flux (Rn), and heat fluxes (latent and sensible) for 2040–2050 for September, October, and November.

3.3. Results

3.3.1. Rainfall validation

To assess the model's skill, I compared its rainfall results with an ensemble of observed precipitation data comprising the GPCC, CHIRPS, and PERSIANN-CDR (described in the Supplementary methods). The CESM simulations behavior (Figure 3.1a-b) was similar to the observed data (Figure 3.1c–d), showing higher precipitation over the northern portion of the Amazon and decreasing the rainfall amount in the southern direction. Most anomalies were between ±2mm/day (Figure 3.e-f), with significant differences in September (Figure 3.1e).

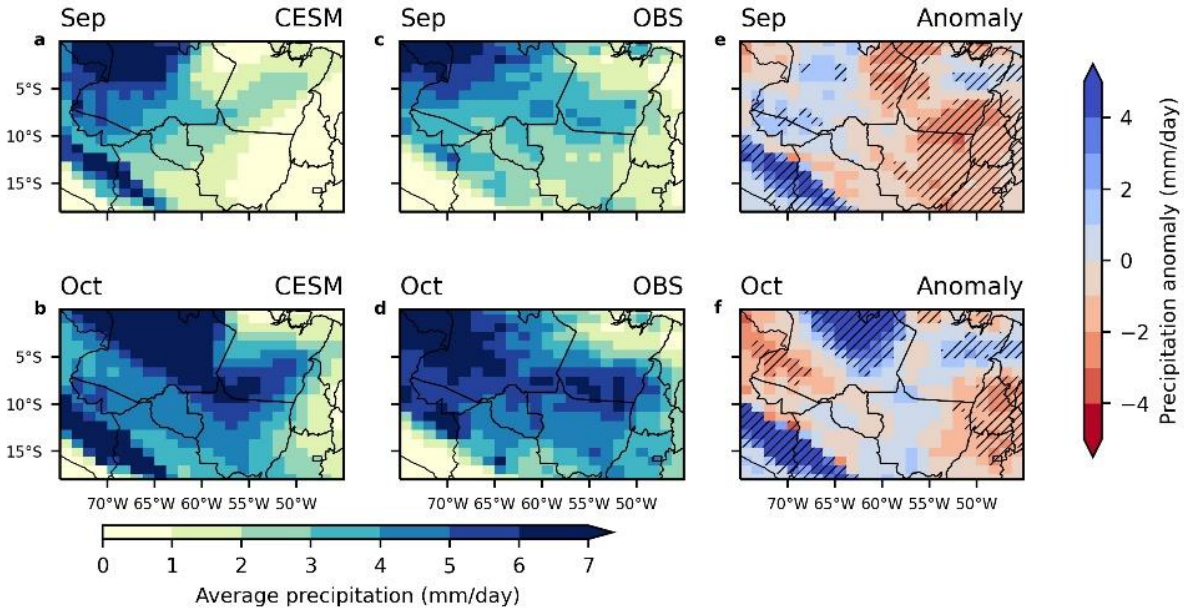

Figure 3.1 – Monthly mean precipitation and anomalies for CESM historical period and the observed data (1990-2005). CESM precipitation (a – b), average observed precipitation (c – d), and precipitation anomalies (e – f). Shaded areas indicate differences significant at $\alpha = 0.05$

3.3.2. Climate response to different environmental governance scenarios

While the SEG deforestation is not much different from 2020 deforestation levels, the WEG pathways promote more extensive and heavier deforestation in SA (Figure 3.2). The difference between the WEG and SEG scenarios is always greater than 5%, but in northern Mato Grosso and along paved roads, the deforestation differences are over 60% (Figure 3.2g).

There was an increase in deforestation for the 2040-2050 decade (Figure 3.2c–f), especially in the WEG scenario AM, MT, and PA frontiers increased deforestation. What showed a change in the PFTs compositions with an expansion in croplands and pasture.

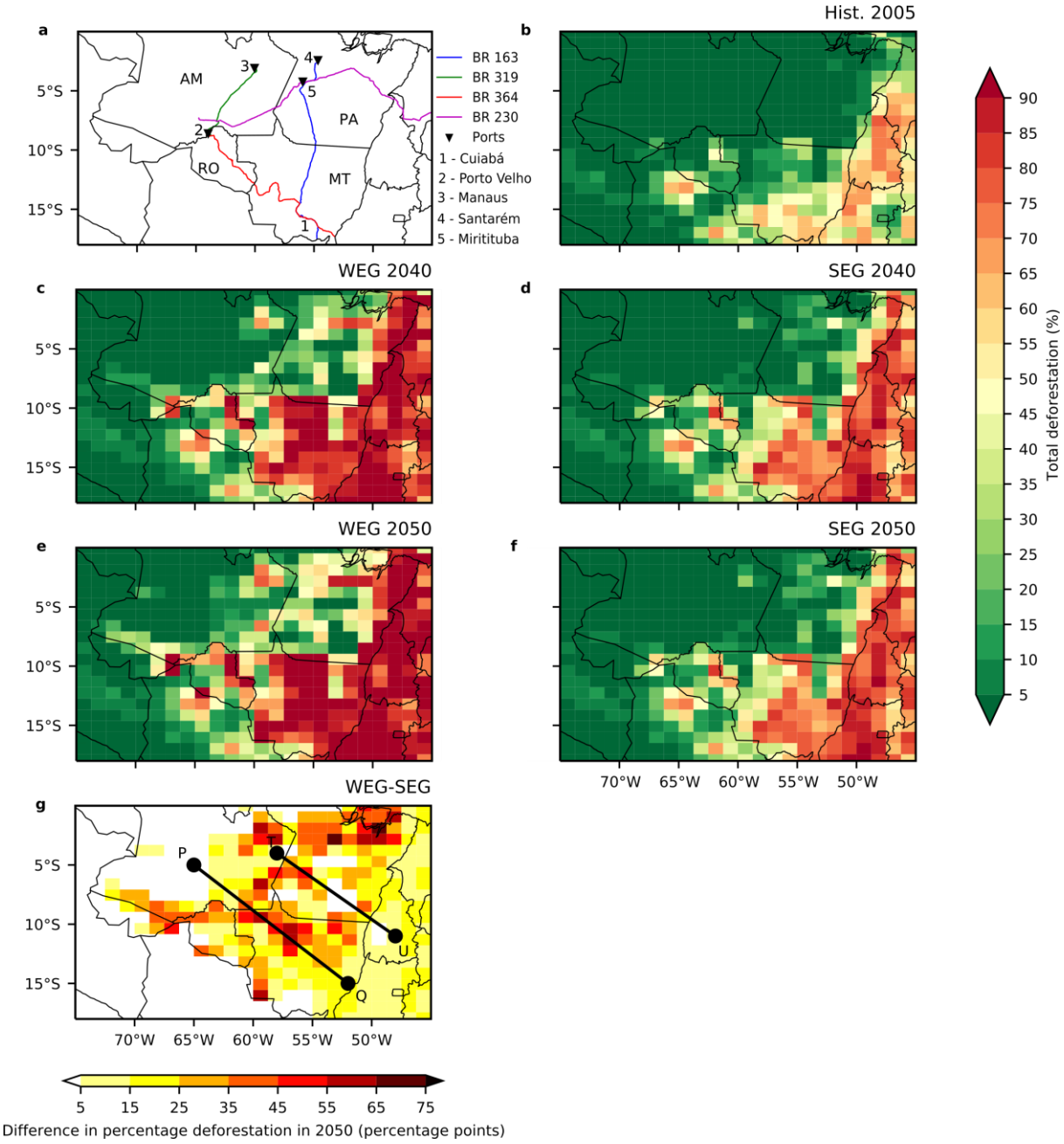

Figure 3.2 – Study area, with main roads, deforestation (historical and scenarios), and scenarios differences. Orientation map (a) with state names (AM – Amazonas, MT – Mato Grosso, PA – Pará, and RO – Rondônia), major cities (numbered), ports (black triangles), and highways (labeled BR). P–Q and T–U indicate two cross-sections for circulation analyses. Total deforestation in 2005 (b), 2040 according to WEG (c) and SEG (d), and 2050 according to WEG (e) and SEG (f) pathways and the difference between them, calculated as WEG − SEG (g).

The differences between deforestation scenarios influence the energy partitioning and distribution over the region, revealing previously unreported shallow synoptic-scale circulation over SA and Mato Grosso (Figure 3.3). This circulation can be as deep as 600 hPa in September and October (Figure 3.3a, b, e, f, i, j, m, and n) and extends from 1,200 to 1,500 km (Figure 3.4). I noticed a clearer circulation for RCP2.6 in September (Figures 3a and i), while RCP8.5

presented a later circulation pattern in October (Figures 3f and n), with sharper circulation behavior (Figures 3e, f, m, and n). This synoptic circulation is absent in November, when the rainy season has already started.

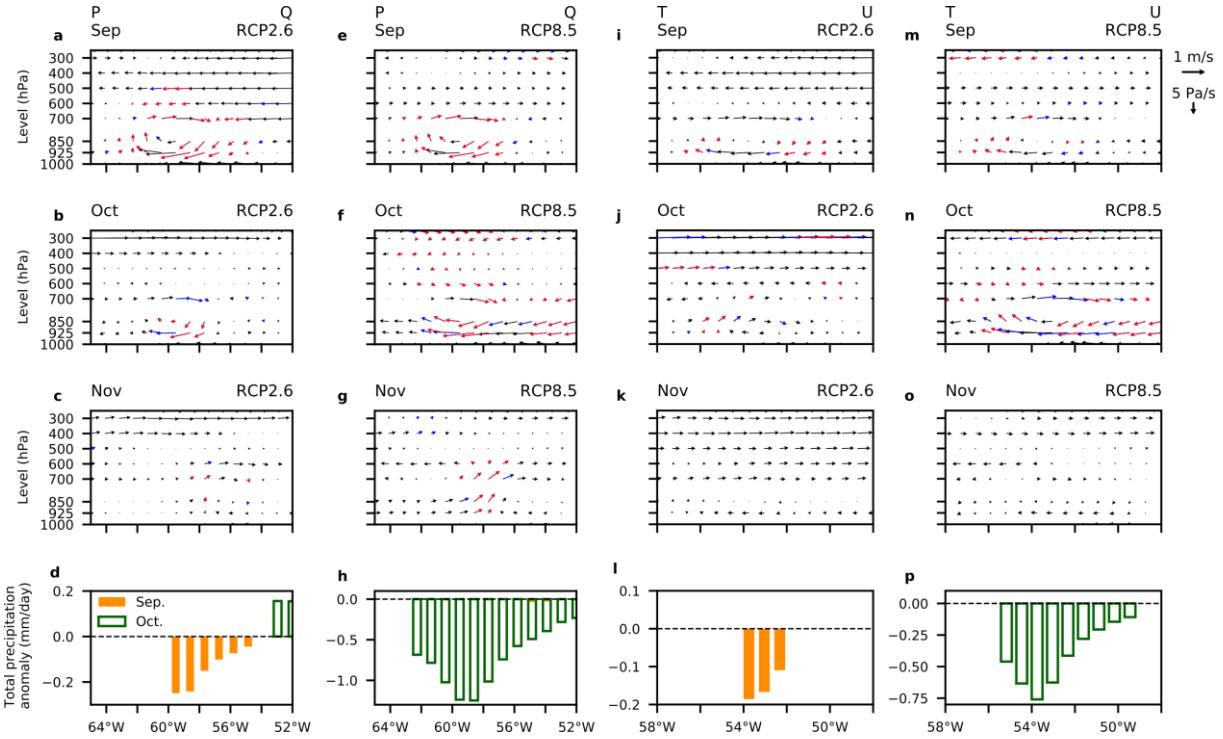

Figure 3.3 – Synoptic-scale circulation and its impacts on precipitation. Zonal winds and vertical velocity anomalies calculated as WEG − SEG over the cross-sections P–Q (a–c, e–g) and T–U (i–k, m–o) for September and October (the rainy season onset months) and for November (when the rainy season is already established); red and blue arrows indicate significant differences at $\alpha = 0.05$ and 0.10, respectively. Total precipitation changes calculated as WEG − SEG over cross-section P–Q for RCP2.6 and RCP8.5 (d and h) and cross-section T–U for RCP2.6 and RCP8.5 (l and p) that are significant at $\alpha = 0.10$; values of precipitation not shown are not significant at $\alpha = 0.10$.

Regarding the circulation pattern, I observed a dipole behavior over SA (Figure 3.3) with a subsidence branch over northern Mato Grosso (MT) and an ascending branch over the southern state of Amazonas (Figure 3.4). In RCP8.5, most of Mato Grosso experiences a subsidence anomaly (Figure 3.4d). These subsidence regions cause a significant ($\alpha = 0.05$) delay in the rainy season onset (Figure 3.5).

The subsidence occurs mostly over regions with a negative net surface radiative flux (Rn) anomaly (Figure S3.3.1a–d), associated with the albedo increase due to deforestation in the region (Figure 3.2g). Rn reductions cause reductions in both sensible heat flux (H) and the injection of water vapor into the atmosphere (reduction in latent heat flux LE) (Figure S3.3.2

and Figure S3.3.3). Similarly, the increased convection occurs where Rn has a positive anomaly, mostly in September (Figure S3.3.1a–b). This spatial energy distribution mirrors the ascending and descending circulation branches, characterizing a thermally induced circulation.

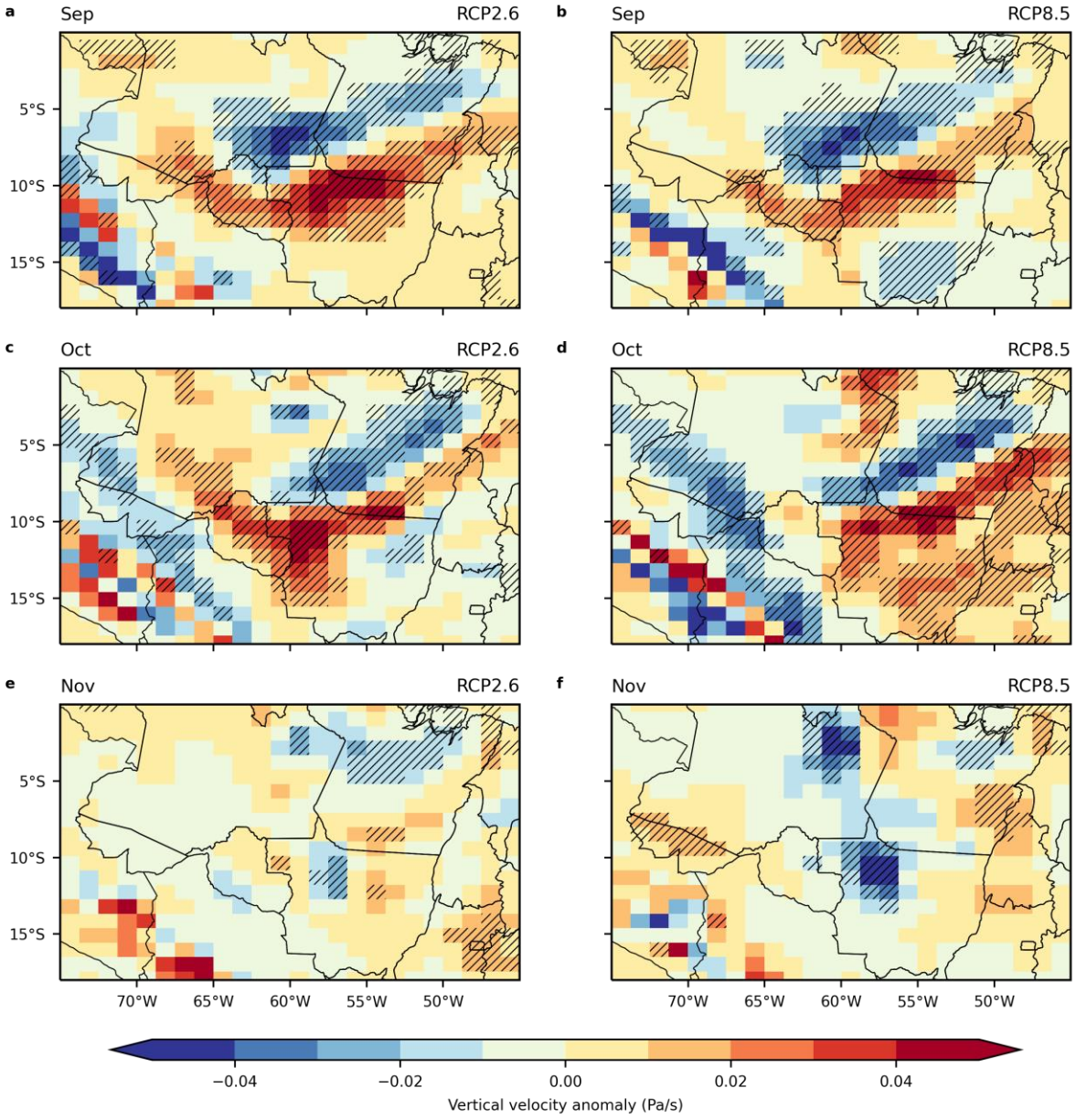

Figure 3.4 – Vertical velocity (omega) anomalies at 850 hPa were calculated as WEG − SEG for RCP2.6 (a, c, e) and RCP8.5 (b, d, f). Shaded areas indicate results significant at α = 0.05.

Global warming and deforestation patterns cause significant rainfall anomalies (Figure S3.3.4) and a significant delay in the rainy season onset (Figure 3.5 and Figure S3.3.5). For my four scenarios in SA, RCP2.6 shows an average onset on September 30 and October 4 for SEG

and WEG, respectively (Figure S3.3.5b and c), while RCP8.5 shows an average onset on October 1 and 7 for SEG and WEG (Figure S3.3.5d and e), respectively.

The circulation anomaly exhibits a predominant subsidence movement over SA and MT during September and October (Figure 3.3 and Figure 3.4a–d) when the rainy season usually begins in these areas (Figure S3.3.5a). In RCP2.6, the circulation affects most of SA, all of MT, and Pará, with anomalies as long as 12 days (Figure 3.5a). The significant anomalies increase spatially for RCP8.5, with a longer delay values (Figure 3.5b). I also observed that, comparing the historical (1990–2005) onset with the worst scenario (RCP8.5 + WEG), the delay in the onset can reach 30–40 days (Figure S3.3.5a and e), and the areas with significant onset delay extend geographically over most of MT (Figure 3.5b).

RCP2.6 is associated with an earlier onset than RCP8.5 (Figure S3.3.5b–e). Rainfall reductions are more significant in September in RCP2.6, while in RCP8.5, the main reductions happen in October (Figures S4a and d).

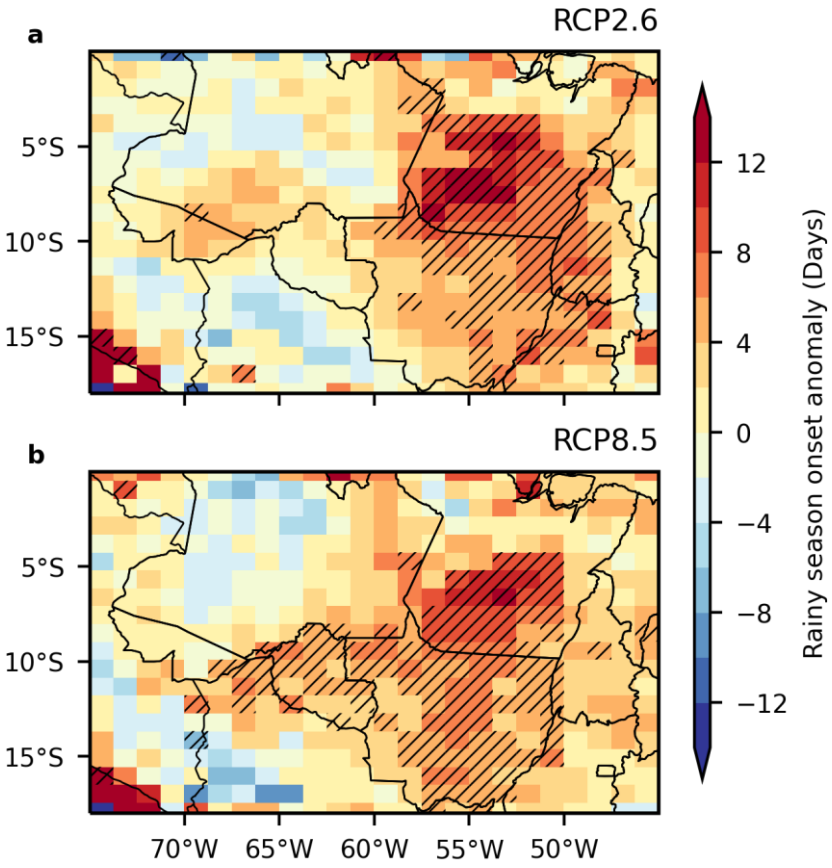

Figure 3.5 – Rainy season onset anomalies, in days, were calculated as WEG − SEG for RCP2.6 (a) and RCP8.5 (b). Shaded areas indicate anomalies significant at $\alpha = 0.05$.

3.4. Discussion

3.4.1. Model validation

My simulation represented the land-atmosphere interactions overAmazon as an energy-limited process, in agreement with observations and other CESM experiments (Baker *et al.*, 2021). Moreover, CESM accurately represented the circulation pattern and its impact on precipitation variability in South America (Olmo *et al.*, 2022). Furthermore, CESM's precipitation behavior was similar to the observations (Figure 3.1), following previous multimodel evaluations, including some underestimation over the Amazon (Firpo *et al.*, 2022; Monteverde *et al.*, 2022). My work is innovative in presenting a monthly scale analysis, which identifies with more detail differences in model simulations compared to annual means.

Previous works suggested good simulations of vegetation water cycles and energy fluxes by land surface models (CLM included) in Amazon (Christoffersen *et al.*, 2014; Restrepo-Coupe *et al.*, 2021). When replacing forests with C4 grasses, CLM tends to produce higher LE values in CESM simulations because C4 grasses are very productive in tropical regions (Boysen *et al.*, 2020). Thus, increased values in LE coinciding with high deforestation regions (Figure S3.3.3c) were related to increased evapotranspiration due to an enhanced C4 plant's leaf area index (LAI) (Figure S3.3.7c). Although this behavior does not match observed evapotranspiration after vegetation loss, neither in forests nor pastures (Spracklen *et al.*, 2018), it could be related to the physiological effects of CO_2 or may be model-specific due to the model parametrization (Boysen et al 2020, Pitman et al 2009) and thus may bring uncertainty to the generalization of the results. However, I keep the original CLM parameterization to maintain full compatibility with the CMIP5 simulations.

Nevertheless, my simulations indicated increased precipitation (Figure S3.3.4c) where the LE and LAI were higher (Figure S3.3.3c and Figure S3.3.7c), demonstrating a cohesive relation between evapotranspiration and rainfall over Amazon, similar to previous ESM analysis (Lawrence and Vandecar, 2015; Boysen *et al.*, 2020; Baker *et al.*, 2021)

3.4.2. Climate response and impacts of different environmental governance scenarios

Large-scale circulation patterns influence rainfall in SA all year (Mu and Jones, 2022; Sierra *et al.*, 2022; Talamoni *et al.*, 2022), while mesoscale circulations induced by deforestation have a much shorter duration (Saad *et al.*, 2010; Lawrence and Vandecar, 2015; Khanna *et al.*, 2017; Sierra *et al.*, 2022). My results showed a deforestation-induced synoptical scale circulation anomaly with a duration of two months (Figure 3.3 and Figure 3.4), impacting the early rainy season in SA.

The additional deforestation disturbed the net radiation balance and partitioning over SA, with negative anomalies in the Rn and LE (Figure S3.3.1 and Figure S3.3.3), creating a subsidence circulation that reduced the rainfall and delayed the rainy season. Moreover, the persistence of the circulation anomaly during the dry-to-wet transition months (September–October) exacerbated the magnitude and spatial extent of the delayed rainy season onset.

Despite the known impact of reducing evaporation and precipitation, highlighting the significance of surface fluxes (Findell *et al.*, 2011; Lee *et al.*, 2012), the role of synoptic-scale phenomena is often overlooked in such cases, particularly in the context of extensive deforestation as discussed herein.

The expansion of roads in the Amazon has been causing deforestation since the 1970s, transitioning forests to agriculture around BR-230 (Moran, 2016; Li *et al.*, 2019). Yet deforestation was constrained by the poor condition of Amazonia's non paved highways. These constraints have recently been removed since the recent expansion and paving of BR-163 and BR-319 (Figure 3.2a). The paving of BR-163 between the Mato Grosso–Pará border and the Miritituba Port between 2019 and 2021 and the ongoing paving of BR-319 linking Porto Velho to Manaus have facilitated access to these regions leading to further deforestation due to land occupation for agriculture expansion (Andrade *et al.*, 2021; Ferrante *et al.*, 2021). Regions closer to Santarém showed higher deforestation over WEG (Figure 3.2g), confirming the negative impact of BR-163 under weak governance (Soares-Filho *et al.*, 2004; Saad *et al.*, 2010). However, a higher-resolution model could provide more detailed information on road-level deforestation.

Deforestation impacted climates in both RCP scenarios through changes in atmospheric circulation, rainy season onset, and rainfall (Figure 3.3, Figure 3.5, and Figure S3.3.4, respectively). These results are consistent with several studies that relate deforestation and global warming to rainfall reduction and rainy season delay (Lawrence and Vandecar, 2015; Khanna *et al.*, 2017; Wright *et al.*, 2017; Costa *et al.*, 2019; Leite-Filho *et al.*, 2020; Baudena *et al.*, 2021; Leite-Filho *et al.*, 2021). However, in this study, I simulated a spatially long (~1,200–1,500 km) and persistent (2 months) circulation pattern.

The effects on the delayed rainy season onset were more spatially extensive in RCP8.5 (Figure 3.5b), affecting most of Mato Grosso and producing a significant reduction in October precipitation (Figure S3.3.4d) (>60% reduction, $\alpha = 0.05$). Mato Grosso's agriculture has already been demonstrated to be extremely sensitive to deforestation and climate change (Costa *et al.*, 2019). Other authors have noted rainfall reductions in RCP8.5 combined with

deforestation (Pires *et al.*, 2016; Sampaio *et al.*, 2021). In RCP2.6, significant ($\alpha = 0.05$) effects of deforestation were most extensive at the rainy season onset (Figure 3.5a) but smaller than in RCP8.5. However, the impacts on total precipitation were mostly non-significant, with significant changes limited to smaller regions (Figure S3.3.4).

Even the original RCP scenarios, which considered limited deforestation scenarios, caused a delayed rainy season onset and precipitation reductions for agriculture and land-use dynamics in the region (Fu *et al.*, 2013; Pires *et al.*, 2016; Costa *et al.*, 2019; Brumatti *et al.*, 2020). In addition, deforestation itself has been shown to reduce precipitation and delay the rainy season onset (Lawrence and Vandecar, 2015; Khanna *et al.*, 2017; Leite-Filho *et al.*, 2020; Leite-Filho *et al.*, 2021). Previous studies have attempted to add the climate effects of global warming and realistic deforestation linearly (Pires *et al.*, 2016; Brumatti *et al.*, 2020), showing that both forcings cause effects in the same direction, but without considering the feedback between them and with the rest of the climate system. Here I have demonstrated that the two effects (increased CO_2 and realistic land use), combined with their feedbacks, may promote a vaster and more persistent impact on rainy season onset (Figure 3.5) and precipitation reductions due to the long-lasting subsidence anomaly described here.

Along with climate change, deforestation and forest degradation will impact the Amazon's hydroclimate, ecosystem services, and ecosystem vulnerability. While forest preservation is an ally to ecosystem services (Strand *et al.*, 2018; Flach *et al.*, 2021; Rattis *et al.*, 2021), a shorter rainy season enhances ecosystem vulnerability (Gatti *et al.*, 2021) and has consequences for agriculture and hydropower generation, as discussed below.

The realistic deforestation scenarios explored here incorporate the likely consequences of the paved road infrastructure that has recently been constructed in the Amazon; this infrastructure is facilitating agricultural expansion and increasing forest fragmentation (Rochedo *et al.*, 2018; Strand *et al.*, 2018; Andrade *et al.*, 2021). This deforestation course—together with rising temperature, increasing vapor pressure deficit, and increasing fires—can destabilize or even collapse the rainforest ecosystem (Brando *et al.*, 2020; Gatti *et al.*, 2021; Oliveira *et al.*, 2022; Xu *et al.*, 2022b). With a shorter rainy season and a vulnerable ecosystem, the risk to biodiversity preservation increases dramatically (Strand *et al.*, 2018; Boulton *et al.*, 2022), thus turning forest conservation into a greater challenge (Brando *et al.*, 2020; Gatti *et al.*, 2021).

Because of the climate feedbacks, agricultural expansion over Amazonia may produce results opposite from what is expected, that is, leading to lower productivity and instigating

several negative economic consequences associated with agricultural activities (Costa *et al.*, 2019; Brumatti *et al.*, 2020; Spera *et al.*, 2020; Leite-Filho *et al.*, 2021; Rattis *et al.*, 2021). Previous studies that did not consider the persistent effects I have found concluded that deforestation could cost SA agriculture US$1 billion annually through the mid-century (Leite-Filho *et al.*, 2021). My results suggest that the impact on agriculture may be even more severe. Mato Grosso is the most affected region, with the longest delay in the rainy season onset (Figure S3.3.5) due to the deforestation-induced circulation. Equivalent results from other studies for the rainy season in Mato Grosso have shown negative impacts for double cropping (Costa *et al.*, 2019; Zhang *et al.*, 2021), damaging the state's economy and productivity (Strand *et al.*, 2018; Spera *et al.*, 2020). Deforestation alone could decrease yield by 20% (Spera *et al.*, 2020). Combining the effects of deforestation and rising greenhouse gases, but without considering the positive feedback between them, yield decreases may lead to US$2.8 billion in annual losses by 2050 (Brumatti *et al.*, 2020). Thus, when considering a persistent circulation that strongly influences the early rainy season, the losses may be stronger, as calculated below.

Moreover, the Tapajós and the Xingu, Amazon River's southern tributaries that drain Mato Grosso, have many hydropower plants in operation, with many others under construction (Couto *et al.*, 2021; Wasti *et al.*, 2022). Most of these plants use the run-of-the-river concept (i.e., they incorporate little to no water storage) to reduce dam flooding impacts (Stickler *et al.*, 2013; Arias *et al.*, 2020; Costa, 2020; Couto *et al.*, 2021). Unfortunately, a run-of-the-river design is largely susceptible to river discharge seasonality (Arias *et al.*, 2020), i.e., to changes in the duration of the dry season. A longer dry season and reduced precipitation could undermine billions of dollars of hydropower infrastructure (Stickler *et al.*, 2013; Arias *et al.*, 2020; Costa, 2020).

My results suggest a delay in the onset and a reduction in the length of the rainy season in Amazonia's Tapajós and Xingu basins (Figure 3.5 and Figure S3.3.6), where most of the hydropower expansion is planned to happen (Couto *et al.*, 2021). This rainy season behavior could diminish hydropower generation during the transitional and dry seasons, enhancing energy insecurity. Future hydropower generation, autonomy, and planning will depend much more on the presence of trees (Costa, 2020; Wasti *et al.*, 2022), especially in dystopic scenarios with dry seasons of longer duration.

Using similar deforestation pathways, Strand *et al* (2018) calculated losses in climate-related ecosystem services that reach US$1.84 ha^{-1} $year^{-1}$ and US$9 ha^{-1} $year^{-1}$ for hydropower generation and agriculture, respectively. Using these relationships, the WEG

scenario (1,700 Mha deforested) would translate to losses of US$3.1 billion year^{-1} for hydropower generation and US$15 billion year^{-1} for agriculture. However, these computations do not consider the persistent circulation discovered in this work, which may enhance the duration of the dry season year after year. Considering the changes in the atmospheric circulation described here, SA could face substantial losses in the agribusiness and hydropower sectors.

Since the atmosphere–biosphere feedback contributes to most of my results, after the loss of the rainforest, effects of this feedback would be difficult to reverse. It would require over a million square kilometers of reforestation to undo them (Baudena *et al.*, 2021; Tuinenburg *et al.*, 2022), reversing the trajectory of the last 50 years' events and the predictions for the next three decades. Additional atmosphere–biosphere feedbacks not considered in this study could lead to savannization, seasonalization, or even dieback of parts of Amazonia's forests (Lovejoy and Nobre, 2018; Boulton *et al.*, 2022), with possibly irreversible consequences.

3.5. Supplementary Material

3.5.1. Supplementary method

3.5.1.1. Study region

The southern Amazon (SA) is a transition region between humid tropical forest and Cerrado with a strong agricultural presence, and it covers 30 to 40% of the Amazon biome (Wright *et al.*, 2017). In recent decades, SA's dry season has lengthened (Fu *et al.*, 2013), which may be related to deforestation impacting the rainy season (Wright *et al.*, 2017; Leite-Filho *et al.*, 2020). My study defines SA as ranging from 5° S to 15° S latitude and from 66° W to 51° W longitude; I also include the state of Mato Grosso due to the possible implications of climate change and the delayed onset of rainfall for agriculture in the state, where a substantial fraction of Brazil's soybean, maize and cotton production is located (Abrahão and Costa, 2018; Brumatti *et al.*, 2020).

3.5.1.2. Plant Functional Types (PFTs)

Table S3.1 – CESM Plant Functional Types (PFT) adapted from land use classes in Rochedo et al. (2018). I used a combination of PFTs with the same fraction as those in Ramankutty and Foley (1999, RF99) primary vegetation maps.

Rochedo et al. (2018) land use class	CESM PFT
Water	Ignored
Urban	Ignored

Pasture	C4 grasses (PFT 14)
Pasture in protected area	C4 grasses (PFT 14)
Savanna	Primary vegetation (RF99)
Savanna in protected area	Primary vegetation (RF99)
Forest	Primary vegetation (RF99)
Forest in protected area	Primary vegetation (RF99)
Soy	Crops (PFT 15)
Sugarcane	Crops (PFT 15)
Maize	Crops (PFT 15)
Cotton	Crops (PFT 15)
Rice	Crops (PFT 15)
Wheat	Crops (PFT 15)
Dry beans	Crops (PFT 15)
Coffee (Arabica)	Crops (PFT 15)
Coffee (Robusta)	Crops (PFT 15)
Oranges	Crops (PFT 15)
Cassava	Crops (PFT 15)
Bananas	Crops (PFT 15)
Cocoa	Crops (PFT 15)
Tobacco	Crops (PFT 15)
Maize (2nd season)	Crops (PFT 15)
Dry beans (2nd season)	Crops (PFT 15)
Planted forest	Broadleaf evergreen trees (PFT 5)
Soy-Maize	Crops (PFT 15)
Soy-Wheat	Crops (PFT 15)
Maize-Wheat	Crops (PFT 15)
Soy-Dry beans	Crops (PFT 15)
Maize-Dry beans	Crops (PFT 15)
Dry beans-Dry beans	Crops (PFT 15)

3.5.1.3. Observed rainfall products

Precipitation retrievals consist 1990-2005 period in a daily timestep for three observation products to describe the regional rainfall behavior: i) The Precipitation Estimation from Remotely Sensed Information using Artificial Neural Networks—Climate Data Record (PERSIANN-CDR) uses artificial neural networks to estimate precipitation based on infrared and images from satellites (Nguyen *et al.*, 2019); ii) The Climate Hazards Group Infrared Precipitation (CHIRPS) consists of a rainfall station and satellite data along with cold cloud duration retrievals to estimate precipitation (Funk *et al.*, 2015); iii) The Global Precipitation Climatology Centre (GPCC) gauge-based product interpolates station observed data to a regular grid (Schamm *et al.*, 2014). I used these datasets to calculate an average observed precipitation for September and October to validate the model's monthly mean precipitation.

3.5.1.4. Rainy season onset

I used a modified anomalous accumulation method (Arvor *et al.*, 2014; Abrahão and Costa, 2018) to calculate the onset of the rainy season (Eq. 1). This method considers a relation between the daily rainfall (R_n) and a reference value (R_{ref}).

$$AA\ (day) = \sum_{n=1}^{dia} R_n - R_{ref} \quad (1)$$

I used 2.5 mm day^{-1} as R_{ref}, representative of water needs for soybean seedlings. This method has already been used in several studies in SA and Mato Grosso(Pires *et al.*, 2016; Abrahão and Costa, 2018; Leite-Filho *et al.*, 2020). Onset values obtained using this method and this R_{ref} value were well correlated with soybean planting dates in the region (Zhang *et al.*, 2021).

I obtained the rainy season onset for all four scenarios. Then, I calculated the anomalies between the environmental governance scenarios (WEG − SEG) for the averages over the decade 2040–2050.

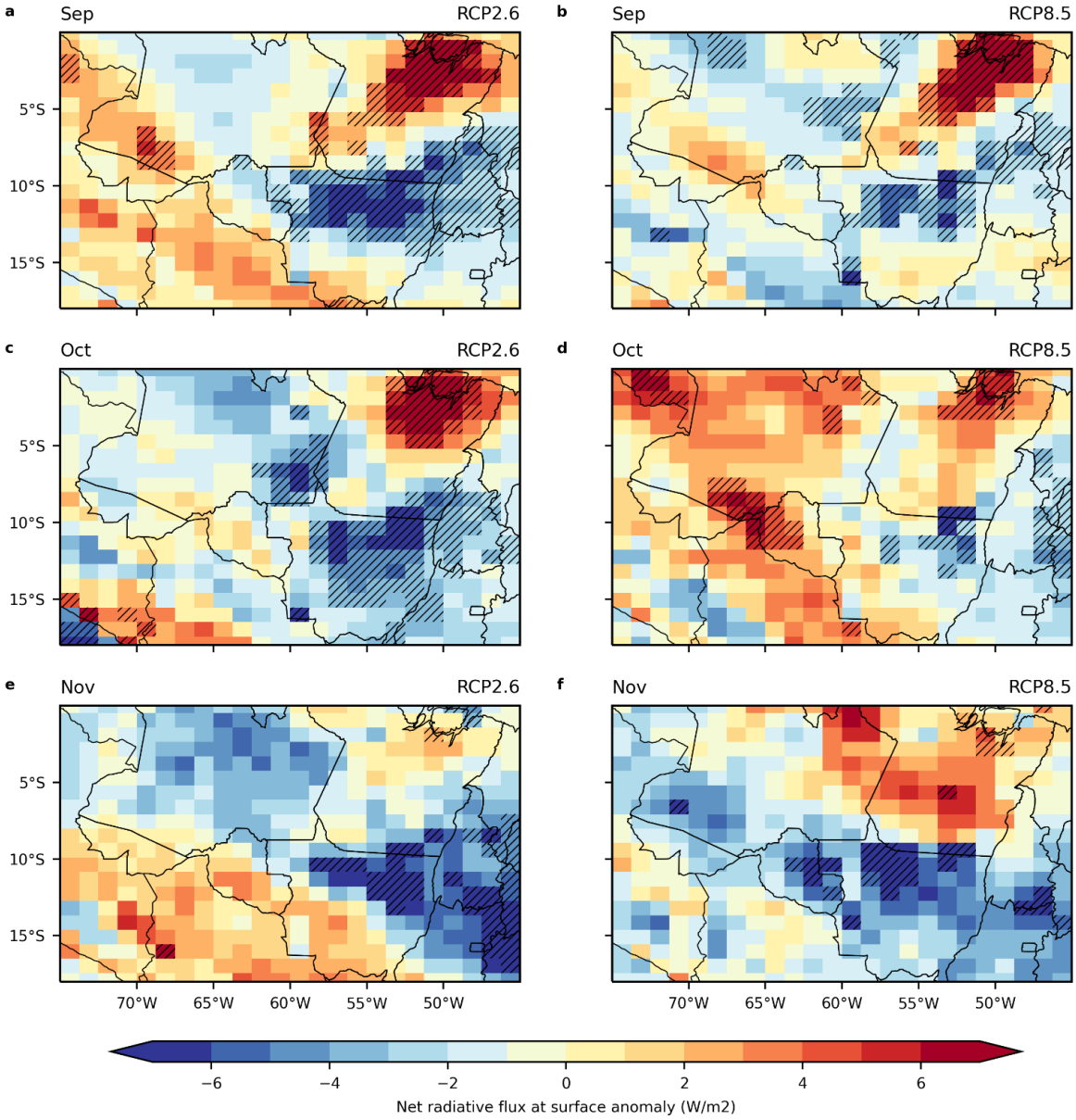

Figure S3.1 – Net radiative flux at surface anomalies calculated as WEG − SEG for RCP2.6 (a, c, e) and RCP8.5 (b, d, f). Shaded areas indicate results significant at $\alpha = 0.05$.

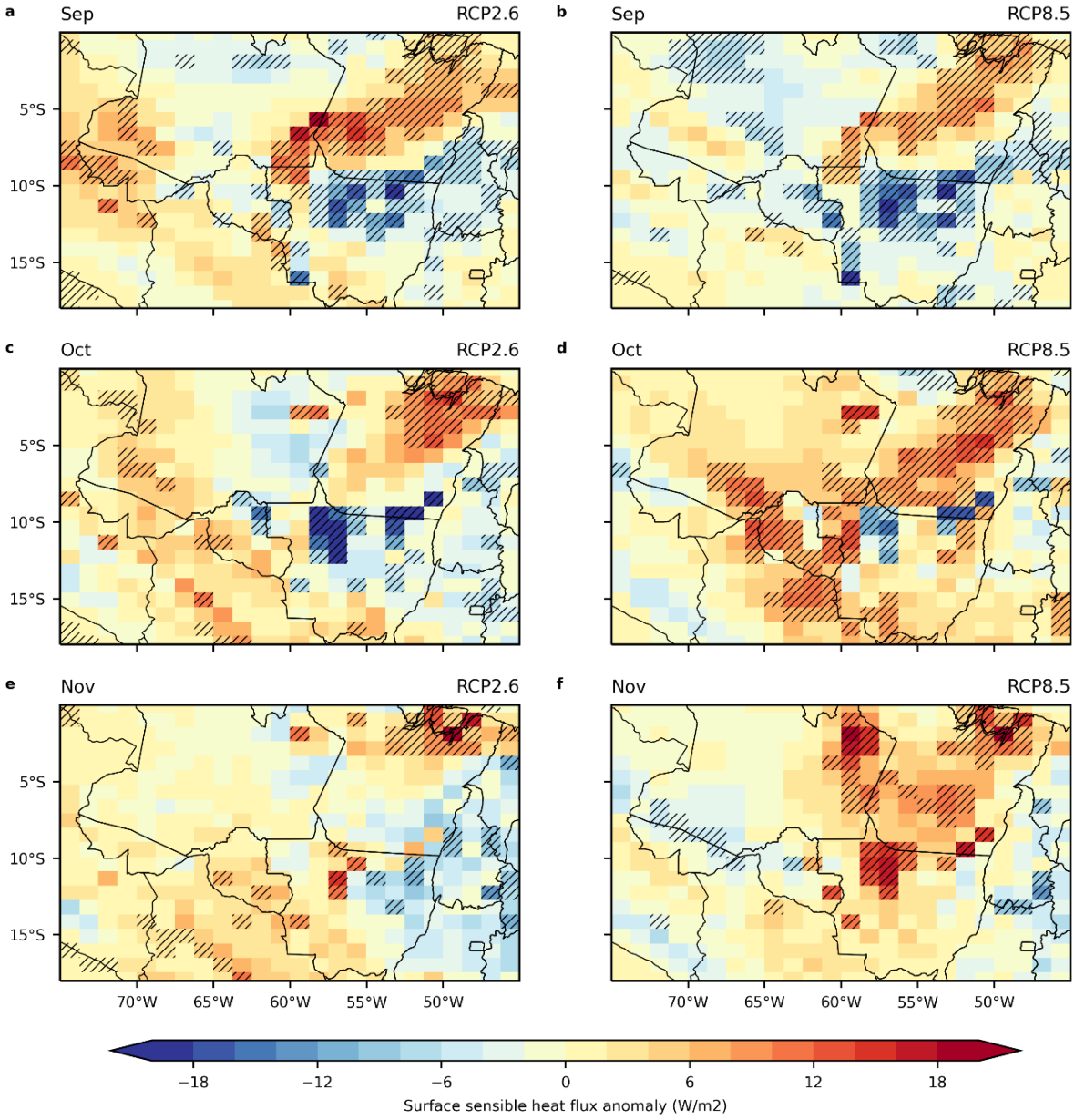

Figure S3.2 – Surface sensible heat flux at surface anomalies calculated as WEG − SEG for RCP2.6 (a, c, e) and RCP8.5 (b, d, f). Shaded areas indicate results significant at $\alpha = 0.05$.

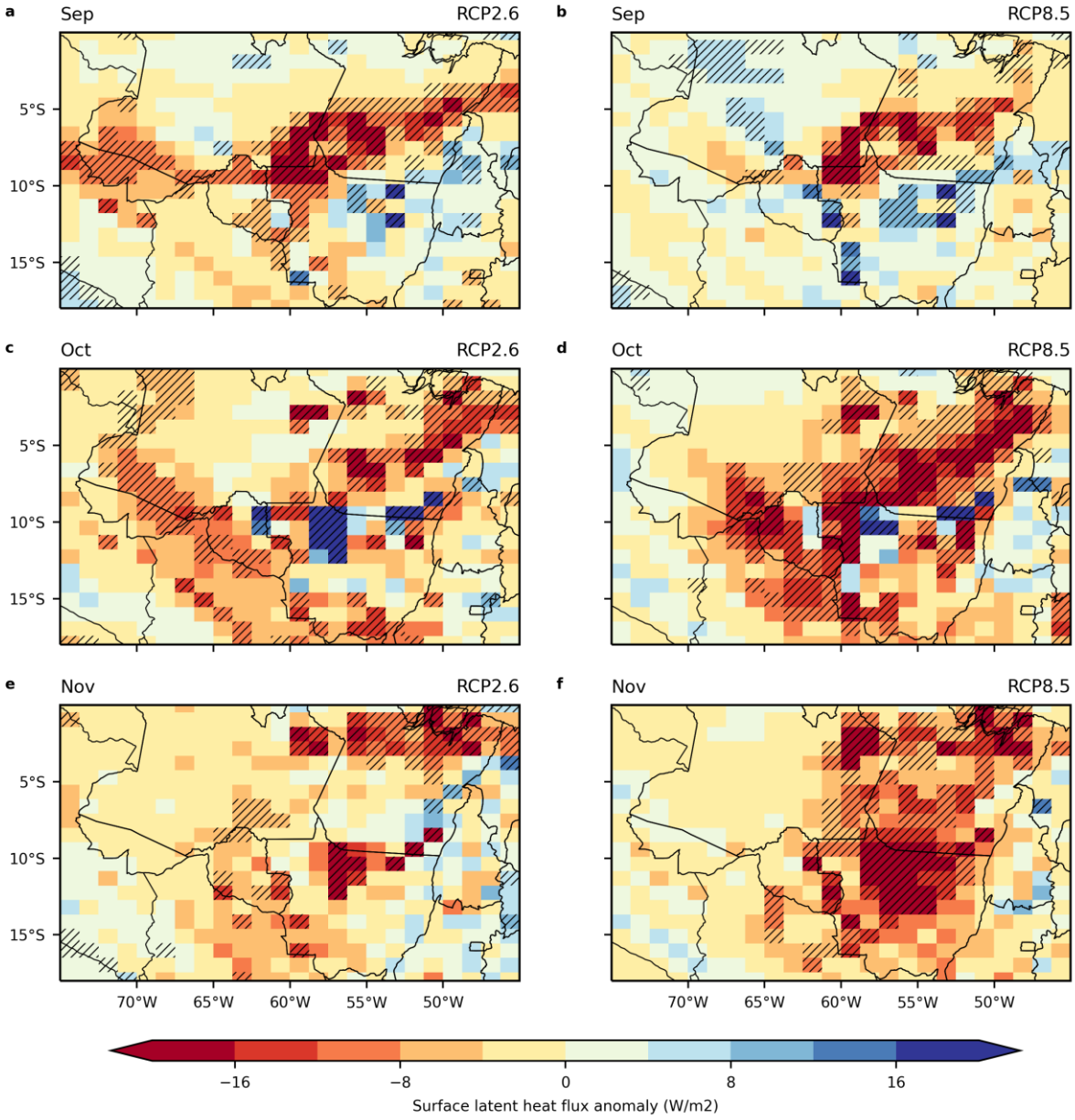

Figure S3.3 – Surface latent heat flux at surface anomalies calculated as WEG − SEG for RCP2.6 (a, c, e) and RCP8.5 (b, d, f). Shaded areas indicate results significant at $\alpha = 0.05$.

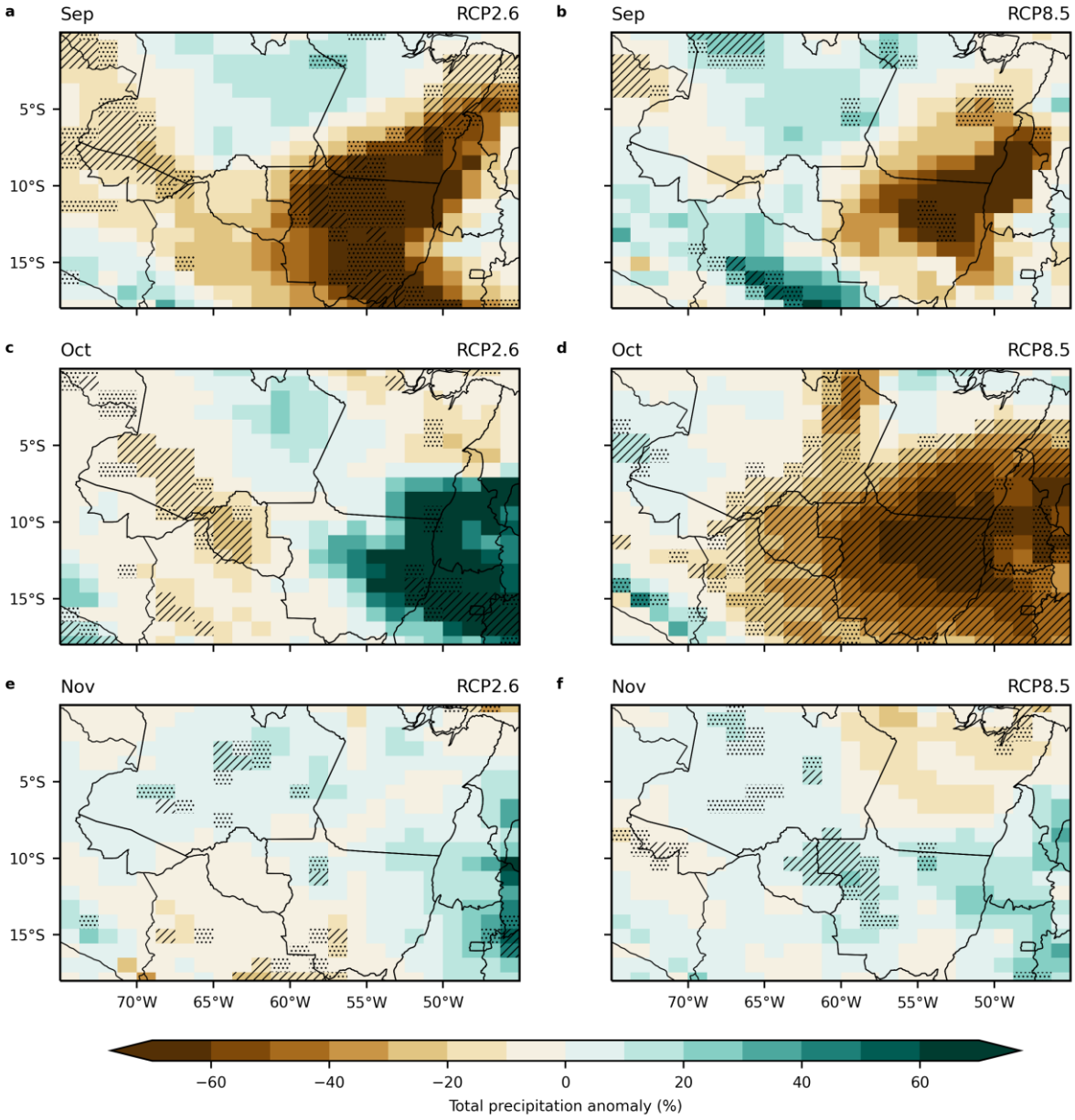

Figure S3.4 – Total precipitation changes calculated as WEG − SEG for RCP2.6 (a, c, e) and RCP8.5 (b, d, f). Dotted and hatched areas indicate results significant at $\alpha = 0.10$ and 0.05, respectively.

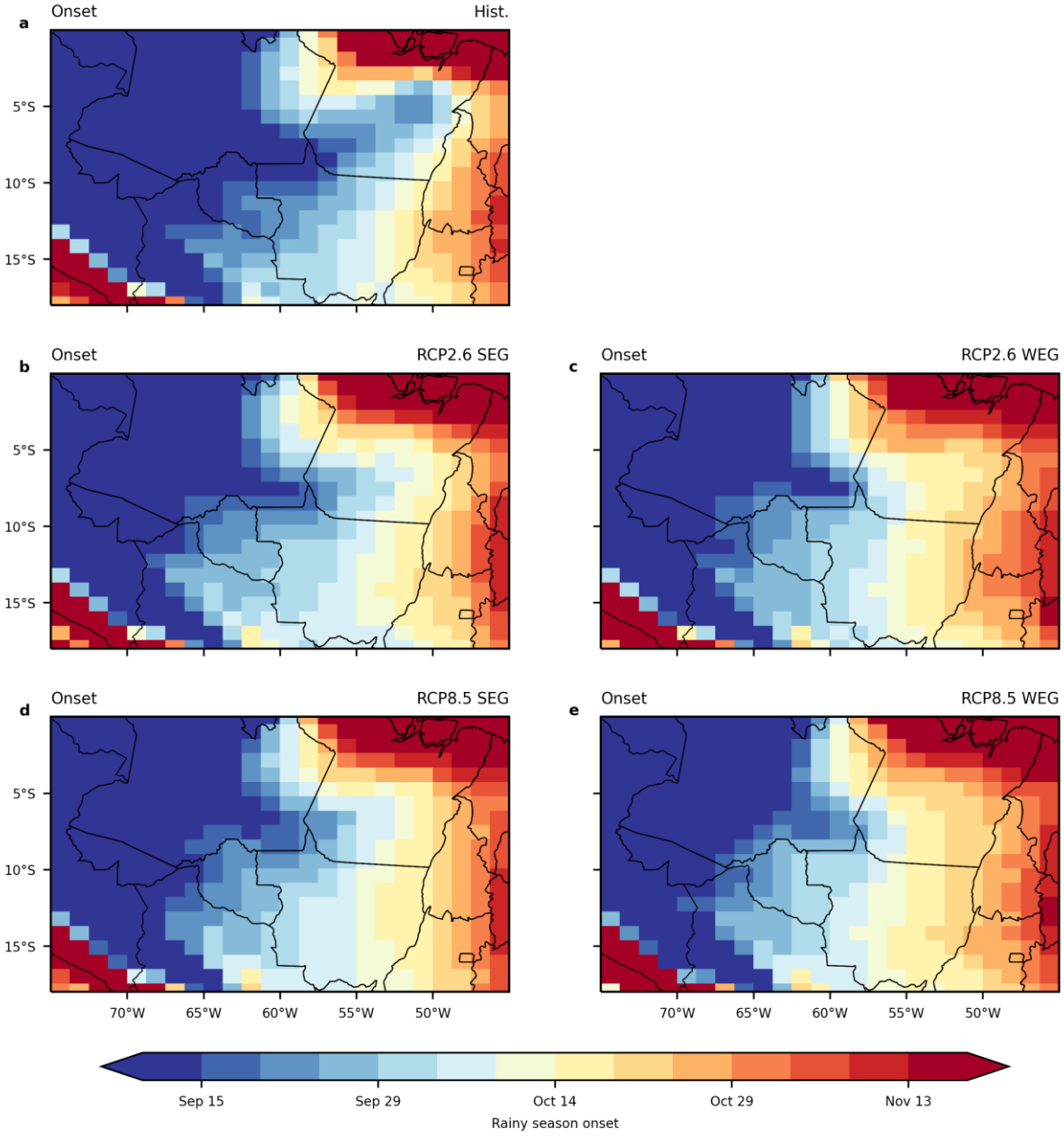

Figure S3.5 – Mean rainy season onset for the historical period (1990–2005) (a); the average of the decade 2040–2050 for four combinations of climate pathways and deforestation scenarios: RCP2.6 and SEG (b), RCP2.6 and WEG (c), RCP8.5 and SEG (d), RCP8.5 and WEG (e).

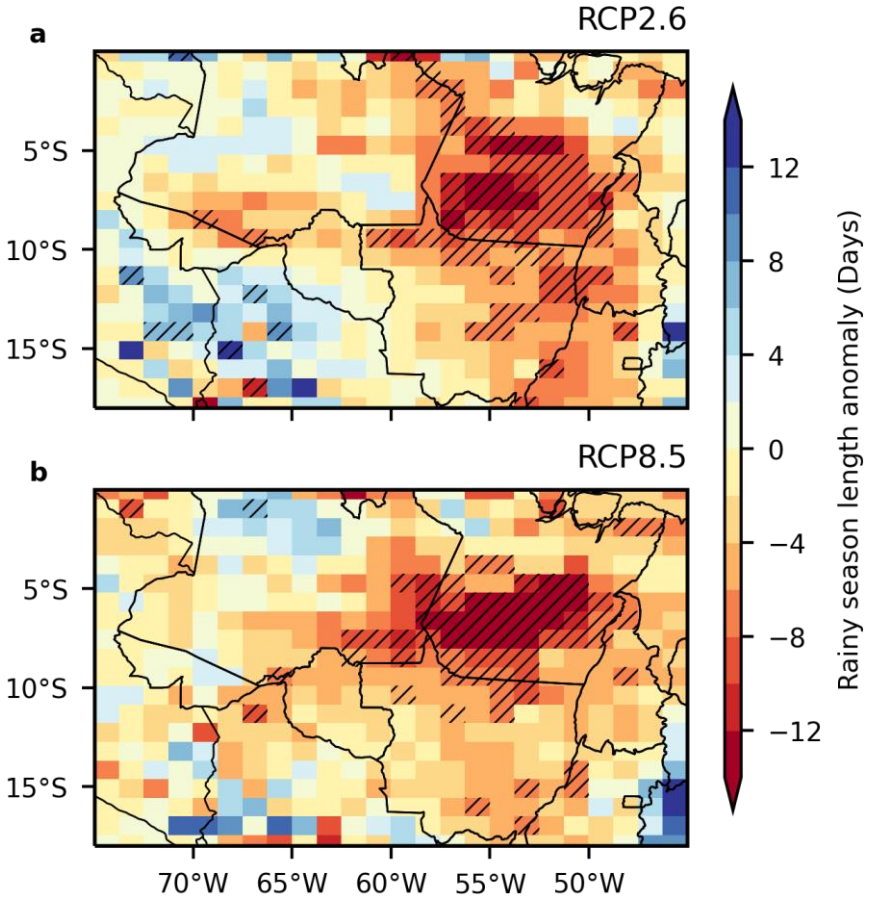

Figure S3.6 – Rainy season length anomalies calculated as WEG − SEG for RCP2.6 (a) and RCP8.5 (b). Shaded areas indicate significant results at a = 0.05.

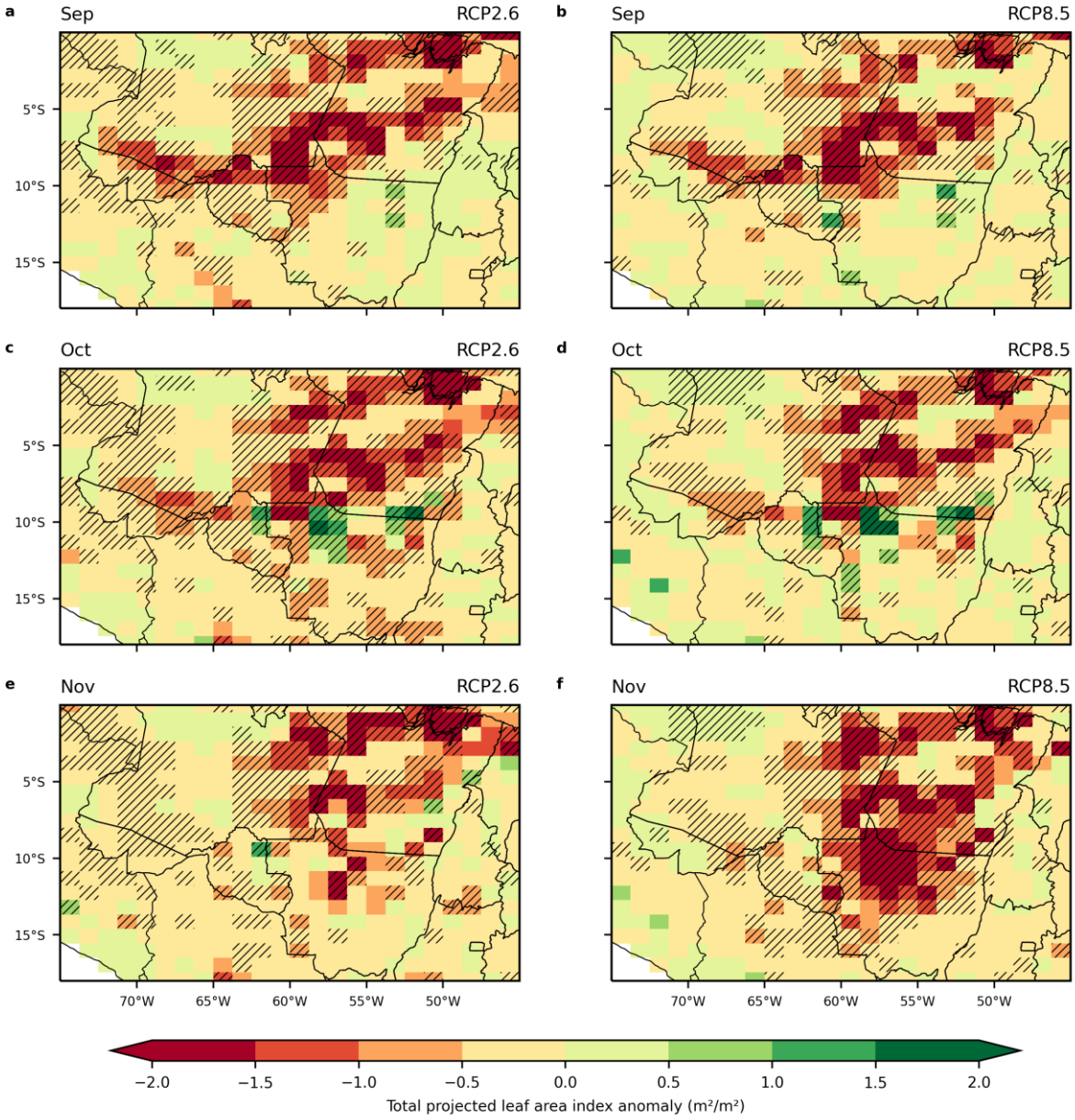

Figure S3.7 – Total projected leaf area index (LAI) anomaly calculated as WEG − SEG for RCP2.6 (a, c, e) and RCP8.5 (b, d, f). Shaded areas indicate significant results at 0.05.

General Conclusions

Deforestation significantly impacts cloud dynamics and the hydroclimate system in tropical regions, leading to a series of effects on the onset and duration of the rainy season. These impacts are evident in the disruption of cloud processes and the changes observed in rainfall and rainy season patterns. By integrating plausible deforestation scenarios with climate change projections, valuable insights into potential economic and ecological losses for the future were generated. This thesis examines the effects of deforestation and climate change on hydroclimatic variability in the southern Amazon, highlighting the complex relationships between land-use changes, atmospheric processes, and seasonal rainfall dynamics. By encompassing multiple spatial scales and temporal periods, from historical trends to projections extending into the mid-century, this approach provides a timely and comprehensive understanding of the region's hydroclimatic processes.

In Chapter 1, I highlighted the critical interplay between deforestation, cloud dynamics, and the onset of the rainy season on the Amazon, revealing significant impacts at varying spatial scales and land cover types. My results demonstrate that deforestation reduces cloud cover at fine scales (11–25 km) and promotes the development of shallower, warmer clouds, which suppress deep convective cloud formation. These effects persist for nearly two months during the dry-to-wet season transition, disrupting regional energy and moisture availability and ultimately delaying the onset of the rainy season. These findings underscore the profound influence of land-use changes on tropical atmospheric processes and emphasize the urgent need to incorporate localized deforestation impacts and broader climatic mechanisms into future climate models.

In Chapter 2, my analysis of rainfall trends in Mato Grosso, combining four decades of observations with climate simulations under realistic deforestation scenarios, reveals a concerning decline in rainfall volumes, delayed rainy season onset, and shorter rainy season durations. Projections suggest further intensifying these patterns by mid-century, with onsets delayed until late October and rainy seasons lasting less than 200 days. These changes threaten Mato Grosso’s double-cropping system, highlighting the urgent need for sustainable agricultural practices and strategic interventions to mitigate agricultural losses and ecosystem degradation. Mato Grosso faces significant challenges due to ongoing and upcoming climate change. Previous agricultural and conservation practices are no longer viable, and immediate action is needed.

In Chapter 3, I evaluated the effects of mid-century realistic deforestation scenarios on the rainy season in the southern Amazon and identified a previously unreported synoptic-scale circulation that delays its onset. Driven by extensive deforestation (around 40%), this anomalous circulation can persist for up to two months, delaying the rainy season onset by 30–40 days compared to historical patterns. Similar to other synoptic-scale processes, this circulation is triggered by differences in surface heating. If current deforestation trends continue, the associated delays could have irreversible consequences for local ecosystems, agriculture, and power generation.

This thesis offered a comprehensive assessment of how deforestation and climate change impact the southern Amazon's rainy season. By examining local deforestation effects through historical data and large-scale interactions using Earth system models, the findings reveal a clear and alarming pattern: deforestation not only delays the onset of the rainy season but also shortens its duration. These changes disrupt the region's water cycle, threatening critical ecosystems, agricultural productivity, and hydropower generation. The compounded effects of delayed and shortened rainy seasons underscore the urgent need for sustainable land-use practices and immediate action to mitigate the escalating threats to Amazon's environment, society, and economy.

To advance the understanding of the hydroclimatic behavior of the Southern Amazon, future research should:

- Investigate how deforested regions influence convective energy and its relationship with the onset and dynamics of the rainy season.
- Explore the atmospheric processes driving convection over deforested areas to identify key mechanisms behind rainfall suppression and delays.
- Utilize a multimodel approach with realistic land-use and land-cover scenarios to improve the accuracy of regional climate projections.
- Employ higher-resolution models incorporating realistic deforestation scenarios to better capture the localized impacts of land-use changes on hydroclimatic processes. Similarly, the employment of artificial intelligence modeling might excel the understanding through modeling for the region.

References

Abera TA, Heiskanen J, Maeda EE, Muhammed MA, Bhandari N, Vakkari V, Hailu BT, Pellikka PKE, Hemp A, Van Zyl PG, Zeuss D. 2024. Deforestation amplifies climate change effects on warming and cloud level rise in African montane forests. *Nature Communications*, 15(1): 6992. https://doi.org/10.1038/s41467-024-51324-7.

Abrahão GM, Costa MH. 2018. Evolution of rain and photoperiod limitations on the soybean growing season in Brazil: The rise (and possible fall) of double-cropping systems. *Agricultural and Forest Meteorology*. Elsevier, 256–257(February): 32–45. https://doi.org/10.1016/j.agrformet.2018.02.031.

Alvares CA, Stape JL, Sentelhas PC, de Moraes Gonçalves JL, Sparovek G. 2013. Köppen's climate classification map for Brazil. *Meteorologische Zeitschrift*, 22(6): 711–728. https://doi.org/10.1127/0941-2948/2013/0507.

Andrade MBT, Ferrante L, Fearnside PM. 2021. Brazil's Highway BR-319 demonstrates a crucial lack of environmental governance in Amazonia. *Environmental Conservation*, 48(3): 161–164. https://doi.org/10.1017/S0376892921000084.

Araujo AG de J, Obregón GO, Sampaio G, Monteiro AMV, da Silva LT, Soriano B, Padovani C, Rodriguez DA, Maksic J, Farias JFS. 2018. Relationships between variability in precipitation, river levels, and beef cattle production in the Brazilian Pantanal. *Wetlands Ecology and Management*, 26(5): 829–848. https://doi.org/10.1007/s11273-018-9612-0.

Arias ME, Farinosi F, Lee E, Livino A, Briscoe J, Moorcroft PR. 2020. Impacts of climate change and deforestation on hydropower planning in the Brazilian Amazon. *Nature Sustainability*. Springer US, 3(6): 430–436. https://doi.org/10.1038/s41893-020-0492-y.

Arvor D, Dubreuil V, Ronchail J, Simões M, Funatsu BM. 2014. Spatial patterns of rainfall regimes related to levels of double cropping agriculture systems in Mato Grosso (Brazil). *International Journal of Climatology*, 34(8): 2622–2633. https://doi.org/10.1002/joc.3863.

Arvor D, Funatsu B, Michot V, Dubreuil V. 2017. Monitoring Rainfall Patterns in the Southern Amazon with PERSIANN-CDR Data: Long-Term Characteristics and Trends. *Remote Sensing*, 9(9): 889. https://doi.org/10.3390/rs9090889.

Baker JCA, Garcia-Carreras L, Buermann W, Castilho de Souza D, Marsham JH, Kubota PY, Gloor M, Coelho CAS, Spracklen DV. 2021. Robust Amazon precipitation projections in climate models that capture realistic land–atmosphere interactions. *Environmental Research Letters*, 16(7): 074002. https://doi.org/10.1088/1748-9326/abfb2e.

Baudena M, Tuinenburg OA, Ferdinand PA, Staal A. 2021. Effects of land-use change in the Amazon on precipitation are likely underestimated. *Global Change Biology*, (January): gcb.15810. https://doi.org/10.1111/gcb.15810.

Bochow N, Boers N. 2023. The South American monsoon approaches a critical transition in response to deforestation. *Science Advances*, 9(40): 1–14. https://doi.org/10.1126/sciadv.add9973.

Boulton CA, Lenton TM, Boers N. 2022. Pronounced loss of Amazon rainforest resilience since the early 2000s. *Nature Climate Change*. Springer US, 12(March). https://doi.org/10.1038/s41558-022-01287-8.

Boysen LR, Brovkin V, Pongratz J, Lawrence DM, Lawrence P, Vuichard N, Peylin P, Liddicoat S, Hajima T, Zhang Y, Rocher M, Delire C, Séférian R, Arora VK, Nieradzik L, Anthoni P, Thiery W, Laguë MM, Lawrence D, Lo M-H. 2020. Global climate response to idealized deforestation in CMIP6 models. *Biogeosciences*, 17(22): 5615–5638. https://doi.org/10.5194/bg-17-5615-2020.

Brando PM, Soares-Filho B, Rodrigues L, Assunção A, Morton D, Tuchschneider D, Fernandes ECM, Macedo MN, Oliveira U, Coe MT. 2020. The gathering firestorm in southern Amazonia. *Science Advances*, 6(2): 1–10. https://doi.org/10.1126/sciadv.aay1632.

Brumatti LM, Pires GF, Santos AB. 2020. Challenges to the Adaptation of Double Cropping Agricultural Systems in Brazil under Changes in Climate and Land Cover. *Atmosphere*, 11(12): 1310. https://doi.org/10.3390/atmos11121310.

Butt N, De Oliveira PA, Costa MH. 2011. Evidence that deforestation affects the onset of the rainy season in Rondonia, Brazil. *Journal of Geophysical Research Atmospheres*, 116(11): 2–9. https://doi.org/10.1029/2010JD015174.

Caballero CB, Ruhoff A, Biggs T. 2022a. Land use and land cover changes and their impacts on surface-atmosphere interactions in Brazil: A systematic review. *Science of the Total Environment*. Elsevier B.V., 808: 152134. https://doi.org/10.1016/j.scitotenv.2021.152134.

Caballero CB, Ruhoff A, Biggs T. 2022b. Land use and land cover changes and their impacts on surface-atmosphere interactions in Brazil: A systematic review. *Science of the Total Environment*. Elsevier B.V., 808: 152134. https://doi.org/10.1016/j.scitotenv.2021.152134.

Cai W, McPhaden MJ, Grimm AM, Rodrigues RR, Taschetto AS, Garreaud RD, Dewitte B, Poveda G, Ham Y-G, Santoso A, Ng B, Anderson W, Wang G, Geng T, Jo H-S, Marengo JA, Alves LM, Osman M, Li S, Wu L, Karamperidou C, Takahashi K, Vera C. 2020. Climate impacts of the El Niño–Southern Oscillation on South America. *Nature Reviews Earth & Environment*. Springer US, 1(4): 215–231. https://doi.org/10.1038/s43017-020-0040-3.

Cao C, Xiong X, Wu A, Wu X. 2008. Assessing the consistency of AVHRR and MODIS L1B reflectance for generating Fundamental Climate Data Records. *Journal of Geophysical Research: Atmospheres*, 113(D9): 2007JD009363. https://doi.org/10.1029/2007JD009363.

Carauta M, Parussis J, Hampf A, Libera A, Berger T. 2021. No more double cropping in Mato Grosso, Brazil? Evaluating the potential impact of climate change on the profitability of farm systems. *Agricultural Systems*. Elsevier Ltd, 190: 103104. https://doi.org/10.1016/j.agsy.2021.103104.

Chakraborty S, Jiang JH, Su H, Fu R. 2020. Deep Convective Evolution From Shallow Clouds Over the Amazon and Congo Rainforests. *Journal of Geophysical Research: Atmospheres*, 125(1). https://doi.org/10.1029/2019JD030962.

Christoffersen BO, Restrepo-Coupe N, Arain MA, Baker IT, Cestaro BP, Ciais P, Fisher JB, Galbraith D, Guan X, Gulden L, van den Hurk B, Ichii K, Imbuzeiro H, Jain A, Levine N, Miguez-Macho G, Poulter B, Roberti DR, Sakaguchi K, Sahoo A, Schaefer K, Shi M, Verbeeck

H, Yang Z-L, Araújo AC, Kruijt B, Manzi AO, da Rocha HR, von Randow C, Muza MN, Borak J, Costa MH, Gonçalves de Gonçalves LG, Zeng X, Saleska SR. 2014. Mechanisms of water supply and vegetation demand govern the seasonality and magnitude of evapotranspiration in Amazonia and Cerrado. *Agricultural and Forest Meteorology*, 191(February): 33–50. https://doi.org/10.1016/j.agrformet.2014.02.008.

Cohn AS, VanWey LK, Spera SA, Mustard JF. 2016. Cropping frequency and area response to climate variability can exceed yield response. *Nature Climate Change*, 6(6): 601–604. https://doi.org/10.1038/nclimate2934.

Commar LFS, Abrahão GM, Costa MH. 2023a. A possible deforestation-induced synoptic-scale circulation that delays the rainy season onset in Amazonia. *Environmental Research Letters*, 18(4): 044041. https://doi.org/10.1088/1748-9326/acc95f.

Commar LFS, Louzada L, Costa MH, Brumatti LM, Abrahão GM. 2024. Mato Grosso's rainy season: past, present, and future trends justify immediate action. *Environmental Research Letters*, 19(11): 114065. https://doi.org/10.1088/1748-9326/ad8588.

Commar LFS, Vitorino FB, Castro M, Pousa R, Costa MH. 2023b. A Hydroclimatic Forecast System to Support Decision-Making and Improve Water Security in an Agricultural Frontier of the Brazilian Cerrado. *Journal of Water Resources Planning and Management*, 150(3): 1–15. https://doi.org/10.1061/JWRMD5.WRENG-6261.

Costa MH. 2020. When more trees mean more power. *Nature Sustainability*. Springer US, 3(6): 410–411. https://doi.org/10.1038/s41893-020-0511-z.

Costa MH, Fleck LC, Cohn AS, Abrahão GM, Brando PM, Coe MT, Fu R, Lawrence D, Pires GF, Pousa R, Soares-Filho BS. 2019. Climate risks to Amazon agriculture suggest a rationale to conserve local ecosystems. *Frontiers in Ecology and the Environment*, 17(10): 584–590. https://doi.org/10.1002/fee.2124.

Costa MH, Foley JA. 2000. Combined effects of deforestation and doubled atmospheric CO2 concentrations on the climate of Amazonia. *Journal of Climate*, 13(1): 18–34. https://doi.org/10.1175/1520-0442(2000)013<0018:CEODAD>2.0.CO;2.

Costa MH, Yanagi SNM, Souza PJOP, Ribeiro A, Rocha EJP. 2007. Climate change in Amazonia caused by soybean cropland expansion, as compared to caused by pastureland expansion. *Geophysical Research Letters*, 34(7): L07706. https://doi.org/10.1029/2007GL029271.

Couto TBA, Messager ML, Olden JD. 2021. Safeguarding migratory fish via strategic planning of future small hydropower in Brazil. *Nature Sustainability*. Springer US, 4(5): 409–416. https://doi.org/10.1038/s41893-020-00665-4.

De Hertog SJ, Havermann F, Vanderkelen I, Guo S, Luo F, Manola I, Coumou D, Davin EL, Duveiller G, Lejeune Q, Pongratz J, Schleussner CF, Seneviratne SI, Thiery W. 2023. The biogeophysical effects of idealized land cover and land management changes in Earth system models. *Earth System Dynamics*. Copernicus Publications, 14(3): 629–667. https://doi.org/10.5194/esd-14-629-2023.

de Moraes JB, Wanderley HS, Delgado RC. 2022. Areas susceptible to desertification in Brazil and projected climate change scenarios. *Natural Hazards*. Springer Science and Business Media B.V., 116(2): 1463–1483. https://doi.org/10.1007/s11069-022-05724-x.

Dirmeyer PA, Shukla J. 1994. Albedo as a modulator of climate response to tropical deforestation. *Journal of Geophysical Research*, 99(D10). https://doi.org/10.1029/94jd01311.

Douville H, K. Raghavan, J. Renwick, R.P. Allan, P.A. Arias, M. Barlow, R. Cerezo-Mota, A. Cherchi, T.Y. Gan JG, D. Jiang, A. Khan, W. Pokam Mba, D. Rosenfeld, J. Tierney and OZ. 2023. Water Cycle Changes. *Climate Change 2021 – The Physical Science Basis*. Cambridge University Press, 1055–1210.

Duveiller G, Filipponi F, Ceglar A, Bojanowski J, Alkama R, Cescatti A. 2021. Revealing the widespread potential of forests to increase low level cloud cover. *Nature Communications*, 12(1): 4337. https://doi.org/10.1038/s41467-021-24551-5.

Eltahir EAB, Bras RL. 1996. Precipitation recycling. *Reviews of Geophysics*, 34(3): 367–378. https://doi.org/10.1029/96RG01927.

Espinoza J-C, Arias PA, Moron V, Junquas C, Segura H, Sierra-Pérez JP, Wongchuig S, Condom T. 2021. Recent changes in the atmospheric circulation patterns during the dry-to-wet transition season in south tropical South America (1979-2020): Impacts on precipitation and fire season. *Journal of Climate*, 34(22): 1–56. https://doi.org/10.1175/JCLI-D-21-0303.1.

Espinoza J-C, Marengo JA, Schongart J, Jimenez JC. 2022. The new historical flood of 2021 in the Amazon River compared to major floods of the 21st century: Atmospheric features in the context of the intensification of floods. *Weather and Climate Extremes*, 35: 100406. https://doi.org/10.1016/j.wace.2021.100406.

Espinoza JC, Sörensson AA, Ronchail J, Molina-Carpio J, Segura H, Gutierrez-Cori O, Ruscica R, Condom T, Wongchuig-Correa S. 2019. Regional hydro-climatic changes in the Southern Amazon Basin (Upper Madeira Basin) during the 1982–2017 period. *Journal of Hydrology: Regional Studies*. Elsevier, 26(June): 100637. https://doi.org/10.1016/j.ejrh.2019.100637.

Fassoni-Andrade AC, Fleischmann AS, Papa F, Paiva RCD de, Wongchuig S, Melack JM, Moreira AA, Paris A, Ruhoff A, Barbosa C, Maciel DA, Novo E, Durand F, Frappart F, Aires F, Abrahão GM, Ferreira-Ferreira J, Espinoza JC, Laipelt L, Costa MH, Espinoza-Villar R, Calmant S, Pellet V. 2021. Amazon Hydrology From Space: Scientific Advances and Future Challenges. *Reviews of Geophysics*, 59(4): 1–97. https://doi.org/10.1029/2020RG000728.

Ferrante L, Andrade MBT, Fearnside PM. 2021. Land grabbing on Brazil's Highway BR-319 as a spearhead for Amazonian deforestation. *Land Use Policy*. Elsevier Ltd, 108(May): 105559. https://doi.org/10.1016/j.landusepol.2021.105559.

Findell KL, Gentine P, Lintner BR, Kerr C. 2011. Probability of afternoon precipitation in eastern United States and Mexico enhanced by high evaporation. *Nature Geoscience*. Nature Publishing Group, 4(7): 434–439. https://doi.org/10.1038/ngeo1174.

Firpo MÂF, Guimarães B dos S, Dantas LG, Silva MGB da, Alves LM, Chadwick R, Llopart MP, Oliveira GS de. 2022. Assessment of CMIP6 models' performance in simulating present-day climate in Brazil. *Frontiers in Climate*, 4. https://doi.org/10.3389/fclim.2022.948499.

Flach R, Abrahão G, Bryant B, Scarabello M, Soterroni AC, Ramos FM, Valin H, Obersteiner M, Cohn AS. 2021. Conserving the Cerrado and Amazon biomes of Brazil protects the soy economy from damaging warming. *World Development*. The Author(s), 146: 105582. https://doi.org/10.1016/j.worlddev.2021.105582.

Foster MJ, Phillips C, Heidinger AK, Borbas EE, Li Y, Menzel WP, Walther A, Weisz E. 2023. PATMOS-x Version 6.0: 40 Years of Merged AVHRR and HIRS Global Cloud Data. *Journal of Climate*, 36(4): 1143–1160. https://doi.org/10.1175/JCLI-D-22-0147.1.

Fu R. 2015. Global warming-accelerated drying in the tropics. *Proceedings of the National Academy of Sciences*, 112(12): 3593–3594. https://doi.org/10.1073/pnas.1503231112.

Fu R, Yin L, Li W, Arias PA, Dickinson RE, Huang L, Chakraborty S, Fernandes K, Liebmann B, Fisher R, Myneni RB. 2013. Increased dry-season length over southern Amazonia in recent decades and its implication for future climate projection. *Proceedings of the National Academy of Sciences*. National Academy of Sciences, 110(45): 18110–18115. https://doi.org/10.1073/pnas.1302584110.

Funatsu BM, Le Roux R, Arvor D, Espinoza JC, Claud C, Ronchail J, Michot V, Dubreuil V. 2021. Assessing precipitation extremes (1981–2018) and deep convective activity (2002–2018) in the Amazon region with CHIRPS and AMSU data. *Climate Dynamics*. Springer Berlin Heidelberg. https://doi.org/10.1007/s00382-021-05742-8.

Funk C, Peterson P, Landsfeld M, Pedreros D, Verdin J, Shukla S, Husak G, Rowland J, Harrison L, Hoell A, Michaelsen J. 2015. The climate hazards infrared precipitation with stations—a new environmental record for monitoring extremes. *Scientific Data*, 2(1): 150066. https://doi.org/10.1038/sdata.2015.66.

Gatti LV, Basso LS, Miller JB, Gloor M, Gatti Domingues L, Cassol HLG, Tejada G, Aragão LEOC, Nobre C, Peters W, Marani L, Arai E, Sanches AH, Corrêa SM, Anderson L, Von Randow C, Correia CSC, Crispim SP, Neves RAL. 2021. Amazonia as a carbon source linked to deforestation and climate change. *Nature*. Springer US, 595(7867): 388–393. https://doi.org/10.1038/s41586-021-03629-6.

Hampf AC, Stella T, Berg-Mohnicke M, Kawohl T, Kilian M, Nendel C. 2020. Future yields of double-cropping systems in the Southern Amazon, Brazil, under climate change and technological development. *Agricultural Systems*. Elsevier Ltd, 177: 102707. https://doi.org/10.1016/j.agsy.2019.102707.

Heidinger AK, Foster MJ, Walther A, Zhao X (Tom). 2014. The Pathfinder Atmospheres–Extended AVHRR Climate Dataset. *Bulletin of the American Meteorological Society*, 95(6): 909–922. https://doi.org/10.1175/BAMS-D-12-00246.1.

Henkes A, Fisch G, Machado LAT, Chaboureau J-P. 2021. Morning boundary layer conditions for shallow to deep convective cloud evolution during the dry season in the central Amazon. *Atmospheric Chemistry and Physics*, 21(17): 13207–13225. https://doi.org/10.5194/acp-21-13207-2021.

Hofmann GS, Silva RC, Weber EJ, Barbosa AA, Oliveira LFB, Alves RJV, Hasenack H, Schossler V, Aquino FE, Cardoso MF. 2023. Changes in atmospheric circulation and evapotranspiration are reducing rainfall in the Brazilian Cerrado. *Scientific Reports*. Nature Publishing Group UK, 13(1): 11236. https://doi.org/10.1038/s41598-023-38174-x.

Hua W, Zhou L, Dai A, Chen H, Liu Y. 2023. Important non-local effects of deforestation on cloud cover changes in CMIP6 models. *Environmental Research Letters*, 18(9): 094047. https://doi.org/10.1088/1748-9326/acf232.

Hurrell JW, Holland MM, Gent PR, Ghan S, Kay JE, Kushner PJ, Lamarque JF, Large WG, Lawrence D, Lindsay K, Lipscomb WH, Long MC, Mahowald N, Marsh DR, Neale RB, Rasch P, Vavrus S, Vertenstein M, Bader D, Collins WD, Hack JJ, Kiehl J, Marshall S. 2013. The community earth system model: A framework for collaborative research. *Bulletin of the American Meteorological Society*, 94(9): 1339–1360. https://doi.org/10.1175/BAMS-D-12-00121.1.

Khanna J, Medvigy D, Fueglistaler S, Walko R. 2017. Regional dry-season climate changes due to three decades of Amazonian deforestation. *Nature Climate Change*, 7(3): 200–204. https://doi.org/10.1038/nclimate3226.

Lawrence D, Vandecar K. 2015. Effects of tropical deforestation on climate and agriculture. *Nature Climate Change*, 5(1): 27–36. https://doi.org/10.1038/nclimate2430.

Lee J-E, Lintner BR, Neelin JD, Jiang X, Gentine P, Boyce CK, Fisher JB, Perron JT, Kubar TL, Lee J, Worden J. 2012. Reduction of tropical land region precipitation variability via transpiration. *Geophysical Research Letters*, 39(19): n/a-n/a. https://doi.org/10.1029/2012GL053417.

Leite-Filho AT, Costa MH, Fu R. 2020. The southern Amazon rainy season: The role of deforestation and its interactions with large-scale mechanisms. *International Journal of Climatology*, 40(4): 2328–2341. https://doi.org/10.1002/joc.6335.

Leite-Filho AT, Soares-Filho BS, Davis JL, Abrahão GM, Börner J. 2021. Deforestation reduces rainfall and agricultural revenues in the Brazilian Amazon. *Nature Communications*, 12(1): 2591. https://doi.org/10.1038/s41467-021-22840-7.

Leite-Filho AT, Soares-Filho BS, de Oliveira U. 2024. Climate risks to soy-maize double-cropping due to Amazon deforestation. *International Journal of Climatology*. John Wiley and Sons Ltd. https://doi.org/10.1002/joc.8381.

Leite-Filho AT, Sousa Pontes VY, Costa MH. 2019. Effects of Deforestation on the Onset of the Rainy Season and the Duration of Dry Spells in Southern Amazonia. *Journal of Geophysical Research: Atmospheres*, 124(10): 5268–5281. https://doi.org/10.1029/2018JD029537.

Leung GR, Grant LD, Van Den Heever SC. 2024. Deforestation-Driven Increases in Shallow Clouds Are Greatest in Drier, Low-Aerosol Regions of Southeast Asia. *Geophysical Research Letters*, 51(10): e2023GL107678. https://doi.org/10.1029/2023GL107678.

Li G, Lu D, Moran E, Calvi MF, Dutra LV, Batistella M. 2019. Examining deforestation and agropasture dynamics along the Brazilian TransAmazon Highway using multitemporal Landsat imagery. *GIScience & Remote Sensing*. Taylor & Francis, 56(2): 161–183. https://doi.org/10.1080/15481603.2018.1497438.

Libonati R, Geirinhas JL, Silva PS, Russo A, Rodrigues JA, Belém LBC, Nogueira J, Roque FO, DaCamara CC, Nunes AMB, Marengo JA, Trigo RM. 2022. Assessing the role of compound drought and heatwave events on unprecedented 2020 wildfires in the Pantanal. *Environmental Research Letters*, 17(1): 015005. https://doi.org/10.1088/1748-9326/ac462e.

Lovejoy TE, Nobre C. 2018. Amazon tipping point. *Science Advances*, 4(2): 1–2. https://doi.org/10.1126/sciadv.aat2340.

Luo H, Quaas J, Han Y. 2024. Decreased cloud cover partially offsets the cooling effects of surface albedo change due to deforestation. *Nature Communications*, 15(1): 7345. https://doi.org/10.1038/s41467-024-51783-y.

Maeda EE, Abera TA, Siljander M, Aragão LEOC, Moura YM de, Heiskanen J. 2021. Large-scale commodity agriculture exacerbates the climatic impacts of Amazonian deforestation. *Proceedings of the National Academy of Sciences*, 118(7). https://doi.org/10.1073/pnas.2023787118.

Marengo JA, Cunha AP, Cuartas LA, Deusdará Leal KR, Broedel E, Seluchi ME, Michelin CM, De Praga Baião CF, Chuchón Angulo E, Almeida EK, Kazmierczak ML, Mateus NPA, Silva RC, Bender F. 2021a. Extreme Drought in the Brazilian Pantanal in 2019–2020: Characterization, Causes, and Impacts. *Frontiers in Water*, 3(February). https://doi.org/10.3389/frwa.2021.639204.

Marengo JA, Jimenez JC, Espinoza J-C, Cunha AP, Aragão LEO. 2021b. Increased Climate Pressure on the New Agricultural Frontier in the Eastern Amazonia-Cerrado Transition Zone. *Scientific Reports*. Nature Publishing Group UK, (0123456789): 1–10. https://doi.org/10.1038/s41598-021-04241-4.

Marin FR, Zanon AJ, Monzon JP, Andrade JF, Silva EHFM, Richter GL, Antolin LAS, Ribeiro BSMR, Ribas GG, Battisti R, Heinemann AB, Grassini P. 2022. Protecting the Amazon forest and reducing global warming via agricultural intensification. *Nature Sustainability*. https://doi.org/10.1038/s41893-022-00968-8.

Mataveli GAV, Pereira G, de Oliveira G, Seixas HT, Cardozo F da S, Shimabukuro YE, Kawakubo FS, Brunsell NA. 2021. 2020 Pantanal's widespread fire: short- and long-term implications for biodiversity and conservation. *Biodiversity and Conservation*. Springer Science and Business Media B.V., 30(11): 3299–3303. https://doi.org/10.1007/s10531-021-02243-2.

Michot V, Corpetti T, Ronchail J, Espinoza JC, Arvor D, Funatsu BM, Dubreuil V. 2024. Seasonal types in homogeneous rainfall regions of the Amazon basin. *International Journal of Climatology*. Wiley. https://doi.org/10.1002/joc.8380.

Monteverde C, De Sales F, Jones C. 2022. Evaluation of the CMIP6 Performance in Simulating Precipitation in the Amazon River Basin. *Climate*, 10(8): 1–18. https://doi.org/10.3390/cli10080122.

Moran EF. 2016. Roads and dams: Infrastructure-driven transformations in the Brazilian Amazon. *Ambiente & Sociedade*, 19(2): 207–220. https://doi.org/10.1590/1809-4422ASOC256V1922016.

Mu Ye, Jones C. 2022. An observational analysis of precipitation and deforestation age in the Brazilian Legal Amazon. *Atmospheric Research*, 271: 106122. https://doi.org/10.1016/j.atmosres.2022.106122.

Nguyen P, Shearer EJ, Tran H, Ombadi M, Hayatbini N, Palacios T, Huynh P, Braithwaite D, Updegraff G, Hsu K, Kuligowski B, Logan WS, Sorooshian S. 2019. The CHRS data portal,

an easily accessible public repository for PERSIANN global satellite precipitation data. *Scientific Data*. The Author(s), 6: 1–10. https://doi.org/10.1038/sdata.2018.296.

Oleson KW, Lawrence DM, Bonan GB, Flanner MG, Kluzek E, Lawrence PJ. 2010. *Technical Description of version 4.0 of the Community Land Model (CLM)*. *NCAR TECHNICAL NOTE*.

Oliveira U, Soares-Filho B, Bustamante M, Gomes L, Ometto JP, Rajão R. 2022. Determinants of Fire Impact in the Brazilian Biomes. *Frontiers in Forests and Global Change*, 5(March): 1–12. https://doi.org/10.3389/ffgc.2022.735017.

Olmo ME, Espinoza J, Bettolli ML, Sierra JP, Junquas C, Arias PA, Moron V, Balmaceda-Huarte R. 2022. Circulation patterns and associated rainfall over South Tropical South America: GCMs evaluation during the dry-to-wet transition season. *Journal of Geophysical Research: Atmospheres*. https://doi.org/10.1029/2022jd036468.

Pires GF, Abrahão GM, Brumatti LM, Oliveira LJC, Costa MH, Liddicoat S, Kato E, Ladle RJ. 2016. Increased climate risk in Brazilian double cropping agriculture systems: Implications for land use in Northern Brazil. *Agricultural and Forest Meteorology*. Elsevier B.V., 228–229: 286–298. https://doi.org/10.1016/j.agrformet.2016.07.005.

Pires GF, Costa MH. 2013. Deforestation causes different subregional effects on the Amazon bioclimatic equilibrium. *Geophysical Research Letters*, 40(14): 3618–3623. https://doi.org/10.1002/grl.50570.

Pousa R, Costa MH, Pimenta FM, Fontes VC, Brito VFA de, Castro M. 2019. Climate Change and Intense Irrigation Growth in Western Bahia, Brazil: The Urgent Need for Hydroclimatic Monitoring. *Water*, 11(5): 933. https://doi.org/10.3390/w11050933.

Ramankutty N, Foley JA. 1999. Estimating historical changes in global land cover: Croplands from 1700 to 1992. *Global Biogeochemical Cycles*, 13(4): 997–1027. https://doi.org/10.1029/1999GB900046.

Rattis L, Brando PM, Macedo MN, Spera SA, Castanho ADA, Marques EQ, Costa NQ, Silverio DV, Coe MT. 2021. Climatic limit for agriculture in Brazil. *Nature Climate Change*. Springer US. https://doi.org/10.1038/s41558-021-01214-3.

Restrepo-Coupe N, Albert LP, Longo M, Baker I, Levine NM, Mercado LM, da Araujo AC, Christoffersen BOD, Costa MH, Fitzjarrald DR, Galbraith D, Imbuzeiro H, Malhi Y, von Randow C, Zeng X, Moorcroft P, Saleska SR. 2021. Understanding water and energy fluxes in the Amazonia: Lessons from an observation-model intercomparison. *Global Change Biology*, 27(9): 1802–1819. https://doi.org/10.1111/gcb.15555.

Rocha Junior AB, Barretto AG de OP, Chamma ALS, Fendrich AN, Gianetti GW, Safanelli JL, Araujo MA de, Takahashi N de F, Coutinho PAQ, Maule RF, Martins SP. 2020. *Análise Territorial para o Desenvolvimento da Agricultura Irrigada no Brasil" Plano de Ação Imediata da Agricultura Irrigada no Brasil para o período 2020-2023*. .

Rochedo PRR, Soares-Filho B, Schaeffer R, Viola E, Szklo A, Lucena AFP, Koberle A, Davis JL, Rajão R, Rathmann R. 2018. The threat of political bargaining to climate mitigation in Brazil. *Nature Climate Change*, 8(8): 695–698. https://doi.org/10.1038/s41558-018-0213-y.

Rodrigues MAM, Garcia SR, Kayano MT, Calheiros AJP, Andreoli RV. 2021. Onset and demise dates of the rainy season in the South American monsoon region: A cluster analysis result. *International Journal of Climatology*, (June): joc.7307. https://doi.org/10.1002/joc.7307.

Ruiz-Vásquez M, Arias PA, Martínez JA, Espinoza JC. 2020. Effects of Amazon basin deforestation on regional atmospheric circulation and water vapor transport towards tropical South America. *Climate Dynamics*. Springer Berlin Heidelberg, 54(9–10): 4169–4189. https://doi.org/10.1007/s00382-020-05223-4.

Saad SI, da Rocha HR, Silva Dias MAF, Rosolem R. 2010. Can the Deforestation Breeze Change the Rainfall in Amazonia? A Case Study for the BR-163 Highway Region. *Earth Interactions*, 14(18): 1–25. https://doi.org/10.1175/2010EI351.1.

Sampaio G, Nobre C, Costa MH, Satyamurty P, Soares-Filho BS, Cardoso M. 2007. Regional climate change over eastern Amazonia caused by pasture and soybean cropland expansion. *Geophysical Research Letters*, 34(17): L17709. https://doi.org/10.1029/2007GL030612.

Sampaio G, Shimizu MH, Guimarães-Júnior CA, Alexandre F, Guatura M, Cardoso M, Domingues TF, Rammig A, von Randow C, Rezende LFC, Lapola DM. 2021. CO2 physiological effect can cause rainfall decrease as strong as large-scale deforestation in the Amazon. *Biogeosciences*, 18(8): 2511–2525. https://doi.org/10.5194/bg-18-2511-2021.

Santos AB, Heil Costa M, Chartuni Mantovani E, Boninsenha I, Castro M. 2020. A Remote Sensing Diagnosis of Water Use and Water Stress in a Region with Intense Irrigation Growth in Brazil. *Remote Sensing*, 12: 3725. https://doi.org/10.3390/rs12223725.

Schamm K, Ziese M, Becker A, Finger P, Meyer-Christoffer A, Schneider U, Schröder M, Stender P. 2014. Global gridded precipitation over land: a description of the new GPCC First Guess Daily product. *Earth System Science Data*, 6(1): 49–60. https://doi.org/10.5194/essd-6-49-2014.

Shukla J, Nobre C, Sellers P. 1990. Amazon Deforestation and Climate Change. *Science*, 247(4948): 1322–1325. https://doi.org/10.1126/science.247.4948.1322.

Sierra JP, Espinoza J-C, Junquas C, Wongchuig S, Polcher J, Moron V, Fita L, Arias PA, Schrapffer A, Pennel R. 2023. Impacts of land-surface heterogeneities and Amazonian deforestation on the wet season onset in southern Amazon. *Climate Dynamics*. Springer Berlin Heidelberg, (0123456789). https://doi.org/10.1007/s00382-023-06835-2.

Sierra JP, Junquas C, Espinoza JC, Segura H, Condom T, Andrade M, Molina-Carpio J, Ticona L, Mardoñez V, Blacutt L, Polcher J, Rabatel A, Sicart JE. 2022. Deforestation impacts on Amazon-Andes hydroclimatic connectivity. *Climate Dynamics*. Springer Berlin Heidelberg, 58(9–10): 2609–2636. https://doi.org/10.1007/s00382-021-06025-y.

Smith C, Baker JCA, Spracklen DV. 2023. Tropical deforestation causes large reductions in observed precipitation. *Nature*. Springer US, (April). https://doi.org/10.1038/s41586-022-05690-1.

Soares-Filho B, Alencar A, Nepstad D, Cerqueira G, Vera Diaz M del C, Rivero S, Solórzano L, Voll E. 2004. Simulating the response of land-cover changes to road paving and governance

along a major Amazon highway: the Santarém-Cuiabá corridor. *Global Change Biology*, 10(5): 745–764. https://doi.org/10.1111/j.1529-8817.2003.00769.x.

Soares-Filho B, Rajão R, Macedo M, Carneiro A, Costa W, Coe M, Rodrigues H, Alencar A. 2014. Cracking Brazil's Forest Code. *Science*, 344(6182): 363–364. https://doi.org/10.1126/science.1246663.

Souza CM, Shimbo JZ, Rosa MR, Parente LL, Alencar AA, Rudorff BFT, Hasenack H, Matsumoto M, Ferreira LG, Souza-Filho PWM, de Oliveira SW, Rocha WF, Fonseca AV, Marques CB, Diniz CG, Costa D, Monteiro D, Rosa ER, Vélez-Martin E, Weber EJ, Lenti FEB, Paternost FF, Pareyn FGC, Siqueira JV, Viera JL, Neto LCF, Saraiva MM, Sales MH, Salgado MPG, Vasconcelos R, Galano S, Mesquita VV, Azevedo T. 2020. Reconstructing three decades of land use and land cover changes in brazilian biomes with landsat archive and earth engine. *Remote Sensing*, 12(17). https://doi.org/10.3390/RS12172735.

Spera SA, Winter JM, Partridge TF. 2020. Brazilian maize yields negatively affected by climate after land clearing. *Nature Sustainability*. Springer US, 3(10): 845–852. https://doi.org/10.1038/s41893-020-0560-3.

Spracklen DV, Baker JCA, Garcia-Carreras L, Marsham JH. 2018. The Effects of Tropical Vegetation on Rainfall. *Annual Review of Environment and Resources*, 43(1): 193–218. https://doi.org/10.1146/annurev-environ-102017-030136.

Spracklen DV, Garcia-Carreras L. 2015. The impact of Amazonian deforestation on Amazon basin rainfall. *Geophysical Research Letters*, 42(21): 9546–9552. https://doi.org/10.1002/2015GL066063.

Staal A, Flores BM, Aguiar APD, Bosmans JHC, Fetzer I, Tuinenburg OA. 2020. Feedback between drought and deforestation in the Amazon. *Environmental Research Letters*. IOP Publishing, 15(4). https://doi.org/10.1088/1748-9326/ab738e.

Stickler CM, Coe MT, Costa MH, Nepstad DC, McGrath DG, Dias LCP, Rodrigues HO, Soares-Filho BS. 2013. Dependence of hydropower energy generation on forests in the Amazon Basin at local and regional scales. *Proceedings of the National Academy of Sciences*, 110(23): 9601–9606. https://doi.org/10.1073/pnas.1215331110.

Strand J, Soares-Filho B, Costa MH, Oliveira U, Ribeiro SC, Pires GF, Oliveira A, Rajão R, May P, van der Hoff R, Siikamäki J, da Motta RS, Toman M. 2018. Spatially explicit valuation of the Brazilian Amazon Forest's Ecosystem Services. *Nature Sustainability*. Springer US, 1(11): 657–664. https://doi.org/10.1038/s41893-018-0175-0.

Talamoni IL, Cavalcanti IFA, Kubota PY, de Souza DC, Baker JCA, Vieira RMSP. 2022. Surface and atmospheric patterns for early and late rainy season onset years in South America. *Climate Dynamics*. Springer Berlin Heidelberg, 2(0123456789). https://doi.org/10.1007/s00382-022-06234-z.

Teuling AJ, Taylor CM, Meirink JF, Melsen LA, Miralles DG, van Heerwaarden CC, Vautard R, Stegehuis AI, Nabuurs G-J, de Arellano JV-G. 2017. Observational evidence for cloud cover enhancement over western European forests. *Nature Communications*, 8(1): 14065. https://doi.org/10.1038/ncomms14065.

Tomas WM, de Oliveira Roque F, Morato RG, Medici PE, Chiaravalloti RM, Tortato FR, Penha JMF, Izzo TJ, Garcia LC, Lourival RFF, Girard P, Albuquerque NR, Almeida-Gomes M, Andrade MH da S, Araujo FAS, Araujo AC, Arruda EC de, Assunção VA, Battirola LD, Benites M, Bolzan FP, Boock JC, Bortolotto IM, Brasil M da S, Camilo AR, Campos Z, Carniello MA, Catella AC, Cheida CC, Crawshaw PG, Crispim SMA, Junior GAD, Desbiez ALJ, Dias FA, Eaton DP, Faggioni GP, Farinaccio MA, Fernandes JFA, Ferreira VL, Fischer EA, Fragoso CE, Freitas GO, Galvani F, Garcia AS, Garcia CM, Graciolli G, Guariento RD, Guedes NMR, Guerra A, Herrera HM, Hoogesteijn R, Ikeda SC, Juliano RS, Kantek DLZK, Keuroghlian A, Lacerda ACR, Lacerda ALR, Landeiro VL, Laps RR, Layme V, Leimgruber P, Rocha FL, Mamede S, Marques DKS, Marques MI, Mateus LAF, Moraes RN, Moreira TA, Mourão GM, Nicola RD, Nogueira DG, Nunes AP, Nunes da Cunha C da, Oliveira MD, Oliveira MR, Paggi GM, Pellegrin AO, Pereira GMF, Peres IAHFS, Pinho JB, Pinto JOP, Pott A, Provete DB, dos Reis VDA, dos Reis LK, Renaud P-C, Ribeiro DB, Rossetto OC, Sabino J, Rumiz D, Salis SM, Santana DJ, Santos SA, Sartori ÂL, Sato M, Schuchmann K-L, Scremin-Dias E, Seixas GHF, Severo-Neto F, Sigrist MR, Silva A, Silva CJ, Siqueira AL, Soriano BMA, Sousa LM, Souza FL, Strussmann C, Sugai LSM, Tocantins N, Urbanetz C, Valente-Neto F, Viana DP, Yanosky A, Junk WJ. 2019. Sustainability Agenda for the Pantanal Wetland: Perspectives on a Collaborative Interface for Science, Policy, and Decision-Making. *Tropical Conservation Science*, 12: 194008291987263. https://doi.org/10.1177/1940082919872634.

Tuinenburg OA, Bosmans JHC, Staal A. 2022. The global potential of forest restoration for drought mitigation. *Environmental Research Letters*, 17(3). https://doi.org/10.1088/1748-9326/ac55b8.

Versieux V, Costa MH. 2024. Local Evapotranspiration Is the Only Relevant Source of Moisture at the Onset of the Rainy Season in South America. *Atmosphere*, 15(8): 932. https://doi.org/10.3390/atmos15080932.

Wang J, Chagnon FJF, Williams ER, Betts AK, Renno NO, Machado LAT, Bisht G, Knox R, Bras RL. 2009. Impact of deforestation in the Amazon basin on cloud climatology. *Proceedings of the National Academy of Sciences*, 106(10): 3670–3674. https://doi.org/10.1073/pnas.0810156106.

Wasti A, Ray P, Wi S, Folch C, Ubierna M, Karki P. 2022. Climate change and the hydropower sector: A global review. *WIREs Climate Change*, 13(2): 1–29. https://doi.org/10.1002/wcc.757.

Wright JS, Fu R, Worden JR, Chakraborty S, Clinton NE, Risi C, Sun Y, Yin L. 2017. Rainforest-initiated wet season onset over the southern Amazon. *Proceedings of the National Academy of Sciences*, 114(32): 8481–8486. https://doi.org/10.1073/pnas.1621516114.

Xavier AC, Scanlon BR, King CW, Alves AI. 2022. New improved Brazilian daily weather gridded data (1961–2020). *International Journal of Climatology*, (October 2021): 1–15. https://doi.org/10.1002/joc.7731.

Xu R, Li Y, Teuling AJ, Zhao L, Spracklen DV, Garcia-Carreras L, Meier R, Chen L, Zheng Y, Lin H, Fu B. 2022a. Contrasting impacts of forests on cloud cover based on satellite observations. *Nature Communications*, 13(1): 670. https://doi.org/10.1038/s41467-022-28161-7.

Xu X, Zhang X, Riley WJ, Xue Y, Nobre CA, Lovejoy TE, Jia G. 2022b. Deforestation triggering irreversible transition in Amazon hydrological cycle. *Environmental Research Letters*, 17(3): 034037. https://doi.org/10.1088/1748-9326/ac4c1d.

Yin L, Fu R, Zhang Y-F, Arias PA, Fernando DN, Li W, Fernandes K, Bowerman AR. 2014. What controls the interannual variation of the wet season onsets over the Amazon? *Journal of Geophysical Research: Atmospheres*, 119(5): 2314–2328. https://doi.org/10.1002/2013JD021349.

Yuan T, Li Z. 2010. General Macro- and Microphysical Properties of Deep Convective Clouds as Observed by MODIS. *Journal of Climate*, 23(13): 3457–3473. https://doi.org/10.1175/2009JCLI3136.1.

Yuan T, Martins JV, Li Z, Remer LA. 2010. Estimating glaciation temperature of deep convective clouds with remote sensing data. *Geophysical Research Letters*, 37(8): 1–5. https://doi.org/10.1029/2010GL042753.

Zhang M, Abrahao G, Thompson S. 2021. Sensitivity of soybean planting date to wet season onset in Mato Grosso, Brazil, and implications under climate change. *Climatic Change*. Springer Netherlands, 168(3–4). https://doi.org/10.1007/s10584-021-03223-9.

Zhao X, Frech J, Foster M, Heidinger A. 2024. Studying the Aerosol Effect on Deep Convective Clouds over the Global Oceans by Applying Machine Learning Techniques on Long-Term Satellite Observation. *Remote Sensing*, 16(13): 2487. https://doi.org/10.3390/rs16132487.